Frauenklinik und Poliklinik der Technischen Universität München
Klinikum rechts der Isar
(Direktorin: Prof. Dr. Marion B. Kiechle)

Molecular assessment of factors of the plasminogen activation cascade in advanced serous ovarian carcinoma tissues: correlation with clinical outcome

Shuo Zhao

Vollständiger Abdruck der von der Fakultät für Medizin der Technischen Universität München zur Erlangung des akademischen Grades eines

Doktors der Medizin (Dr.med.)

genehmigten Dissertation.

Vorsitzender: Prof. Dr. Ernst J Rummeny

Prüfende/-r der Dissertation:

1. Prof. Dr. Manfred Schmitt
2. Prof. Dr. Marion B. Kiechle

Die Dissertation wurde am 04.10.2016 bei der Technischen Universität München eingereicht und durch die Fakultät für Medizin angenommen

For my family

1. Introduction

1.1 Diagnosis, treatment, and prognosis of ovarian cancer

Ovarian cancer (OC) is in most cases diagnosed in women over the age of 50, and is the seventh deadliest form of cancer worldwide, following cancer of the lung, breast, colorectum, cervix uteri, stomach, and corpus uteri (WHO report, 2014). In 2012, 238,719 women around the world were diagnosed with OC worldwide, with more than 151,917 deaths according to GLOBOCAN v1.1 (Cancer Epidemiology and Genetic Databases) (Ferlay et al., 2014). The highest incidence of OC is present in Europe and Northern America affecting approximately, 9.9 in 100,000 people in Europe, and 8.1 in 100,000 in Northern America. Africa and Asia have the lowest incidence of OC, with 4.8 diagnoses per 100,000 people in Africa and 5 diagnoses per 100,000 people in Asia (Ferlay et al., 2014). OC is ranked as the fifth most commonly diagnosed female cancer in Europe following carcinoma of the breast, colorectum, lung, and uterus (Ferlay et al., 2014). In 2012 alone, it was estimated that 65,538 new cases of OC were diagnosed, with 42,704 related deaths. Unfortunately, the 5-year survival rate for women with OC is less than half, at 46%, compared to the 89% 5-year survival rate for breast cancer patients (Howlader et al., 2015).

Early detection is the key to survival, with a very optimistic 5-year survival probability of 92% for patients diagnosed at the early stages of this disease (FIGO IA/IB). Sadly, only 15% of OC patients are diagnosed at this stage. The majority of patients (up to 60%) are diagnosed at a very late stage when cancer has metastasized, contributing to a much poorer prognosis and 5-year survival rate of only 28% (Howlader et al., 2015). Reasons for late detection include ambiguous symptoms that hinder the feasibility of early diagnosis, in addition to a lack of effective screening.

The cause, clinical origins and mechanism of disease progression for OC remains poorly understood. It is currently suspected that OC reflects dysfunction in normal reproduction processes, particularly ovulation. A number of factors contribute to increased risk of developing OC. One major risk is increasing age: women >50 years of age have the highest risk of development of OC (Roett et al., 2009); OC is most frequently diagnosed among women aged 55-64, and the median age at diagnosis is 63. The death rate of OC is high among women aged 65-74, and the median age at death is 70 (Howlader et al., 2015). Women with mothers or sisters who were afflicted with ovarian, breast, or uterine cancer have an elevated risk of developing OC. For example, genetic aberrations including mutations in either the BRCA1 or BRCA2 gene are associated with breast or OC (Permuth et al., 2009). Other risk factors include a

history of infertility, use of assisted reproductive technologies, endometriosis, hormone replacement therapy (Kauff et al., 2006). The Hereditary Nonpolyposis Colorectal Cancer (HNPCC) syndrome (also known as Lynch syndrome) is associated with a 9 to 12% increase in lifetime risk for OC. Obesity, smoking, and a sedentary lifestyle have also been linked to increased risk of developing OC (Roett et al., 2009).

Diagnosis of OC is difficult, particularly at its early stage with few or no symptoms (Ledermann et al., 2013). Advanced-stage OC may cause few, nonspecific symptoms that are often mistaken for other serious conditions, such as constipation or an irritable bowel (http://www.cancer.org/cancer/ovariancancer/index, American Cancer Society, 2015; http://www.cancerresearchuk.org/health-professional/cancer-statistics/statistics-by-cancer-type/ovarian-cancer#heading-Zero, Cancer Research UK, 2015). Some of the more common symptoms of OC include: abdominal bloating or swelling, early satiety after eating little, weight loss, discomfort or pain in the pelvis area, changes in bowel habits, vaginal bleeding, or a frequent need to urinate (Permuth et al., 2009; http://www.cancer.org/cancer/ovarian-cancer/index, American Cancer Society, 2015).

After diagnostic tests, such as transvaginal ultrasound and the CA125 blood test, have been performed, one or more treatment options may be recommended. The primary treatment for OC is surgery with subsequent chemotherapy, endocrine therapy, other targeted GENE therapy, and radiation. Almost all OC patients require surgery. Treatment options for OC patients depend on the stage and type of the disease. Disease staging for OC is performed according to the Fédération Internationale de Gynécologie et d'Obstétrique (FIGO) standards. The stage of the cancer is determined using the T-, N-, M-classification system (T: size of the primary tumor; N: number of regional lymph nodes; M: incidence of distant metastasis). Carcinomas account for 90% of OCs (Polterauer et al., 2012), and at least 5 subtypes are currently distinguished based on histopathology and immunohistochemistry: high-grade serous carcinoma (70%), endometrioid carcinoma (10%), clear-cell carcinoma (10%), mucinous carcinoma (3%), and low-grade serous carcinoma (<5%) (Prat et al., 2012).

Several established biological and clinical factors are recognized as important in predicting clinical outcomes for OC patients: age, FIGO stage, histology, nuclear grade, ascitic fluid volume, performance status, the extent of residual tumor mass after debulking surgery, and findings of second-look laparotomy (Berman et al., 2003). FIGO stage and residual tumor mass after primary surgery are the most clinically relevant factors (Winter et al. 2007). On the one hand, at the early stage of OC (FIGO IA/IB), patients have a favorable prognosis and may benefit from adjuvant chemotherapy; on the other hand, at the advanced stage (FIGO III/IV), most patients will benefit from debulking surgery followed by paclitaxel-carboplatin-based chemotherapy (Harries et

al., 2002). The amount of residual tumor mass after cytoreductive surgery is considered another clinically relevant factor for the treatment of advanced ovarian patients with adjuvant therapy. Patients afflicted with epithelial ovarian cancer (EOC) FIGO IIA-IV experience a favorable outcome after surgical cytoreduction compared with patients with persistent residual disease (Polterauer et al., 2012). Various studies have shown that ascitic fluid volume is also a relevant clinical factor in predicting patients' outcome. It has been reported that the incidence of a large volume of ascitic fluid (>500 ml) could be used to identify FIGO III patients who would benefit from neoadjuvant chemotherapy (Kuhn et al., 2001).

1.2 Biomarkers of ovarian cancer

A disease biomarker is "a biological molecule found in blood, other body fluids, or tissues that is a sign of an abnormal process, or of an unphysiological condition or disease" (https://www.cancer.gov/publications/dictionaries/cancer-terms?cdrid=45618, National Cancer Institute, USA). Disease biomarkers may be used to distinguish an affected patient from a person without the disease. Important groups of biomarkers include proteins and peptides (e.g. an enzyme or receptor) or nucleic acids (e.g. mRNA, microRNA, or other non-coding RNA).

Clinical applications of cancer biomarkers involve screening for occult primary cancer, identification of healthy from malignant tissues, distinguishing one type of malignancy from another, and predicting the clinical outcome (prognosis), response of patients to therapy (prediction), as well as the status of the disease (Henry and Hayes, 2012).

An ideal cancer biomarker should meet three important criteria: 1) high specificity for a given tumor type, with the ability to detect early-stage disease and monitor treatment; 2) high sensitivity to avoid false-positive results; 3) high precision to provide an accurate prognosis for treatment, if the purpose is disease monitoring to detect recurrence during follow-up (Sweep, et al., 2006). Some biomarkers are limited to only one application, while others can serve more than one purpose. For example, prostate-specific antigen (PSA) is used for both prostate cancer screening and monitoring, while detection of BRCA germline mutations is used only to assess the risk of breast and/or OC development.

With respect to OC screening, biomarkers are urgently needed. Transvaginal ultrasound (TVU) screening, the primary method of detection at present, is an unreliable tool (van Nagell et al., 2000). Furthermore, an annual gynecologic pelvic examination is not sensitive enough to detect early stage OC. Cancer antigen 125 (CA125) and human epididymis protein 4 (HE4) are two biomarkers currently used to monitor OC. At

present, there are no acceptable biomarkers for early disease detection. Other potential OC biomarkers have been described in the literature, including CA15-3 (MUC-1), HMPG1/G2, cancer associated serum antigen (CASA), CA50, CA54-61, CA19-9, MAM-6, NB/70K, and ovarian serum antigen (OSA), but none of these markers have yet demonstrated an acceptable efficacy required for clinical practice (Terry et al., 2004).

1.2.1 CA125 and HE4

Cancer antigen 125 (CA125) is an established OC biomarker for detecting disease recurrence and monitoring therapy response and was first characterized in 1981 by Robert Bast and his colleagues (Bast et al., 1981). CA125 is encoded by the MUC16 gene. The N-terminal extracellular region of the CA125 is expressed by epithelial cells of various origins, including malignant cells, and released into the blood of OC patients, including EOC (O'Brien et al., 2002). Expression of CA125 is <60% during early-stage OC, but it can increase up to 90% in late-stages (Visintin et al., 2008). However, CA125 alone is inadequate as a cancer-screening biomarker owing to its high rate of false-positive cases and its lower sensitivity for patients with early stage disease or benign gynecologic conditions compared with patients with late stage (Scholler et al., 2007).

HE4, a protease inhibitor, is highly expressed in OC, particularly in serous and endometrioid histotypes, and has been proposed as an alternative biomarker (Simmons et al., 2013). Some reports suggest that HE4 has higher specificity than CA125, as it may be more precise in distinguishing benign and malignant tumors (Escudero et al., 2011). At present, CA125 and HE4 are the only diagnostic markers of OC that are approved by the U.S. Food and Drug Administration (Simmons et al., 2013).

In one study, a panel of serum biomarkers obtained from women who presented with a pelvic tumor mass were evaluated and showed that dual biomarker detection of HE4 and CA125 had increased sensitivity and specificity over CA125 alone in the risk evaluation of malignancy (Moore et al., 2007). The utilization of ROMA (**R**isk of **O**varian **M**alignancy **A**lgorithm) prompts to improve sensitivity and specificity even further (Anastasi et al., 2010; Moore et al., 2010). The combination of dual biomarker detection and ROMA increased the sensitivity of the test to 90% (95% in non-mucinous tumors) with a specificity of 82% (Molina et al., 2011).

1.2.2 Other ovarian cancer biomarkers

Other OC-associated biomarkers include cytokines, hormones, cytokeratins, lipids, lipoproteins, autoantibodies, proteases, and inhibitors. One of the well-recognized OC biomarkers is the macrophage-colony stimulating factor (M-CSF) with 80-100% sensitivity for early stage EOC when M-CSF is combined with CA125 and/or HE4

(Będkowska et al., 2015). Tumor necrosis factor (TNF)-α also belongs to this group. TNF-α inhibits tumor growth by increasing the rate of apoptosis. Additional markers in this category include interleukins (IL) and haptoglobin-α, which is usually combined with CA125 to yield higher sensitivity and specificity (Kodama et al., 1999). The category of hormones, growth or inhibition factors, is largely represented by transforming growth factor (TGF)-β. Mesothelin, representing the growth factor group, was identified for its gene upregulation in late-stage OC (Scholler et al., 1999). P53, another EOC biomarker, is expressed at low levels in the early stage and increases in the later stage of the disease (Kohler et al., 1993). Other biomarkers, such as lysophosphatidic acid (LPA), apolipoprotein, and carcinoembryonic antigen (CEA) are of additive value only for detecting ovarian carcinomas when combined with CA125. Other biomarkers include autoantibodies to the epithelial cell adhesion molecule (Ep-CAM), alpha-fucosidase, galactosyltransferase, lactate dehydrogenase (LDH), RNAase A, or osteopontin. These are related to OC incidence, yet lack specificity, because they may be present in non-neoplastic conditions as well.

A promising group of biomarkers consists of proteases, their receptors, and inhibitors. Serine proteases, such as the urokinase-type plasminogen activator (uPA) and the kallikrein-related peptidases (KLKs), have been shown to be associated with OC. Up-regulation of twelve (KLK3-11 and KLK13-15) of the fifteen KLKs at the mRNA and/or protein expression level are characteristic for OC, compared to expression in normal ovarian tissues. Clinical assessment of KLK expression indicates that KLK4-7, KLK10, and KLK15 are correlated with poor outcome; while expression of KLK8-9, KLK11, KLK13, and KLK14 is correlated with a more favorable outcome. KLK5-8, KLK10, KLK11, and KLK13 are regarded as promising predictive biomarkers of OC (Schmitt et al., 2013). Combined with CA125, several KLKs, e.g. KLK10, can improve sensitivity and specificity of OC screening (Luo et al., 2003).

1.3 The urokinase-type plasminogen activator system

The urokinase-type plasminogen activator (uPA) system, which plays a significant role in tumor invasion and metastasis, encompasses the urokinase plasminogen activator (uPA), several plasminogen activator inhibitors (PAI-1, PAI-2, PAI-3, PAI-4), the urokinase plasminogen activator receptor (uPAR or CD87) and activating protease plasmin (McMahon et al., 2015). In OC, plasmin is known to cleave fibrin, similar to the biological process of dissolving fibrin-containing-blood clots into soluble fragments (e.g. D-dimer), known as fibrinolysis. Plasminogen, the proenzyme form of plasmin, is produced in the liver and released into the blood. Plasminogen is cleaved into plasmin by active uPA (high-molecular-weight-/low-molecular-weight-uPA: HMW/LMW-uPA).

HMW-uPA is the full-length two-chain active form of uPA and harbors two domains with the A-chain, the growth-factor-like domain (GFD), which is responsible for interaction with the uPA receptor, and the so-called the kringle domain. B-chain, which is covalently attached to the A-chain, encompasses the serine protease domain (SPD). In contrast, LMW-uPA represents a proteolytically cleaved form of HMW-uPA, by which most of the A-chain including with the GFD and kringle domain is removed. Thus, LMW-uPA is still an active protease, but incapable to interact with uPAR. Both forms, HMW-uPA and LMW-uPA can be inhibited by its natural inhibitors (Vincenza Carriero et al., 2009). Interaction of uPA with its receptor uPAR focuses HMW-uPA and pro-uPA to the cell surface. Since also plasmin(ogen) interacts with cell surface-associated binding proteins, the reciprocal conversion of pro-uPA by plasmin and of plasminogen by uPA occurs with a cell higher efficiency than in solution (Novokhatny et al., 1992). The uPA binding uPAR then activates the near-cell conversion of plasminogen to plasmin. Inhibition of the uPA system occurs via inactivation of HMW-uPA or LMW-uPA mainly by PAI-1 (Mengele et al., 2010). Despite its established role in fibrinolysis, the clinical significance of uPA in vascular biology, matrix remodeling, tumor growth and dissemination, wound healing, and infection was largely unknown until around 1985. As cancer metastasis results from the process of cancer cell detachment from its original tissue localization, cancer cell migration and invasion into the surrounding tissue requires adhesion to and subsequent degradation of extracellular matrix (ECM).

The broad-spectrum serine protease plasmin is involved in thrombolysis, the degradation of blood clots. In OC, plasmin does not only activate the proenzyme form of uPA, pro-uPA, but also cleaves other proteins, for example fibrin, a major constituent of the extracellular tumor stroma (Davidson et al., 2014). Moreover, plasmin activates latent transforming growth factor-β1 (TGF-β1) and vascular endothelial growth factor (VEGF), and the zymogen forms of matrix metalloproteases.

Amino-terminal glutamic acid (Glu) plasminogen is the circulating form of plasminogen (the zymogen pro-form of plasmin), a single-chain multidomain glycoprotein of 90 kDa composed of 791 amino acids. It is composed of seven structural domains: an N-terminal pre-activation peptide (amino-terminal glutamic acid (Glu) plasminogen N-terminal peptide), five kringle domains, and the C-terminal trypsin-like serine protease domain carrying the catalytic triad His603, Asp646, and Ser741 (Petersen et al., 1990). Plasminogen and plasmin binding to proteins or cells is regulated by the kringle domains. Kringle domains consist of homologous triple-loop structures. Four out of the five domains (K1, K2, K4, and K5) include lysine-binding sites (LBS) that enable plasminogen to bind to proteins with carboxyl-terminal lysines or conformational mimetics of these residues. K1 mediates plasminogen recruitment to the

matrix protein fibrin or to the cell surface, and thus activity of plasminogen is associated with the cell surface (Deryugina et al., 2012). The structure of first three or four kringle domains of plasminogen is known as angiostatin or recombinant angiostatin. Angiostatin is produced by autoproteolytic cleavage of plasminogen and inhibits angiogenesis (Javaherian et al., 2011). Other kringle LBS initiates the change in conformation of the compact-closed-state of plasminogen to its open-extended-state. Conversion of the closed to the open form of plasminogen stimulates conversion of plasminogen to plasmin that is boosted when plasminogen is attached to fibrin or to associated cells. Glu-plasminogen, as the circulating form of plasminogen, exhibits a closed, compact and spiral confirmation, the activation site is buried within the molecule, and it is a poor substrate for plasminogen activators (Law et al., 2012). Then, plasmin hydrolyzes peptide bonds of Glu-plasminogen, producing a small N-terminal peptide and the 714-amino-acid variant Lys-plasminogen. Lys-plasminogen (the more readily activated form) becomes the predominant substrate for plasminogen activators on the cell surface (Xue et al., 2012). Next, Lys-plasminogen is converted to plasmin by cleavage of the activation site, leading to the two-chain plasmin molecule, composed of a light chain and a heavy chain.

Plasminogen, plasmin, and uPA are often co-localized on cells. Localization of the proteolytic activity of plasmin to cell surfaces enhances the cells' ability to degrade surrounding ECM and thereby to facilitate cell migration through activation of other matrix-related proteolytic enzymes and growth factors. Interaction of plasminogen with cells plays a pivotal role in the recruitment of macrophages within pathophysiological processes such as the inflammatory response, tumor cell invasion, and metastasis. Apart from that, it also plays a major part in non-malignant situations, such as wound healing, tissue remodeling, neurite outgrowth, and skeletal myogenesis (Law et al., 2013).

Enzymatically active uPA is a serine protease that predominantly catalyzes the plasminogen/plasmin conversion. The *uPA* gene is located on chromosome 10q24. The 6.4 kb human gene codes for *uPA*, consisting of 11 exons and 10 introns. uPA is considered to play a central role in the regulation of extracellular proteolysis in various physiological and pathological processes. As a thrombolytic agent, enzymatically active uPA was explored for the treatment of pulmonary embolism, acute myocardial infarction, ophthalmic clot and hemorrhage and peripheral arterial occlusion (Crippa et al., 2007). uPA also serves as an important biomarker in prognosis and therapy response in a number of other forms of cancer (McMahon et al., 2015).

uPA initially exists as an almost proteolytically inactive precursor form (pro-uPA) accompanied by its enzymatically active molecular forms: HMW-uPA and LMW-uPA. HMW-uPA binds to the cell surface receptor uPAR initiating conversion of plasminogen to plasmin. Pro-uPA is activated via cleavage of the Lys158-Ile159 peptide bond into HMW-uPA by different proteases (e.g., plasmin, cathepsin B and L, kallikrein, trypsin or thermolysin), and subsequently into its LMW-uPA form (Su et al., 2016). Such activation of pro-uPA by plasmin is representative of feedback activation. Plasminogen can also be cleaved by proteases to liberate kringle domains called angiostatin. The inhibitor (serpin) PAI-1 controls the proteolytic conversion of plasminogen to plasmin by inactivating HMW-uPA or LMW-uPA. In cancer, PAI-1 forms a one-to-one covalent complex with uPA and is released by various tumor-associated cells. Only the HMW-uPA and PAI-1 complex, when bound to uPAR, will induce cellular internalization of the trimeric uPAR/HMW-uPA/PAI-1 complex. Internalization of this complex in a piggyback fashion is assisted by a member of the low-density lipoprotein receptor-related protein (LRP) family, LRP-1. Following the internalization, the uPAR/HMW-uPA/PAI-1 complex is degraded in lysosomes. However, uPAR is left intact, and recycled from the endocytotic compartment back to the cell surface (Nykjaer et al., 1990). The details of the uPA activation system are shown in Figure 1.

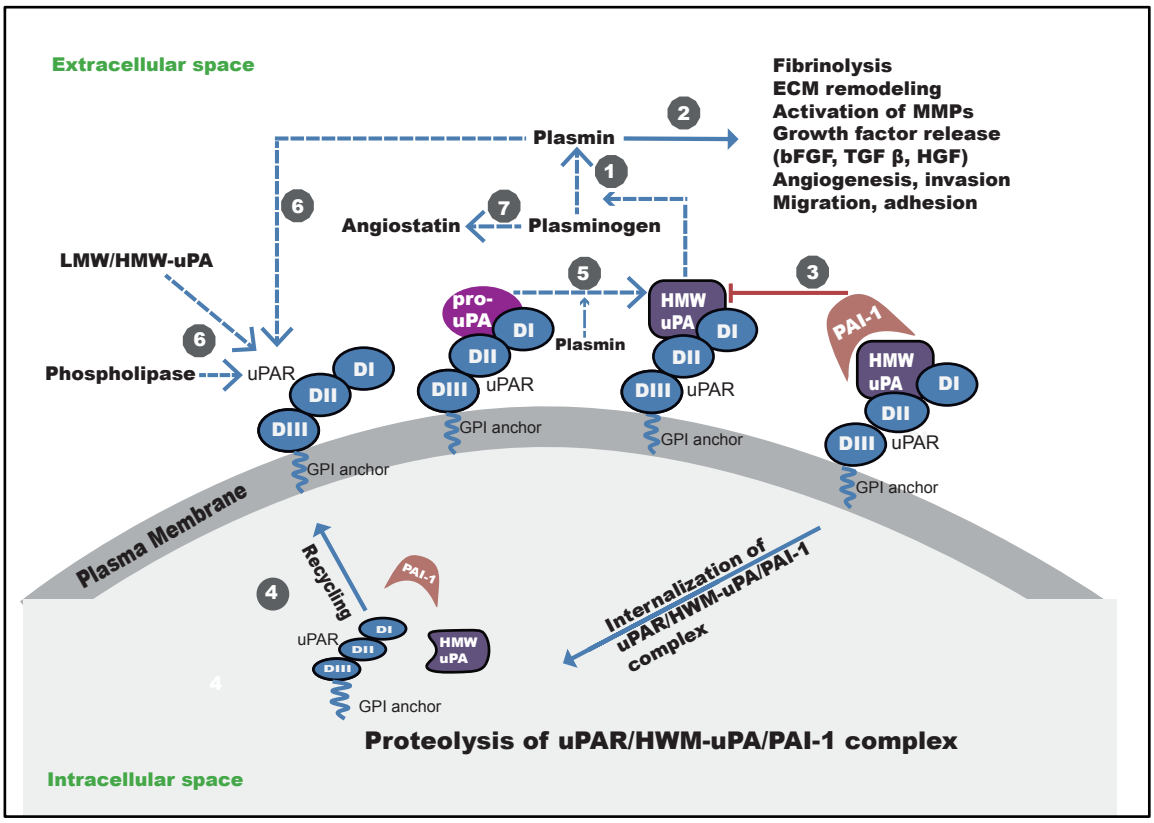

Figure 1. Known steps of the activity scheme of the cellular plasminogen/plasmin system.

(1) Plasminogen is converted to plasmin by activation of HMW-uPA. (2) Plasmin then induces fibrinolysis and conversion of pro-metalloproteinases to metalloproteinases (MMPs). Both plasmin and MMP can trigger the breakdown of the ECM; plasmin also activates latent growth factors, thereby affecting cell migration and adhesion, angiogenesis and tumor invasion. (3) PAI-1 inactivates HMW-uPA. After formation of the uPAR/HMW-uPA/PAI-1 complex, the trimeric uPAR/HMW-uPA/PAI-1 complex will be internalized. (4) Following internalization, the uPAR/HMW-uPA/PAI-1 complex is degraded and uPAR is recycled back to the cell surface. (5) Plasmin, in turn, activates the conversion of pro-uPA to HMW-uPA. (6) uPAR can be cleaved by plasmin, LMW/HMW-uPA, or phospholipase. (7) Angiostatin is produced by autoproteolytic cleavage of plasminogen.

Activation is shown as arrows, inhibition as flat-headed arrows. Proteolytic cleavage is represented by dashed-line arrows. LMW/HMW-uPA: low/high-molecular-weight-urokinase-type plasminogen activator; uPAR: urokinase-type plasminogen activator receptor; DI-DIII: domain I-III of uPAR; GPI: glycosyl-phosphatidyl-inositol; PAI-1: plasminogen activator inhibitor-1. (Adapted from “The apparent uPA/PAI-1 paradox in cancer: more than meets the eye.” Kwaan et al., 2013).

uPAR, the receptor for uPA, is a cysteine-rich glycoprotein (55-60 kDa). uPAR integrates into the cell membrane through glycosyl-phosphatidyl-inositol (GPI) anchor that is covalently attached to carboxy-terminus. uPAR was first described in 1985 as a high-affinity-binding cell surface entity for the amino-terminus of uPA (Stoppelli et al., 1985; Vassalli et al., 1985). uPAR is highly glycosylated and consists of 283 amino acids (35 kDa). uPAR does not contain any transmembrane or cytosolic domains (Wang et al., 1995). Soluble uPAR variants, lacking the GPI anchor, have been detected in conditioned medium of tumor cell lines and in the ascitic fluid of OC patients (Pedersen et al., 1993). Not only uPA is known to bind to uPAR, but also vitronectin, integrins, G-protein-coupled receptors, and other uPAR-associated proteins interact with uPAR (Ploug et al., 2003).

Both uPAR and uPA are jointly expressed at the invasive foci in many different types of human cancer tissues. Non-malignant stromal cells expressing uPAR and/or uPA, such as macrophages and fibroblasts, show that these cells actively support the invasive cancer process (Ohtani et al., 1995). Apart from cancer, uPA and uPAR have also been found to be up regulated in atherosclerotic plaques. Inhibition of uPAR also results in inhibition of pathological vascular remodeling (Kanno et al., 2008). Both uPA

and uPAR may serve as potential targets for cancer treatment to affect tumor growth and metastasis, or other diseases associated with tissue remodeling (Danø et al., 1999).

PAI-1, as an efficient inhibitor of uPAR-bound HMW-uPA, promotes internalization of receptor-bound uPA, allowing for recycling of uPAR to the cell surface. PAI-1 is a well-studied member of the serpin superfamily, a family encompassing more than 100 members besides PAI-1 (Gils et al., 2004). There are two groups of serpins: inhibitory and noninhibitory. PAI-1 belongs to the first group, which is a 47 kDa single chain glycoprotein (van de Craen et al., 2012). PAI-1 is secreted by a large number of cell types, including endothelial cells, stromal cells, platelets, monocytes, smooth muscle cells, trophoblasts, myofibroblasts, adipocytes, hepatocytes, and cancer cells. Several agents also stimulate synthesis and secretion of PAI-1, such as growth factors (TNF-α and TGF-β), thrombin, interleukin-1, insulin, tumor necrosis factor, endotoxins, dexamethasone, lipopolysaccharide, very-low-density lipoprotein (VLDL), and low-density lipoprotein (LDL) (Loskutoff et al., 1987). Other factors may influence PAI-1 expression, e.g. estrogen, hyperglycemic conditions, certain cytokines (Mengele et al., 2010).

1.4 The urokinase-type plasminogen activator system in human cancers

A large number of studies reported that the uPA system is involved in multiple steps of tumor progression (Duffy et al., 2004). Several studies showed that the uPA system is consistently overexpressed in OC, compared to the normal ovarian tissue (Kenny et al., 2011; Al-Hassan et al., 2012). Enhancement of over-expression of uPA in OC might be affected by lysophosphatidic acid (LPA) production, stimulating metastasis in OC cells (Li et al., 2005). Another study found that PAI-1 expression was significantly elevated in EOC over benign ovarian tumors (Kuhn et al., 1994; Kuhn et al., 1999). In OC, PAI-1 was found to be a statistically independent factor for overall survival. In addition, PAI-1 protein expression is significantly associated with advanced FIGO stage, poor histological differentiation, and lymph node metastasis, suggesting that PAI-1 is implicated in OC invasion and metastasis (Schmalfeldt et al., 1995; Chambers et al., 1998; Koensgen et al., 2006; Dorn et al., 2011; Zhang et al., 2013b).

Most studies have been concentrated on two approaches in terms of uPA as a therapeutic target: one approach is inhibition of uPA catalytic activity by selective low-molecular-weight inhibitors; another approach is preventing uPA from binding to uPAR by use of antagonistic peptides or antibodies (Duffy et al., 2004; Schmitt et al., 2010; Schmitt et al., 2011). Previously, the uPA inhibitor WX-671 (also known as Mesupron® or Upamostat) (Wilex, Munich, Germany), a pro-drug of WX-UK1, has completed a phase Ib trial for the treatment of patients with head and neck cancer

(Meyer et al., 2008). It has also completed two of phase II trials in patients with advanced breast or pancreatic cancer (Heinemann, et al., 2013; Leurer et al., 2015). Yet, no clinical studies have been prepared to target the uPA system in OC patients. Although only few uPA inhibitors have entered the clinical trial, other studies have shown other drugs can block the uPA system both *in vitro* and *in vivo* animal models (Ulisse et al., 2009; Mazar et al., 2011; Zhang et al., 2013a; Mashiko et al., 2015). uPAR expressed in OC augments cell proliferation, mesothelial adhesion, and invasiveness. Although many researchers have developed peptides that antagonize uPA-uPAR interaction, most of them have not reached clinical testing (Duffy et al., 2004).

Particularly, uPA was shown to be an important prognostic marker in human breast cancer (Duffy et al., 1988; Jänicke et al., 1989). In 2007, assessment of uPA and PAI-1 levels using ELISA have been recommended by the American Society of Clinical Oncology (ASCO) to determine the risk of disease recurrence in breast cancer patients (Schmitt et al., 2010). Elevated expression of uPA and uPAR are associated with poor prognosis and are correlated with advanced breast cancer, including the occurrence of metastasis (Foekens et al., 2000). The prognostic value of uPA and PAI-1 has also been validated by the EORTC-RBG (European Organization for Research and Treatment of Cancer-Receptor and Biomarker Group) meta-analysis, encompassing 8,377 breast cancer patients (Look et al., 2002). This study reported that increased levels of uPA and PAI-1 are associated with poor disease-free survival and poor overall survival in untreated node-negative breast cancer patients. These characteristics and many other studies indicated the uPA and PAI-1 are promising biomarkers in breast cancer and candidate targets for breast cancer therapy (Roy et al., 2014).

In other types of cancer, elevation of the uPA system members plays an important part in tumor progression as well. Increased expression of uPA, uPAR, and/or PAI-1 is associated with poor prognosis in cancer of the breast, ovary, cervix uteri, prostate, colon and rectum, stomach, esophagus, pancreas, liver, kidney, lung, glioma, and bone (Kobayashi et al., 1994; Kuhn et al., 1994; Hsu et al., 1995; Cantero et al., 1997; De Petro et al., 1998; Nekarda et al., 1998; Swiercz et al., 1998; Häckel et al., 2000; Look et al., 2002; Hataji et al., 2004; Ji et al., 2005; Riisbro et al., 2005; Al-Janabi et al., 2014). Various studies support the clinical impact of uPA and uPAR as biomarkers. Expression of uPA and uPAR were both found to be elevated in gastric cancer tissues and increased uPA and uPAR expression were associated with high mortality in human gastric cancer (Ji et al., 2005). Nekarda et al. (1994; 1998) also reported that uPA and PAI-1 could be used as a diagnostic and a prognostic marker in gastric cancer and adenocarcinoma of the esophagus. With respect to colorectal cancer studies, it was

shown that higher preoperative levels of the soluble form of uPAR (suPAR) correlated with increased mortality (Stephens et al., 1999). A rectal cancer study reported that increased preoperative uPAR levels are of statistically independent prognostic value (Riisbro et al., 2005). Another study demonstrated that uPAR expression is correlated with survival of small cell lung cancer patients (Gutova et al., 2007). Other studies reported that overexpression of uPA and uPAR is associated with mesothelioma, osteosarcoma, and chondrosarcoma (Shetty et al., 1995; Häckel et al., 2000; Fisher et al., 2001). uPA and uPAR are also involved in prostate cancer metastasis. Both uPA and uPAR have been found to be overexpressed in the advanced stage of prostate cancer (Piironen et al., 2006). A glioma study showed that tumor grade is associated with uPA expression. It was found that overexpression of uPAR is one of the main reasons that tumor cells grow fast in gliomas; tumor growth declined by blocking uPAR (Bu et al., 2004). A higher content of uPAR protein was also found in patients with more aggressive and late stage endometrial cancer (Memarzadeh et al., 2002). Cervical cancer patients with strong immunohistochemical staining of uPA and PAI-1 had poor prognosis and survival rates, and higher likelihood of lymph nodes metastasis (Kobayashi et al., 1994). uPA and PAI-1 antigen levels also presented as unfavorable prognostic factors in thyroid carcinoma patients (Herceg et al., 2013). It was reported that uPA, uPAR, and PAI-1 were all overexpressed in kidney cancer compared with normal tissue, e.g. in squamous cell carcinoma and clear cell renal cell carcinoma (Hofmann et al., 1996; Swiercz et al., 1998; Fuessel et al., 2014).

2. Aim of the study

The aim of the present study was:

- to set up standard-operating-procedures (SOPs) for the qualitative and quantitative assessment of plasmin(ogen) (PLG), uPA, and PAI-1 by immunohistochemistry and qPCR in ovarian cancer tissues;
- to compare the expression levels of PLG, uPA, and PAI-1 both at the mRNA and protein level;
- to analyze for associations between expression of PLG, uPA, and PAI-1 with clinical and histomorphological features of advanced serous ovarian cancer patients;
- to analyze whether expression of PLG, uPA, and PAI-1 is associated with progression-free and overall survival of advanced serous ovarian cancer patients.

3. Patients, material, and methods

3.1 Ovarian cancer patients and tissue collection

The ovarian cancer (OC) tumor tissue samples used in this study were obtained from patients enrolled in the Department of Obstetrics and Gynecology, Klinikum rechts der Isar, Technical University of Munich (TUM), Germany, between the years 1990 and 2012. Tissue samples were organized into two cohorts (Table 1 and 2). Tissues were inspected for malignancy by a local pathologist and then snap-frozen for storage in liquid nitrogen. In parallel, FFPE (formalin-fixed, paraffin-embedded) tumor tissue blocks were routinely prepared by the Institute of Pathology and Pathological Anatomy, TUM. Cores taken from the central tumor region of the FFPE blocks were transferred to the recipient tissue microarray paraffin blocks (cohort 1, n=103). Full-face tissue sections for cohort 2 (n=50) were obtained from FFPE tumor tissue blocks. mRNA was isolated from 29 frozen tumor specimens matched with samples of cohort 2. uPA and PAI-1 protein content from cohort 2 was determined before by the Femtelle uPA/PAI-1 ELISA (enzyme-linked immunosorbent assay) (Sekisui, Stamford, CT, USA).

For total RNA isolation, 200 mg tissue was pulverized in the deep-frozen state by use of the micro-dismembrator II bead mill apparatus (Sartorius, Goettingen, Germany) (Schmitt et al, 2007). Then the RNA was extracted from 100 mg of the still frozen tissue powder employing the TRIzol reagent protocol (see Chapter 3.6.1).

This biomarker study was approved by the Ethics Committee of the Medical Faculty of the Technical University of Munich. Written informed consent to use tumor tissue specimens for research purposes was obtained from all patients included in this study.

Table 1. **Clinical data of advanced serous ovarian cancer patients in cohort 1 (n=103).**

Clinicopathological factors	Number	Percentage
All patients	103	
Median observation time of patients alive (range)	39 (1-181) months	
Median age (range)	63 (23-86)	
Age		
≤60 years	42	40.8
>60 years	61	59.2
Nuclear grade		
2	15	14.6
3	88	85.4
FIGO stage		
III	82	79.6
IV	21	20.4
Ascitic fluid volume		
No	11	10.7
≤500 ml	25	24.3
>500 ml	53	51.5
No data	14	13.5
Residual tumor mass		
Tumor-free	30	29.1
>0 and ≤10 mm	42	40.8
>10 mm	31	30.1
Disease recurrence		
Yes	79	76.7
No	10	9.7
No data	14	13.6
Alive		
Yes	27	26.2
No	71	68.9
No data	5	4.9
Response to carboplatin/taxol		
Complete remission	35	34.0
Partial remission	15	14.5
No change	3	2.9
Progression	15	14.6
No data	35	34.0
CA125 (median value)		
≤699 U/ml	36	35.0
>699 U/ml	35	34.0
No data	32	31.0

Table 2. Clinical data of advanced serous ovarian cancer patients in cohort 2 (n=50).

Clinicopathological factors	Number	Percentage
All patients	50	
Median observation time of patients alive (range)	46 (5-161) months	
Median age (range)	63 (35-82)	
Age		
≤60 years	23	46.0
>60 years	27	54.0
Nuclear grade		
2	4	8.0
3	46	92.0
FIGO stage		
III	37	74.0
IV	13	26.0
Ascitic fluid volume		
No	9	18.0
≤500 ml	14	28.0
>500 ml	23	46.0
No data	4	8.0
Residual tumor mass		
Tumor-free	14	28.0
>0 and ≤10 mm	19	38.0
>10 mm	13	26.0
No data	4	8.0
Disease recurrence		
Yes	32	64.0
No	16	32.0
No data	2	4.0
Alive		
Yes	22	44.0
No	26	52.0
No data	2	4.0
Response to carboplatin/taxol		
Complete remission	21	42.0
Partial remission	3	6.0
No change	0	0.0
Progression	20	40.0
No data	6	12.0
CA125 (median value)		
≤892.5 U/ml	23	46.0
>892.5 U/ml	23	46.0
No data	4	8.0

3.2 Reagents and material

Table 3. Reagents and material.

Cell culture	
Cell culture flask (25 cm^2, 75 cm^2, 175 cm^2)	Greiner Bio-one GmbH, Frickenhausen, Germany
Cell culture microscope	CK30, Olympus, Tokyo, Japan
Centrifuge	Rotina 48R, Andreas Hettich, Tuttlingen, Germany
CO_2-incubator	Heraeus Function Line Serie 7000
Collagen, Type I from rat tail	#L120M7011V, Sigma-Aldrich, Taufkirchen, Germany
Cryogenic vials	Thermo Fisher Scientific Inc., Rochester, NY, USA
DMEM (dulbecco's modified eagle's medium)+ Glutamax	#61965-026, Gibco, Invitrogen, Paisley, United Kingdom
DMSO (dimethyl sulfoxide)	#317275, Merck Chemicals, Darmstadt, Germany
EDTA (ethylenediaminetetraacetic acid), 1% (w/v)	#L2113, Biochrom GmbH, Berlin, Germany
FBS (Fetal bovine serum)	#10270-106, Invitrogen, Carlsbad, USA
Hemocytometer	0.1 mm, Neubauer improved chamber, Laboroptik Ltd, United Kingdom
HEPES (4-(2-hydroxyethyl)-1-piperazineethanesulfonic acid)	#15630-080, Gibco, Invitrogen, Darmstadt, Germany
Laminar flow cabinet (Hera Safe)	M1199, Heraeus, Hanau, Germany
L-arginine	#A8094, Sigma, Munich, Germany
L-asparagine	#A7094, Sigma, Munich, Germany
Microscope coverslip	#005540 Menzel-Glaeser, Braunschweig, Germany
Molecular Imager ChemiDo XRS System, Bio-Rad	Bio-Rad Laboratories Inc., Munich, Germany
PBS (phosphate-buffered saline)	#10010-015, Gibco, Invitrogen, Carlsbad, CA, USA
RPMI 1640 medium plus Glutamax minus phenol red	#11835-30, Gibco, Invitrogen, Paisley, United Kingdom
Serological pipette	Greiner Bio-one GmbH, Frickenhausen, Germany
Trypan Blue	#T-8154, Sigma, Taufkirchen, Germany
Trypsin/EDTA 0.5%/0.2% (w/v) in PBS without Ca^{2+} 10X	Biochrom GmbH, Berlin, Germany

Immunohistochemistry	
Antibody diluent 500 ml ready to use	#ZUC025-500, Zytomed Systems GmbH, Berlin, Germany
Coverslip	#1130287, R. Langenbrinck, Teningen, Germany
DAB (diaminobenzidine)	#247-DA, DAB 5000 plus, Zytomed Systems GmbH, Berlin, Germany
Ethanol	Department of Pathology, Technical University of Munich, Germany
Formalin	Department of Pathology, Technical University of Munich, Germany
HCl 37% (hydrochloric acid)	#3957.2, Carl Roth, Karlsruhe, Germany
Hematoxylin	#S2020, Dako REAL, Glostrup, Denmark
Hydrogen peroxide 30 % (H_2O_2)	1.07210.0250, Merck, Darmstadt, Germany
Isopropanol	Department of Pathology, Technical University of Munich, Germany
Light microscope	Axioskop, Carl Zeiss, Jena, Germany
Manual Tissue Arrayer	MTA-1, Beecher Instruments, Sun Prairie, WI, USA
Microcentrifuge 5417R	Eppendorf, Hauppage, NY, USA
Microscope slides	SuperFrost Plus, # 03-0060, R. Langenbrinck, Teningen, Germany
NaCl (sodium chloride)	1.06404, Merck, Darmstadt, Germany
Na_2HPO_4 -2 H_2O (sodium phosphate dibasic dihydrate)	S-0876, Sigma-Aldrich, Taufkirchen, Germany
NaH_2PO_4 -2H_2O (sodium phosphate monobasic dihydrate)	#2370, Carl Roth, Karlsruhe, Germany
NaOH (sodium hydroxide)	S-0899, Sigma-Aldrich, Taufkirchen, Germany
NanoZoomer Virtual Microscope and software NDP2.0	Hamamatsu Photonics, Hamamatsu, Japan
Paraffin	Department of Pathology, Technical University of Munich, Germany
Paraformaldehyde	#31628.01 Serva Electrophoresis, Heidelberg, Germany
pH Meter	SCHOTT Instruments Analytics, Mainz, Germany
Pertex (mounting medium)	PER3000, Medite, Burgdorf, Germany
Pressure cooker (Ankoch-Automatik)	WMF, Geislingen Steige, Germany
Toploader balance	#Z267074, Model BP310S, Sartorius, Goettingen, Germany
Trizma Base	T1503, Sigma-Aldrich GmbH, Taufkirchen, Germany
Tris-buffered saline (TBS)	60.5 g Trizma Base, 1 L distilled H_2O, 2 N hydrogen chloride, 90 g sodium chloride. Adjust to pH 7.6 solution for use: add distilled H_2O up to 1 L stock solution
Tween-20	#P1379, Sigma-Aldrich GmbH, Taufkirchen, Germany
Ventana DISCOVERY® XT	N750-BMKTX-FS, Ventana, Tucson, AZ
Xylene	Department of Pathology, Technical University of Munich, Germany
Zytochem plus HRP One-Step polymer anti-mouse/rabbit/rat	#ZUC053-100, Zytomed Systems, Berlin, Germany

qPCR	
Brilliant III Ultra-Fast RT-PCR Master Mix with Low ROX	#600890, Agilent Technologies, Boeblingen, Germany
Cloned AMV first-strand cDNA synthesis kit	#12328-040, Invitrogen, Darmstadt, Germany
Mx3005P quantitative PCR	Agilent Technologies, Boeblingen, Germany
Nanodrop	Thermo Scientific, Peqlab, Erlangen, Germany
PCR 96-well TW-MT-plate, clear	#52450, Qiagen, Hilden, Germany
Qiacube	Thermo Scientific, Peqlab, Erlangen, Germany
RNase-free DNase set (50)	SensoQuest, Goettingen, Germany
RNeasy Mini Kit	Biozym Diagnostik, Hessisch Oldendorf, Germany
Sterile aerosol pipette tips	Biozym, Biozym Diagnostik, Hessisch Oldendorf, Germany
Thermal cycler	Qiagen, Hilden, Germany
TRIzol® LS reagent	#10296-010, Invitrogen, Carlsbad, CA, USA

3.3 Paraffin block preparation and Tissue Microarray (TMA) construction

FFPE blocks were received from the Department of Pathology, TUM, Germany, where the tissues were trimmed, fixed and paraffin-embedded. FFPE blocks were used for full-face slides and TMA construction.

The tissue microarray (TMA) technology is different from the traditional multi-tissue block technique, which has often been used in pathology laboratories for antibody specificity testing (Battifora et al., 1986). Advantages of TMA technology include increased capacity, negligible damage caused to the original tissue block, precise positioning of tissue specimens, and parallel utility of these tissues in different kinds of molecular analyses. This technology enables the generation of multiple replicate microarray blocks, each with the identical coordinates and the same specimens for the same analyses.

TMA construction was performed using a Beecher Instrument according to the Tissue Arrayer Instruction Manual (MTA-1) (Tan et al., 2004). First, tumor regions of each FFPE specimen were viewed and pre-marked by a pathologist with reference to hematoxylin-eosin (H&E) stained slides. Three different 1 mm-wide tissue punches were retrieved from each donor block and transferred to the recipient array block. A schematic diagram of a TMA set-up is depicted in Figure 2. Core samples of normal tissue blocks, including liver, were placed between tumor core samples for orientation of histological specimens (W in Figure 2). An H&E section was recorded for each tissue for the re-evaluation of the transferred tissue cores.

	0	1	2	3	4	5	6	7	8	9	10	11	12	0
0	w	w	w											
1	w	w	w	w	w	w	w	w	w	w	w	w	w	w
2	w	1	1	1	2	2	2	3	3	3	4	4	4	w
3	w	5	5	5	6	6	6	7	7	7	8	8	8	w
4	w	9	9	9	10	10	10	11	11	11	12	12	12	w
5	w	13	13	13	14	14	14	15	15	15	16	16	16	w
0	w	w	w	w	w	w	w	w	w	w	w	w	w	w

Figure 2. Tissue microarray map template.

The area marked yellow is the tumor specimens' area (row 1-16). W=wall (liver reference sample). Row 0: TMA orientation walls.

The tumor tissue array recipient block was first placed in a warm chamber (37°C) for 10 to 15 min and gently pressed on a flat surface to ensure the block was leveled. After, the paraffin core was punched out of the recipient block according to the template shown in Figure 2. Next, the needle was switched to the donor block, and core punches containing tumor tissues were extracted from the donor block and transferred to the recipient block. This workflow was repeated until the recipient block was completely filled with all of the donor paraffin punch cores. Finally, the recipient block was heated to 42°C for 40 min and then cooled down to 20°C before being cut into 3 µm-thick sections for H&E staining or immunohistochemistry (IHC).

3.4 Immunohistochemistry (IHC)

3.4.1 Polymer technology – EnVision™ method

Despite the widespread use of streptavidin-biotin labelling in immunohistochemistry, there are certain limits to this method. First, the presence of endogenous biotin in tissues, such as the ovary, can lead to significant background staining. To overcome this issue, polymer-based immunohistochemical methods that do not rely on biotin have been introduced; such as Dako EnVision Systems' chemistry, which relies on biotin-free dextran polymer technology, that permits binding of numerous enzymes (e.g. horseradish peroxidase or alkaline phosphatase) to a secondary antibody via the dextran backbone (Figure 3). In brief, the primary antibody is applied to the tissue to bind the target molecule, followed by addition of the enzyme-labeled polymer linked to the secondary antibody, after which the chromogenic substrate is added. After processing of the chromogenic substrate, the colored product is precipitated due to the enzymatic reaction.

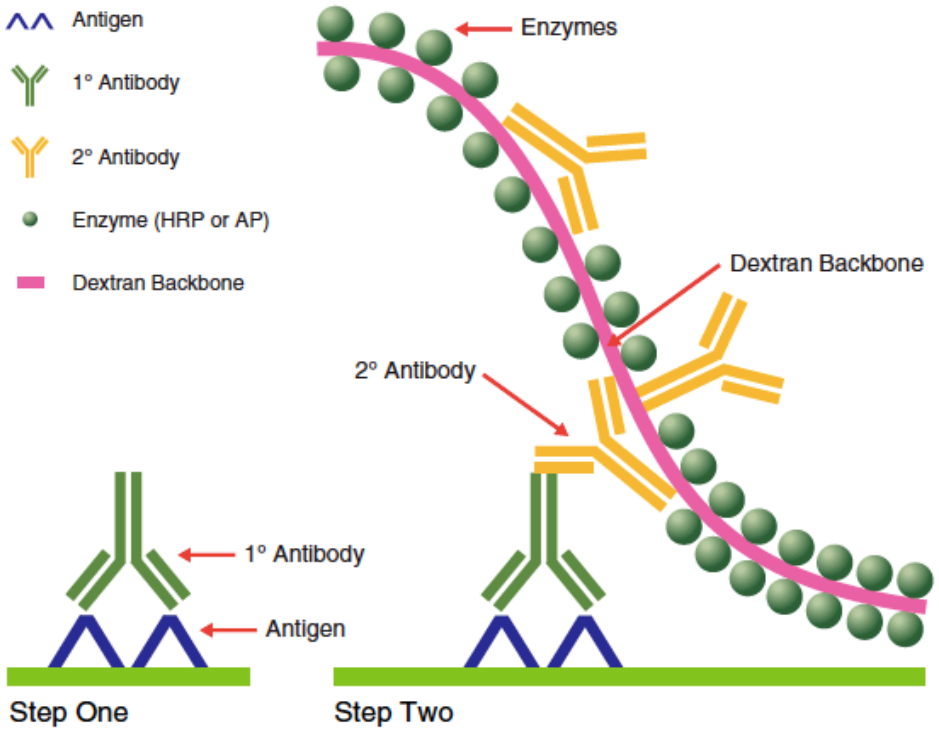

Figure 3. Graphic representation of the two-step polymer EnVision™ system method.

Source: DAKO Education Guide IHC Staining Methods, 5th edition, www.dako.com

3.4.2 Manual immunohistochemical staining protocol for PLG, uPA, and PAI-1

The antibody for PLG (ab10178, stock concentration: 2 mg/ml; named anti-PLG) does not require filtration or centrifugation. The antibody for uPA (#3689, stock concentration: 1 mg/ml; named anti-uPA) was pre-diluted with the DAKO antibody diluent to 1:200 in a final volume of 5 ml and was then filtered with a Minisart® NML Syringe Filter (28 mm size 0.2 µm, Sartorius, Goettingen, Germany). Afterwards, the antibody to PAI-1 (#3786, stock concentration: 0.42 mg/ml; named anti-PAI-1) was centrifuged at high speed (6 min, 8°C) in a microcentrifuge (Eppendorf, NY, USA). After centrifugation, the supernatant was carefully transferred to an Eppendorf tube.

FFPE sections mounted on microscope slides were heated to 58°C to remove the paraffin. Samples were rehydrated the next day in a descending row of xylene-alcohol (2 x 10 min xylene; 2 x 100% ethanol, 1 x 96% ethanol，1 x 70% ethanol, for 5 min each). The sections were washed twice with Tris-buffered saline with 0.05% Tween 20 (TBST) (2.5 min each). For anti-PLG staining, but not for anti-uPA or anti-PAI-1, antigen retrieval was performed. 1.116 g EDTA (ethylenediaminetetraacetic acid) was dissolved in 3 L H_2O, adjusted with NaOH to pH 8.0. EDTA-buffer (1 L) was heated in an open

pressure cooker until boiling. Subsequently, slides were incubated in boiling buffer for 4 min. After pressure-cooking, the pot was cooled under running tap water; the slides were retrieved and washed twice with TBST (2.5 min each).

Some of the tissues in question may contain endogenous peroxidases. This endogenous background must be reduced by the pre-treatment of FFPE-sections with H_2O_2 prior to incubation with the HRP-conjugated antibody polymer. For this, tissue sections were immersed in 3% H_2O_2 in a Glass Coplin jar (20 min, room temperature). Subsequently, the slides were rinsed with tap water and then transferred to TBST.

For IHC, 100 µl of the appropriate primary antibody dilution was applied as specified in Table 4. As a negative control, 100 µl of antibody diluent replaced the primary antibody. Following overnight incubation at 4°C of the primary antibody in a humidified slide chamber was performed. Then after TBST washing step, 120 µl of the polymer-one-step solution (Zytomed, Berlin, Germany) was applied and incubated for 30 min at room temperature. Next, slides were washed with TBST twice for 5 min and then 120 µl of DAB(diaminobenzidine)-high-contrast substrate (Zytomed, Berlin, Germany) was applied (8 min, room temperature). Then the slides were washed twice with TBST and counterstained with hematoxylin, rinsed under tap water, then transferred to distilled H_2O. Next, the sections were dehydrated in an ascending ethanol series: 1 x 70% ethanol, 1 x 96% ethanol, 2 x 100% ethanol, followed by 2 x xylene, for 3 min each. Slides were mounted with section adhesive Pertex and sealed with a coverslip (see detailed protocol in Appendix 7.1).

Table 4. Primary antibodies to human PLG, uPA, and PAI-1 proteins.

Antibody directed to	Antibody (Lot number)	Concentration of antibody stock solution	Company
Plasminogen	ab10178 (190569-1)	2 mg/ml	Abcam, Cambridge, United Kingdom
Urokinase-type plasminogen activator	#3689 (70830)	1 mg/ml	American Diagnostica (Sekisui), Stamford, CT, USA
Plasminogen activator inhibitor-1	#3786 (AK 1006/01.1)	0.42 mg/ml	American Diagnostica (Sekisui), Stamford, CT, USA

3.4.3 IHC protocol using the Ventana DISCOVERY® XT automated staining system

The Ventana DISCOVERY® XT automated staining system (Ventana Medical Systems, Tucson, Arizona) (Figure 4) is a fully automated slide processing system with a barcode-labeled slide recognition unit, standardized ready-to-use buffers, and automated workflow protocol (see Appendix 7.2). Heat-induced antigen retrieval was carried out using the cell conditioning solution (CC1, Ventana Medical Systems) in subsequent incubation steps at 93°C for 8 min, 100°C for 4 min, and, finally, room temperature for 40 min. Detection was performed using peroxidase-DAB-Map chemistry with automated stainer (Ventana DISCOVERY® XT, Ventana, Tucson, AZ, USA). The Ventana DISCOVERY® XT system can process a maximum of 30 slides for each staining cycle.

Figure 4. The Ventana DISCOVERY® XT system

(A) Ventana Medical System **(B)** DISCOVERY® XT software
(C) The slides rack.

3.4.4 Quantification of immunostaining

Three separate punch cores for each tumor tissue FFPE block were included in each TMA block. Stained TMAs and full-face tissue sections were scanned by the Hamamatsu Photonics NPD scanner (Hamamatsu, Japan) and staining intensities for PLG, uPA, and PAI-1 were scored. The following semi-quantitative scoring system for immunostaining assessment of tumor cells was used (Table 5).

Table 5. Immunoreactive score (IRS).

Immunoreactive scoring (IRS) system	
Score (IRS)	**Staining intensity**
0	None
1	Weak/moderate
2	Strong

Scoring of all of sections was performed independently by two pathologists under the Zeiss AxioSkop microscope (Carl Zeiss, Goettingen, Germany). Micrographs were captured with the Hamamatsu Nanozoomer XT virtual microscope at 40x magnification and visualized with NDP scan software (Version 2.2.60). Representative staining is shown in Figures 8-10.

3.5 Cell culture

3.5.1 Cultivation of ovarian cancer and liver cancer cells

OV-MZ-6 is a human epithelial ovarian cancer (EOC) cell line obtained from Prof. Dr. med. Volker Möbus, Frankfurt, Germany. This cell line was retrieved and cultivated from a 70-year-old female with serous adenocarcinoma of the ovary FIGO stage IV (Möbus et al., 1992). HepG2 is a human liver carcinoma cell line, derived from neoplastic liver tissue of a 15-year-old Caucasian male afflicted with a well-differentiated hepatocellular carcinoma. Both cell lines grow adherently in T75 plastic culture flasks (37°C, humidified chamber of 95% air/5% CO_2 (v/v)).

The OV-MZ-6 cells were cultured in dulbecco's modified eagle's medium (DMEM) supplemented with 10% fetal bovine serum (FBS), 1% 4-(2-hydroxyethyl)-1-piperazineethanesulfonic acid (HEPES) and 0.2% arginine/asparagine (ARG/ASN). The medium was changed every 3 days with cells passaged every 7 days (1:10). HepG2 cells were cultured in complete RPMI 1640 medium. Major components of the complete medium were 10% FBS, 1% HEPES, and 0.2 % ARG/ASN. Before culturing the HepG2 cells, flasks were pre-coated with 0.01% collagen I from rat tail 6-10 mg/cm^2 at 2-8°C overnight to minimize clumping and vacuole formation during cell growth. The culture medium was changed twice a week and cells were passaged every 3 days (1:5).

3.5.2 Thawing and freezing of cells

Before the thawing step, 100% FBS (3-4 ml) in a T75 flask was stored in the incubator overnight (37°C, humidified chamber of 95% air/5% CO_2 (v/v)). Cryovials containing deep-frozen cells, which were stored in the gas phase of liquid nitrogen, were cleaned

with 70% ethanol on the outside prior to opening. Pre-warmed complete growth medium (DMEM for OV-MZ-6 cells, RPMI 1640 for HepG2 cells) was added to cryovials containing still-frozen cells and immediately transferred to a centrifuge tube adjusted to 10 ml of medium. The cell suspension was centrifuged (320 × g, 5 min, room temperature) and the supernatant was discarded. Fresh medium was added and the centrifugation step repeated twice. Finally, the supernatant was carefully aspirated without disturbing the cell pellet. Then the cells were gently resuspended in 1.5 ml of the medium and transferred to the culture flask containing 6.5 ml of fresh medium.

For cryopreservation of cultivated cells, the freezing medium was prepared as follows. Cells were detached from the culture flask using 1% EDTA (OV-MZ-6 cells) or trypsin/EDTA 0.5%/0.2% (w/v) (HepG2 cells), and centrifuged (320 × g, 5 min). The supernatant was aspirated and the cells quickly resuspended in 10% DMSO/FBS (10^6 cells/ml) on ice. Aliquots (1.5 ml) of the cell suspension were transferred to cryogenic storage vials (Nalgene & Nunc, NY, USA) on ice. Cryovials were transferred to a controlled rate cryo-freezing container (Mr. Frosty, Nalgene & Nunc, NY, USA), decreasing the temperature approximately by 1°C/ min. The container was frozen at -80°C for up to 24 hours and cryovials were transferred to liquid nitrogen and stored in the gas phase at -196°C.

3.6 Real-time polymerase chain reaction (qPCR)

3.6.1 RNA isolation from frozen ovarian tumor tissue using TRIzol®

Frozen OC tumor tissues were pulverized on ice by use of dismembrator II. The still-frozen powder (30 to 100 mg) was homogenized in 1 ml of TRIzol® (TRI) reagent solution (Invitrogen, Carlsbad, CA, USA). The solution was vortexed and then thoroughly mixed by repetitive pipetting until the powder was homogenized. After incubation of the solution for 5 min at room temperature to allow for complete dissociation of the nucleoprotein complexes, 200 µl of chloroform (without isoamyl alcohol) per 1 ml of TRI Reagent® solution was added. Samples were mixed vigorously for 15 seconds and incubated for 10 min at room temperature followed by centrifugation (12,000 x g, 15 min, 4°C). Centrifugation separated the mixture into the upper colorless aqueous phase, the interphase, and the lower, red, phenol-chloroform phase. The aqueous phase was transferred to a 1.5 ml Eppendorf tube and RNA precipitated by mixing with 500 µl of isopropanol per 1 ml of TRI reagent solution® used for sample homogenization. After vortexing at moderate speed for 5-10 seconds, the samples were incubated (10 min, room temperature) and then centrifuged (12,000 x g, 8 min, 4°C). Precipitated RNA formed a white pellet at the bottom of the tube. The supernatant was

carefully removed without disturbing the pellet and the pelleted RNA was washed with 1 ml of 75% ethanol (37.5 ml of 96% ethanol plus 12.5 ml of nuclease-free water, 4°C). After centrifugation (12,000 x g, 5 min, 4°C), the wash solution was removed. The pellet was air-dried and dissolved in RNAase-free water by careful pipetting. The resuspension volume was determined by the size of the RNA pellet (use 5 to 30 µL of RNA storage solution).

3.6.2 RNA isolation from cell lines using QIAcube and Qiagen RNA isolation kits

The RNeasy® Mini kit (Qiagen, Hilden, Germany) was used for RNA extraction from OV-MZ-6 and HepG2 cells. Fully automated purification of RNA was achieved by use of the QIAcube system employing the QIAcube protocol "Purification of total RNA from animal tissues and cells including DNase digestion" with the RNeasy® mini Kit. For each cell line, 2 x 10^6 cells were harvested and lysed in 350 µl of RLT buffer supplemented with 1% β-mercapto-ethanol. Tissue lysates were centrifuged at full speed in a standard tabletop microcentrifuge (3 min, room temperature). Supernatants were transferred to 2 ml microcentrifuge tubes without disturbing the pellet. The supernatants were inserted into the sample rack of the QIAcube machine along with the RNeasy® mini spin columns and all the consumables according to the manufacturer's recommendations. Buffers were a mixture of DNase I incubation mix (e.g. 27 µl DNase mix in 186 µl buffer RDD for 2 samples), RW1 buffer, RPE buffer (11 ml concentrate plus 44 ml ethanol), 70% ethanol and RNase-free water. After running the QIAcube program, RNA was eluted into a 1.5 ml tube with 50 µl final elution volume.

All RNA extracted, either by TRIzol® reagent or the Qiacube system, was quantified by the Nanodrop ND1000 spectrophotometer (NanoDrop, Peqlab, Germany). Absorbance ratios at A260/280 nm and 260/230 nm were determined to quantify RNA concentration and purity. RNA samples were stored at -80°C until further use.

3.6.3 cDNA synthesis

Reverse transcription for samples with up to 1 µg of RNA was conducted using the cloned AMV first strand cDNA Synthesis Kit (Invitrogen, Darmstadt, Germany) according to the manufacturer's instructions. First, annealing of primers was performed using 1 µl random hexamer primers (50 ng/µl); 1 µg total RNA (the RNA volume depends on the RNA concentration) and 2 µl 10 mM dNTP was then adjusted with DEPC-treated H_2O to a total volume of 12 µl in a 200 µl PCR reaction tube. The reverse transcription absent of template control (RT0) is the control using RNase-free water instead of sample RNA in the reverse transcription.

The PCR reaction tubes were immediately transferred to a thermal cycler (10 min, 65°C), then transferred on ice to allow primer annealing to the RNA template. Master reaction mix for one reaction, containing 4 µl 5 x cDNA synthesis buffer, 1 µl DTT (0.1 M), 1 µl RNaseOUT (40 units/µl), 1 µl DEPC-treated water, 1 µl cloned AMV RT (15 units/µl), was prepared on ice and mixed gently before use. After retrieval of the reaction tube from the thermal cycler, 8 µl of the master reaction mix was pipetted into a reaction tube on ice. Then the reaction tubes were transferred to a thermal cycler with the following program applied: step 1: 10 min, 25°C; step 2: 50 min, 50°C; step 3: 5 min, 85°C.

For the RNA derived from frozen ovarian tissues, the resulting cDNA was diluted to 10 ng/µl with RNase-free water. For cell lines, the resulting cDNA (OV-MZ-6/HepG2) was diluted with RNase-free water to 5 ng/µl prepared for serial dilutions and calibrator (OV-MZ-6). All of the cDNA samples were stored at -80°C until further use.

3.6.4 qPCR using the Roche Universal Probe Library

The TaqMan® Probe-based chemistry was employed for the quantitative polymerase chain reaction (qPCR) method, which uses fluorogenic probes specifically targeted to the gene of interest, that accumulate proportionally with amplification, as displayed in Figure 5. The higher the initial copy number of the nucleic acid target, the sooner a fluorescence signal is observed (Bustin et al., 2009). Universal Probe Library (UPL) assays are compatible with all qPCR instruments capable of detecting fluorescein, FITC, FAM, and/or SYBR Green I, and follow standard cycling protocols for hydrolysis probe assays. The UPL probe offers extensive transcript coverage due to its short length of 8-9 nucleotides. While nucleic acids are incorporated into the sequence of each UPL probe to increase the annealing temperature of the probe, specificity and thermal stability are maintained (Universal Probe Library Technology, Roche Diagnostics).

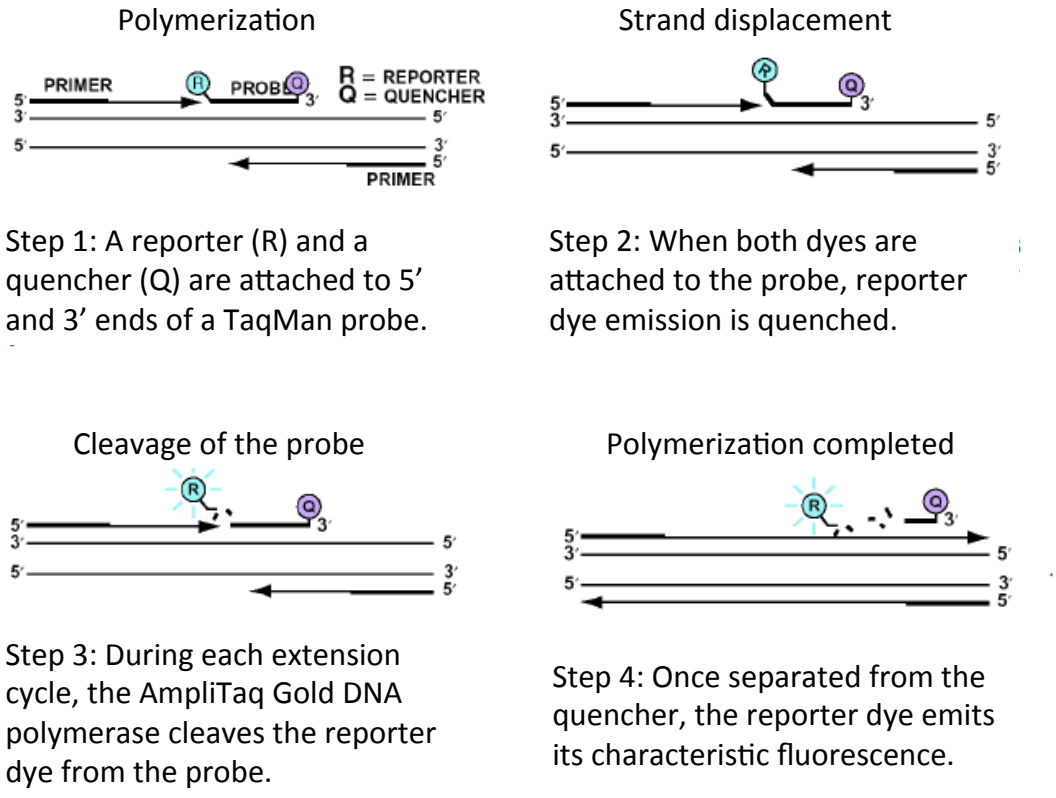

Figure 5. Process of TaqMan probe-based chemistry.

Representation of how the 5'-nuclease chemistry uses a fluorogenic probe to enable detection of a specific PCR product. Source: Real-Time PCR Systems Chemistry Guide (Applied Biosystems, US, 2005)

The gene-specific primers for *PLG*, *uPA*, *PAI-1*, and *HPRT1* were designed online with the UPL Assay Design Center (Roche probe library 2015; web link: https://life-science.roche.com/shop/products/universal-probelibrary-system-assay-design). Based on a study by de Kok et al. (2005), the housekeeping gene *HPRT1* was selected for normalization of the expression levels of the analyzed biomarkers. The following gene-specific primers (Metabion, Martinsried, Germany) and hydrolysis probes from UPL (Roche, Penzberg, Germany) were used in this study:

PLG (NM_000301): forward 5'-CAGGGGGCTTCACTGTTC-3' (197-214);
reverse 5'-TGTTGCTCTTTACTGTGATATTGGA-3' (303-327);
PLG-probe: 5'-FAM-GAGCAGGA-3'-dark quencher; amplicon size: 131 bp.

uPA (NM_002658): forward 5'-CTGACCCACAGTGGAAAACA-3' (1234-1253);
reverse 5'-TTGTCCTTCAGGGCACATC-3' (1342-1360);
uPA-probe: 5'-FAM- CTGGGGCC-3'-dark quencher; amplicon size: 127 bp.

PAI-1 (NM_000602): forward 5'-AAGGCACCTCTGAGAACTTCA-3' (126-146);

reverse 5'-CCCAGGACTAGGCAGGTG-3' (169-186);

PAI-1-probe: 5'-FAM-CTCCAGCC-3'-dark quencher; amplicon size: 61 bp.

HPRT1 (NM_000194): forward 5'-TGACCTTGATTTATTTTGCATACC-3' (218-241);

reverse 5'-CGAGCAAGACGTTCAGTCCT-3' (300-319);

HPRT1-probe: 5'-FAM-GCTGAGGA-3'-dark quencher; amplicon size: 102 bp.

The experimental reaction was prepared by combining the components described in Table 6. A single mastermix was prepared for triplicate experimental reactions, including the positive control and calibrator (OV-MZ-6 cells expressing the target genes; and RNA from OV-MZ-6 cells was used as the calibrator), and negative controls (amplification can indicate contamination of reagents) for triplicates. Negative controls are no-template control (water as substrate), reverse transcription absent of template control (RT0), genomic cDNA (OV-MZ-6 cells) and no-RT control (untranscribed RNA from cell line as substrate).

Table 6. qPCR Mastermix.

Materials provided	Quantity	Volume	Final concentration
Brilliant III Ulra-Fast Probe Low Rox QPCR Master Mix	2 x 2 ml	10 µl	1X
Primer forward	20 µM	0.4 µl	400 nM
Primer reverse	20 µM	0.4 µl	400 nM
UPL probe	10 µM	0.4 µl	200 nM
H_2O		5.8 µl	
Total amount		17 µl	

The solution was gently mixed to avoid bubbles and then distributed to a 96-well qPCR reaction plate (Biozym, Hamburg, Germany). Afterwards, 3 µl of cDNA (30 ng) was added to each reaction well. The plate was centrifuged (3,000 x g, 3 min) and then transferred to the Agilent Mx3005P instrument. The cycling program was performed using the MxPro software version 4.1. The instrument was programmed to detect and report fluorescence at each cycle during the 60°C annealing/extension step (Table 7).

Table 7. qPCR cycling program.

Segment	Number of cycles	Temperature	Duration of time
1	1	95°C (Polymerase activation)	3 min
2	40	95°C (Denaturation) 60°C (Extension)	15 sec 1 min

3.6.5 Standard dilution series for assay establishment

Due to variation in RNA concentration and quality, standardization of the various steps of RNA extraction and of the qPCR method was crucial. There are several ways to estimate qPCR efficiency. An established method is based on serial dilutions. The resulting amplification rate is calculated based on a linear regression slope of a dilution row. Efficiency (E) can be determined based on the equation "E = 10 [–1/slope]" (Higuchi et al., 1993; Rasmussen, 2001). The efficiency usually varies in the range of E = 1.60 to 2. Typically, the relationship between delta Ct and the logarithm of the cDNA input of the target sequence should remain linear for up to five RNA orders of magnitude by log10 in the calibration curve.

For this method, the liver cancer cell line HepG2 was used for the *PLG* cDNA dilution series; the OC cell line OV-MZ-6 was used for the *uPA* and *PAI-1* cDNA dilution series. The input volume for cDNA was 3 µl. Two-fold serial dilutions were performed with five dilution steps (D0: 5ng; D1: 2.5ng; D2: 1.25ng; D3: 0.625ng; D4: 0.3125).

For *PLG*, two cDNA dilution series were prepared; each dilution series was analyzed twice. Since HepG2 cells strongly express *PLG* (Malgaretti et al., 1990), it was employed as test samples for standard dilution series. OV-MZ-6 cells were used for standard dilution series of *uPA/PAI-1.* For *uPA*, one dilution series was prepared, which was analyzed twice. For *PAI-1*, three dilution series were prepared; each dilution series was analyzed twice. Later, it has been found the *PLG* gene expression in OV-MZ-6 cells as well. Thus, the OV-MZ-6 cells were chosen as a positive control and calibrator for all of the 3 genes.

3.6.6 Final qPCR evaluation method

Quantitative mRNA expression analysis for *PLG*, *uPA,* and *PAI-1*, was performed using the comparative threshold cycle ($2^{-\Delta\Delta Ct}$) method. Ct values of target genes were normalized to respective Ct values of the endogenous control gene *HPRT1* [ΔCt = Ct (*target gene*) – Ct (*HPRT1*)] with subsequent normalization to cell line OV-MZ-6-derived template cDNA as the calibrator [ΔΔCt = ΔCt (tumor sample) – ΔCt (calibrator)].

All kinds of measurement are associated with an intrinsic error. Therefore, random errors in observable quantities are estimated by computing the error propagation. In statistics, error propagation is the effect of the variables' uncertainties (or errors) on the uncertainty of a function based on them. When the variables are the values of experimental measurements, they have uncertainties due to measurement limitations, which propagate to the combination of variables in the function. Relative error propagation (EP) was calculated for each step by the following formula:

EP (DCt) = SQRRoot (((STDEV$_{target\ gene}$)^2 +(STDEV $_{HPRT1}$)^2)/2);

EP (DDCt) = SQRRoot (((STDEV Ct $_{tumor\ sample}$)^2 +(STDEV Ct $_{calibrator}$)^2)/2).

Absolute error propagation was calculated by the following formula: ln2*EP (ΔΔCt)*2$^{-\Delta\Delta Ct}$ (sample) (STDEV: standard deviation; SQRRoot: square root; ln for natural logarithm).

If this absolute error propagation value is >30%, the value has too much variability and the result for this sample should be disregarded (Nordgard et al., 2006). The layout of the experiment is that all samples are analyzed in triplicates, including the negative controls. Samples were excluded with an error propagation >30%, and/or a Ct value of *HPRT* >35.

3.7 Statistical analyses

Association of IHC expression (IRS) of PLG, PAI-1 (cohort 1), and uPA (cohort 2) with clinical and histomorphological parameters was evaluated by the Chi-square test. Outcome variables were progression-free survival (PFS) and overall survival (OS). PFS was defined by the time between the date of the first diagnosis and the date of the diagnosis of disease recurrence. Overall survival is defined by time between the date of the first diagnosis and the date of patient death. Evidence of tumor mass is defined as macroscopic tumor-free (absent) or macroscopically visible residual tumor mass (>0 mm). Other clinical factors are ascitic fluid volume (≤500 vs. >500 ml), age (≤60 vs. >60 years), CA125 (dichotomized by the median value). The relation of IRS for PLG, uPA, and PAI-1 with OS and PFS as well as that of the clinical/histomorphological factors with PFS and OS was calculated by univariate and multivariate Cox regression analysis and expressed as the hazard ratio (HR), plus its 95% confidence interval (CI). Survival curves were plotted according to Kaplan-Meier (Kaplan and Meier, 1958); and a weighted log-rank test is proposed for comparing group differences of survival functions.

The non-parametric Mann-Whitney U test was applied for analysis of the relation of IRS with mRNA/antigen expression. Correlations between continuous variables were calculated by Spearman rank correlation (r_s). Box plots were drawn to indicate differences.

All calculations were performed by use of the IBM SPSS statistical package, released 2013 (IBM Corp., Armonk, NY, USA, version 22.0). P-values ≤0.05 were considered statistically significant.

4. Results

4.1 Immunohistochemistry and qPCR assay establishment for PLG, uPA, and PAI-1 expression

4.1.1 Immunohistochemical assay establishment

Optimization of staining protocols plays a pivotal role in immunohistochemical technique establishment. For the present study, all of the antibodies applied were assessed by manual and automatic staining protocols. Anti-PLG and anti-PAI-1 were employed for staining of tissue microarrays of ovarian cancer (OC) tissues (n=103; cohort 1). Anti-uPA was employed for staining of full-face sections of OC tissue samples (n=50; cohort 2). The process to establish the various protocols is shown in Figure 6. Automatic staining of anti-uPA was not applicable for OC tissues. Therefore, its workflow was optimized for a manual staining protocol. For anti-PLG and anti-PAI-1, manual staining protocol was not efficient, while the automated staining protocol greatly improved staining.

Initially, the staining procedure for anti-uPA and anti-PAI-1 expression was associated with profound background artefacts (Figure 7). In order to remove aggregates that would result in false-positive signals, anti-uPA was filtered and anti-PAI-1 was centrifuged (Note: anti-PAI-1 should not be filtered, due to an otherwise heavy loss of antibody during subsequent filtration). Different dilutions of anti-uPA (1:200, 1:400, and 1:600) were applied for testing. Centrifuged anti-PAI-1 was diluted to 1:100, 1:50, and 1:25 with the Zytomed antibody diluent. Anti-PLG was diluted to 1:70, 1:100, and 1:150 with antibody diluent.

In the end, the IHC protocol for anti-PLG and anti-PAI-1 was established on the automatic Ventana platform with a dilution of 1:100 (20 µg/ml) and 1:25 (16.8 µg/ml) respectively; and anti-uPA staining was optimized by applying the polymer-based EnVision™ system manual protocol with a dilution of 1:400 (12.5 ng/ml) post-filtration (pre-dilution 1:200) For the protocols and antibody information see Appendix 7.1-7.3.

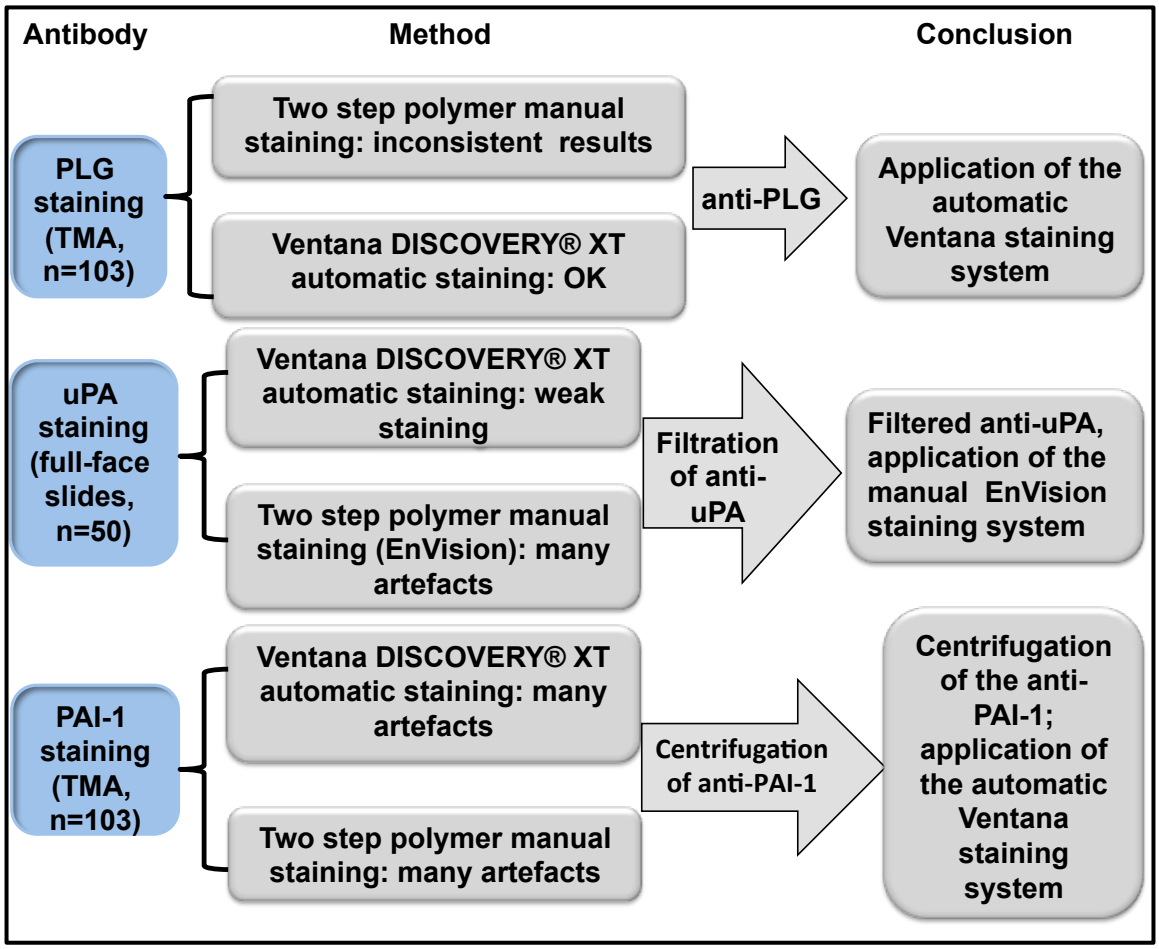

Figure 6. **Optimization of immunohistochemical staining protocols for antibodies to PLG, uPA, and PAI-1.**

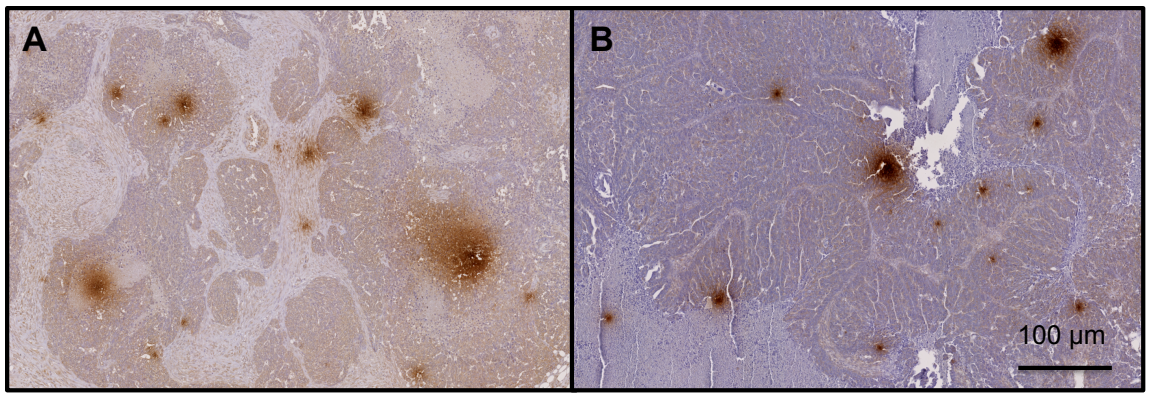

Figure 7. **uPA and PAI-1 immunoexpression in ovarian cancer tissues: demonstration of initial artefacts.**

Test tumor tissue samples were manually stained using the polymer-based EnVision™ system (Dako). Intensive brown spots staining were observed for both uPA and PAI-1 expression. **(A)** anti-uPA (0.66 µg/ml). **(B)** anti-PAI-1 (1.05 µg/ml). Micrographs were captured with the Hamamatsu Nanozoomer XT virtual microscope and visualized with the NDP.scan software (Version 2.2.60).

4.1.2 qPCR assay establishment

To validate sensitivity and efficiency of qPCR assays for the target genes *PLG, uPA,* and *PAI-1*, the amplification rate was calculated based on a linear regression slope of serial dilution series. The qPCR efficiency was calculated to assess differences in efficiency of the respective target genes against the housekeeping gene *HPRT*. Efficiency (E) describes the amplification rate for each cycle, which can be determined by the dilution series method. The efficiency of the assays should be 95-100%, with a value of E ranging from 1.6 to 2. (Ruijter et al., 2013).

A 2-fold serial dilution curve for *PLG* and the reference gene *HPRT* was performed with the cDNA of a positive control (HepG2 cells). Ct values were plotted against the logarithm of cDNA input (60-3.75 ng, log input 1.778-0.574) in two independent experiments with two repetitions of each dilution series. Slopes of the lines were parallel between the target genes *PLG* and *HPRT*. Average efficiency values of *PLG* and *HPRT* of four dilution series were 2.10 and 2.17 respectively. Thus, efficiencies were comparable and efficiency correction was not required for normalization in subsequent cancer sample analyses. Linear regression coefficients were with R^2 = 0.995 (*PLG*) and R^2 = 0.997 (*HPRT*), demonstrating concordance of dilution steps over the applied DNA input range. Similarly, OV-MZ-6 cells were used for establishing standard dilution curves for *uPA/PAI-1*. Although *PLG* is strongly expressed in HepG2 cells, we found it is expressed in OV-MZ-6 cells too. Therefore, OV-MZ-6 cells, not HepG2 cells, were used as the calibrator and positive controls for *PLG, uPA,* and *PAI-1*, which were employed in the subsequent cancer sample analyses.

The dilution curve for *PLG* was representative for all assays (Figure 8). Since the last dilution of the sample in the first dilution row had a very high Ct value (>35), the dilution series was repeated. Standard deviation (SD) of $2exp^{(-\Delta CT)}$ of D0 (first dilution) is 0.013, which is <20%. Similarly, all SDs of $2exp^{(-\Delta CT)}$ of *PLG* of D1-D4 were <20% (Figure 9). SDs of Efficiency values of *PLG* (E1 = 2.16, E2 = 2.14; E3 = 1.94, E4 = 2.08) and *HPRT* (E1 = 2.40, E2 = 2.10; E3 = 2.0, E4 = 2.18), and all SDs of $2exp^{(-\Delta CT)}$ of *HPRT* of D1-D4 were also <20%.

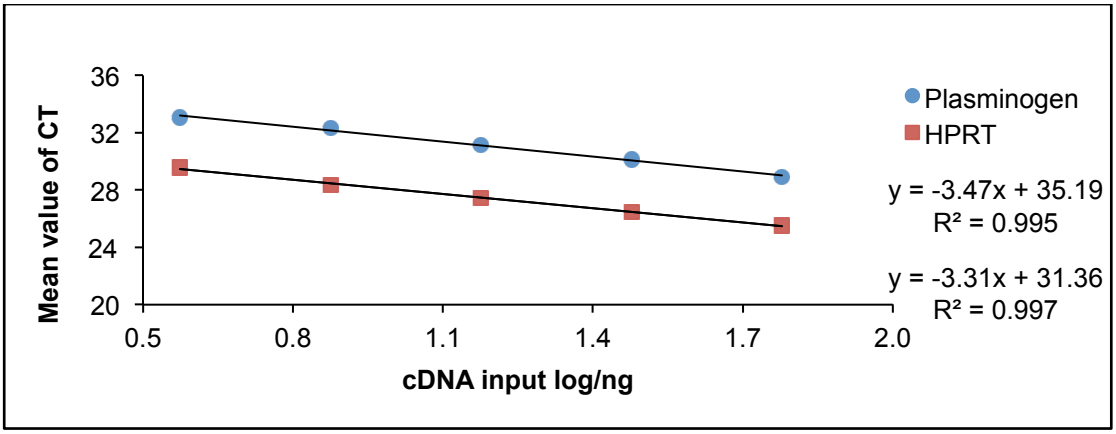

Figure 8. Exemplary dilution series for *PLG* cDNA and *HPRT* cDNA by qPCR.

Reference gene is *HPRT*. Total RNA was extracted from the liver cell line HepG2 and reverse transcribed (cDNA input range: 3.75-60 ng). *PLG*: slope = -3.31, E = 2.00; *HPRT:* slope = -3.47, E = 1.94.

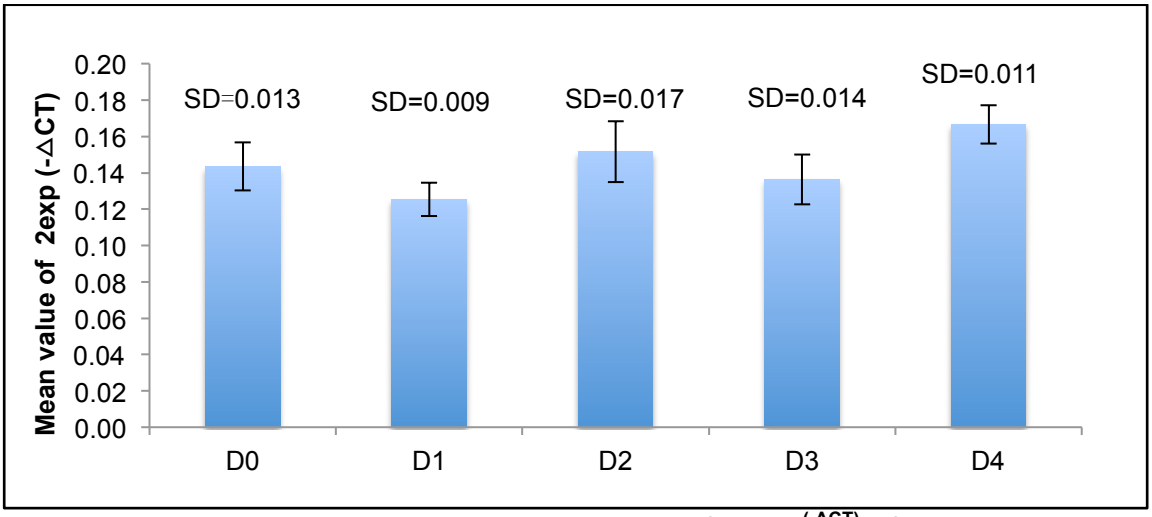

Figure 9. Mean values and standard deviations of 2exp $^{(-\Delta CT)}$ of individually diluted samples representing four independent *PLG* qPCR experiments, normalization against *HPRT* cDNA.

Overview of four separate qPCR experiments representing five dilutions for the *PLG* qPCR assay. 1:2 fold dilution, from the first dilution (D0) to the fifth dilution (D4) are displayed (cDNA from HepG2; cDNA input range: 3.75-60 ng).

For the *uPA* cDNA qPCR assay, only one dilution series was performed with two independent runs. The linear regression curve was parallel for the target gene *uPA* and the reference gene *HPRT*. The amplification efficiency was consistent for comparable samples (Appendix 7.4, Figure A). The SDs of 2exp$^{(-\Delta CT)}$ of two qPCR experiments were <20% (Appendix 7.4, Figure B).

Three dilution series for *PAI-1* have been applied, and each one with two repetition runs (for a representation, see Appendix 7.4, Figure C). Two separate dilution series with two analyses each were performed, resulting in different Efficiency values of *PAI-1* (E1 = 1.79, E2 = 1.86; E3 = 2.05, E4 = 2.04) and *HPRT* (E1 = 1.98, E2 = 1.96; E3 = 1.96, E4 = 1.95). To validate the assay, a third dilution series was performed. Although

the Efficiency value of *PAI-1* from the third dilution series replicate experiments was not the same (*PAI-1*: E5 = 2.00, E6 = 1.87; *HPRT*: E5 = 1.97, E6 = 1.93), all SDs of $2exp^{(-\Delta CT)}$ of D0-D4 were <20% (Appendix 7.4, Figure D), therefore, <20% intra-assay-variation was achieved.

Fifty fresh-frozen OC tissue samples were available for RNA extraction, subsequent cDNA synthesis, and qPCR analysis. All samples were analyzed by qPCR for *PLG, uPA, PAI-1,* and *HPRT expression* including triplicate measurements for each sample. A second qPCR experiment included repetitions of samples of the first experiment, which showed insufficient for qPCR quality checks (see chapter 3.6 in Material and Methods: >30% error propagation, and/or mean value (MV) of Ct of *HPRT* >35) and additional independent repetitions of samples for inter-assay-variation analysis. In total, 24 samples were measured for *PLG, uPA,* and *PAI-1*. After two experiments, samples with an error propagation >30% for both repetitions, and/or MV of Ct of HPRT >35 were excluded from data analysis.

MVs and SDs of $2^{-\Delta\Delta CT}$ of 24 samples analyzed in two separate runs for all three markers. A quality control cut-off was defined: if more than 100% difference between absolute $2exp^{(-\Delta\Delta CT)}$ values in two separate qPCR runs (%SD is 47.1%) was observed, samples were disregarded. The analysis of *PLG* expression showed that 10 samples out of 11 repeated samples had a %SD <47.1%. Identically, the analysis of *uPA* expression also exhibited 10 samples out of 10 repeated samples with %SD <47.1% (Figure 11). However, for target gene *PAI-1*, only 6 out of 15 samples had a %SD <47.1%. Therefore, a cut-off ($2exp^{(-\Delta\Delta CT)} = 0.6$) was set to distinguish high from low *PAI-1* mRNA expression in a dichotomized manner (Figure 12).

After qPCR assessment, only samples from patients who underwent initial stage-related primary radical debulking surgery followed by adjuvant treatment according to current standards of treatment were selected for further evaluation. Samples from patients who received neoadjuvant therapy before primary surgery were also excluded. Therefore, a total of 29 samples for *PLG* and *uPA*, and 28 samples for *PAI-1* were included in the final statistical analysis.

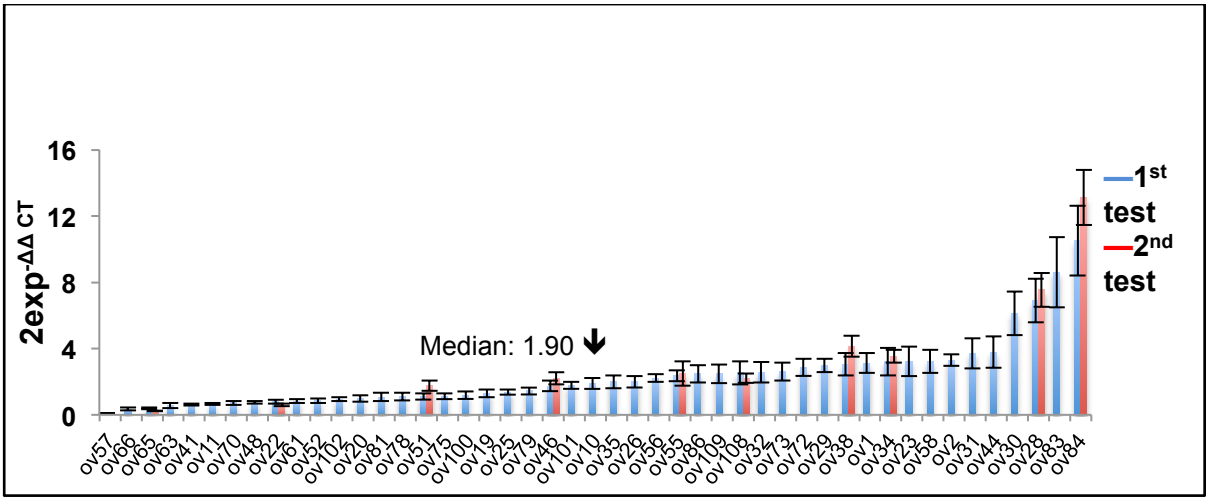

Figure 10. Overview of the qPCR analysis of *PLG* mRNA expression.

PLG mRNA expression in ovarian cancer tissues. Housekeeping gene *HPRT* and calibrator (OV-MZ-6 cells) were used for normalization. Samples of the first experiment (n=47) and the second experiment (n=11) are displayed. OV: sample names of ovarian cancer tissues. The median is positioned at ov10 with a value of $2^{-\Delta\Delta CT}$ = 1.90.

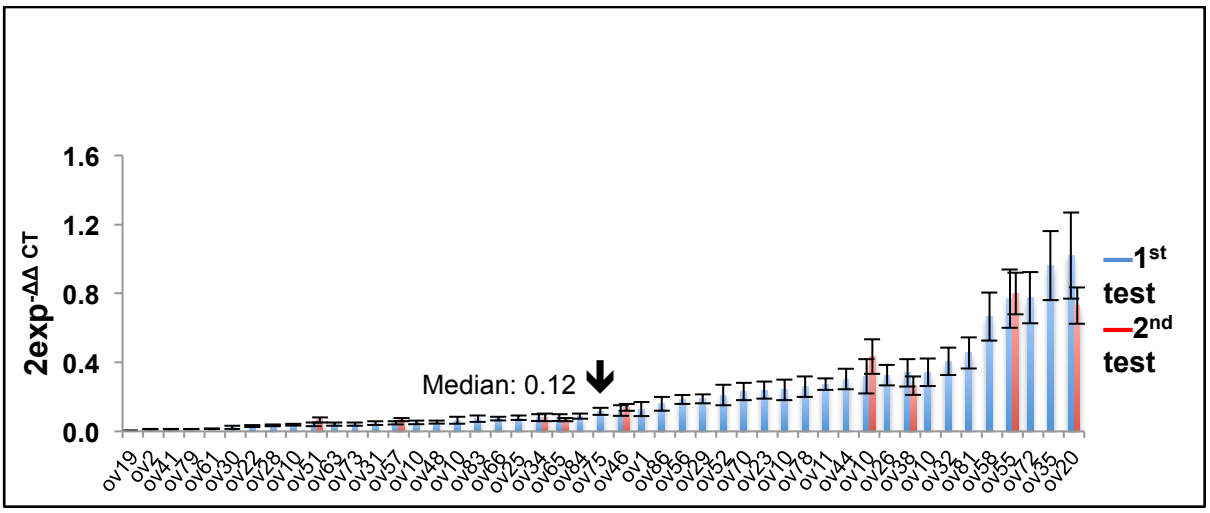

Figure 11. Overview of the qPCR analysis of *uPA* mRNA expression.

uPA mRNA expression in ovarian cancer tissues. Housekeeping gene *HPRT* and calibrator (OV-MZ-6 cells) were used for normalization. Samples of the first experiment (n=47) and the second experiment (n=10) are displayed. OV: sample names of ovarian cancer tissues. The median is positioned at ov75 with a value of $2^{-\Delta\Delta CT}$ = 0.12.

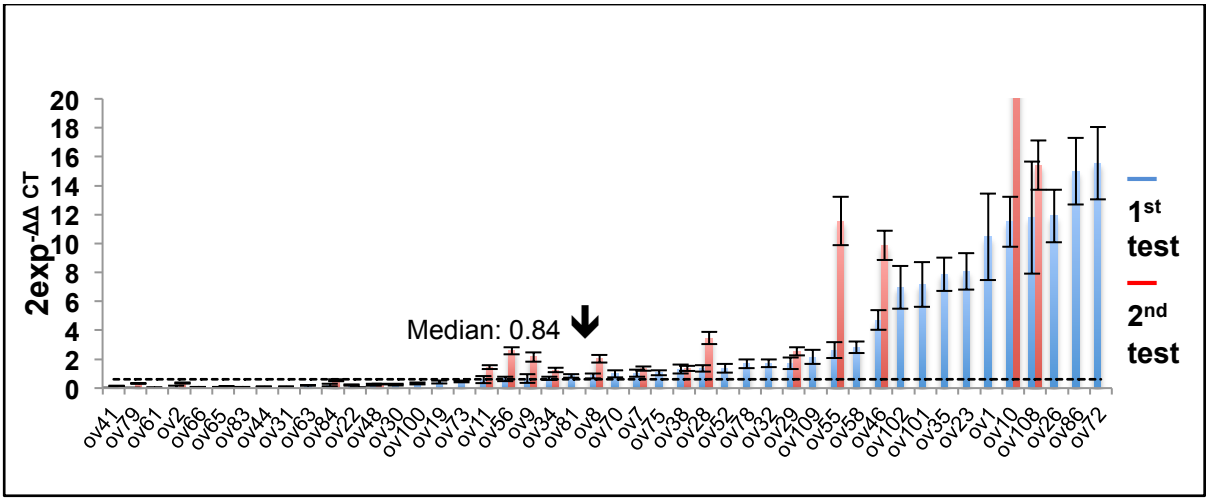

Figure 12. Overview of the qPCR analysis of *PAI-1* mRNA expression.

PAI-1 mRNA expression in ovarian cancer tissues. Housekeeping gene *HPRT* and calibrator (OV-MZ-6 cells) were used for normalization. Samples of the first experiment (n=47) and the second experiment (n=15) are displayed. The cut-off value is marked as a dashed line ($2^{-\Delta\Delta CT}$ = 0.6); the median is positioned at ov8 with a value of $2^{-\Delta\Delta CT}$ = 0.84. OV: sample names of ovarian cancer tissues.

4.2 Protein expression of uPA and PAI-1 determined by ELISA

Antigen expression levels of uPA and PAI-1 in OC tissue extracts were available from previous measurements by colleagues of the Department of Obstetrics and Gynecology, Klinikum rechts der Isar, TUM, Germany, who assessed 45 samples of the 50 contained in cohort 2. For Cohort 1, insufficient data were available. uPA antigen values ranged from 0.00 to 7.60 ng/mg protein, the median value was 0.78 ng/mg protein. PAI-1 antigen values ranged from 0.00 to 247.50 ng/mg protein, the median value was 11.65 ng/mg protein. Cut-off values for uPA (0.90 ng/mg protein) and PAI-1 (13.50 ng/mg protein) were chosen to subdivide patients into low and high expression uPA/PAI-1 groups according to a previous study by Kuhn et al. (1994).

4.3 Immunohistochemical assessment of PLG, uPA, and PAI-1 protein expression in ovarian tumor tissues

A semi-quantitative scoring system, whereby a score of '0' indicated 'No expression', '1' – 'Moderate expression', and '2' – 'High expression', was utilized for estimation of PLG, PAI-1 (cohort 1), and uPA (cohort 2) immunoreactivity in tumor cells of advanced (FIGO III/IV) high-grade serous OC patients. High expression was present in 5/103 (4.9%) specimens only. Most tissues demonstrated moderate staining in 65/103 (63.1%), while no expression was observed in 33/103 (32.0%) of specimens (Figure 13). uPA staining was distributed evenly over the tumor tissue. High expression of uPA was detected in 16/50 (32%) of cases, while moderate expression was observed in 21/50 (42%). No

expression was detected in 13/50 (26%) of cases. Figure 14 presents the representative images of stained tissues for various levels of PAI-1 staining in tumor cells. PAI-1 expression was high in 20/103 (19.4%) and moderate in 42/103 (40.8%) of the cases. No staining was detected in 41/103 (39.8%) of the cases. Figure 15 shows the representative image of stained tissues for different levels of PAI-1 staining in tumor cells. PAI-1 expression in OC tissues displayed a similar pattern compared to a previous study that showed high-density staining of OC cells (Ren et al., 2013).

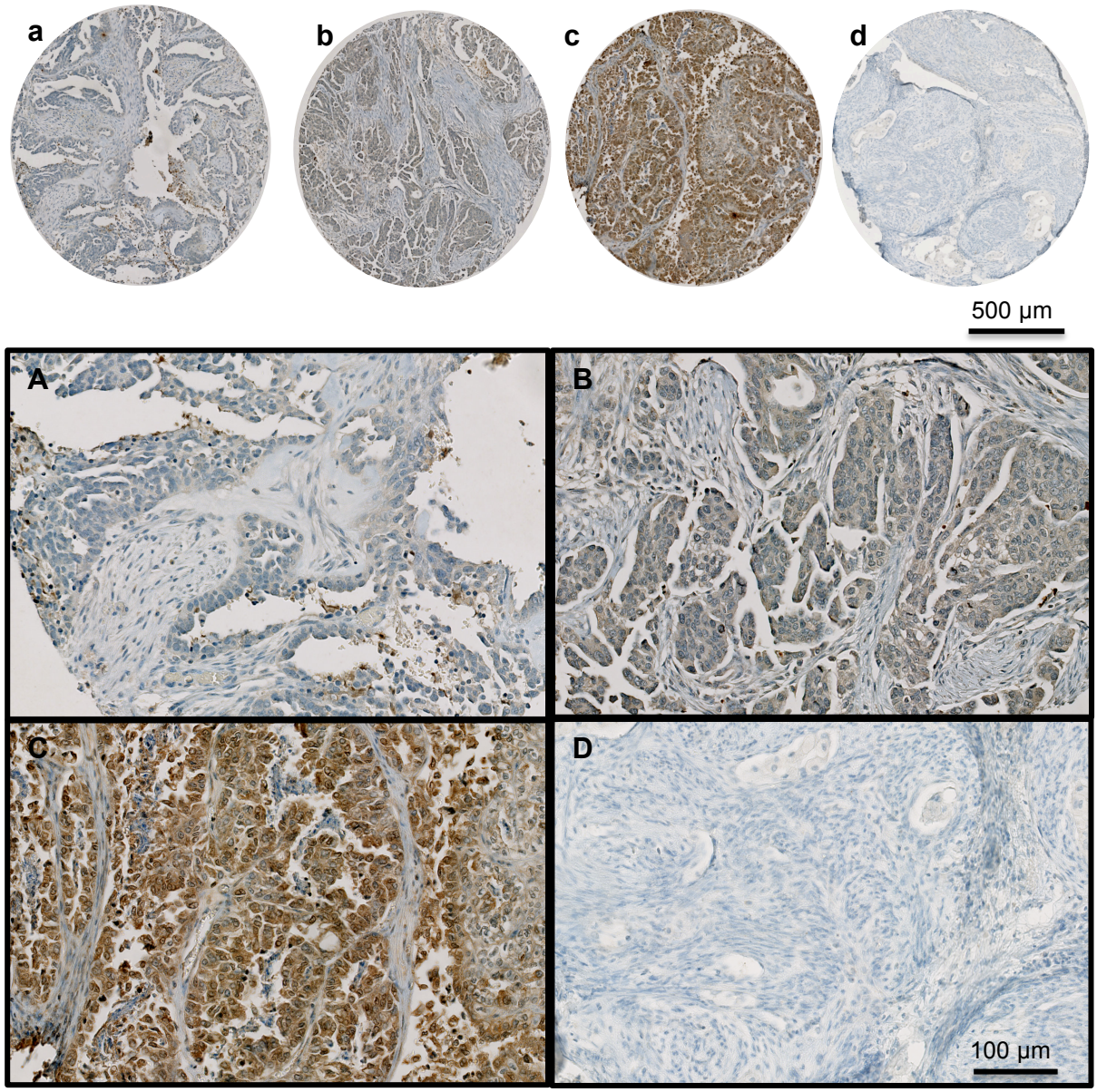

Figure 13. Immunohistochemical visualization of PLG protein expression in ovarian tumor tissue specimens.

Tissue microarrays were prepared from serous ovarian cancer tissue FFPE specimens and the plasmin(ogen) (PLG) protein expression in tumor cells visualized by reaction of tissue sections with antibody ab10178 (20 µg/ml) (brown) employing the Ventana Medical System. Sections were counterstained with hematoxylin (blue). Representative stained tumor tissue core drills with adjacent selected areas at higher magnification. **(A, a)** Immunoreactive score (IRS): 0 (no expression, n=33); **(B, b)** IRS: 1 (moderate expression; n=65); **(C, c)** IRS: 2 (high expression, n=5); **(D, d)** Negative control (Zytomed antibody diluent was applied without primary antibody). Micrographs were captured with the Hamamatsu Nanozoomer XT virtual microscope and processed with the NDP scan software (version 2.2.60).

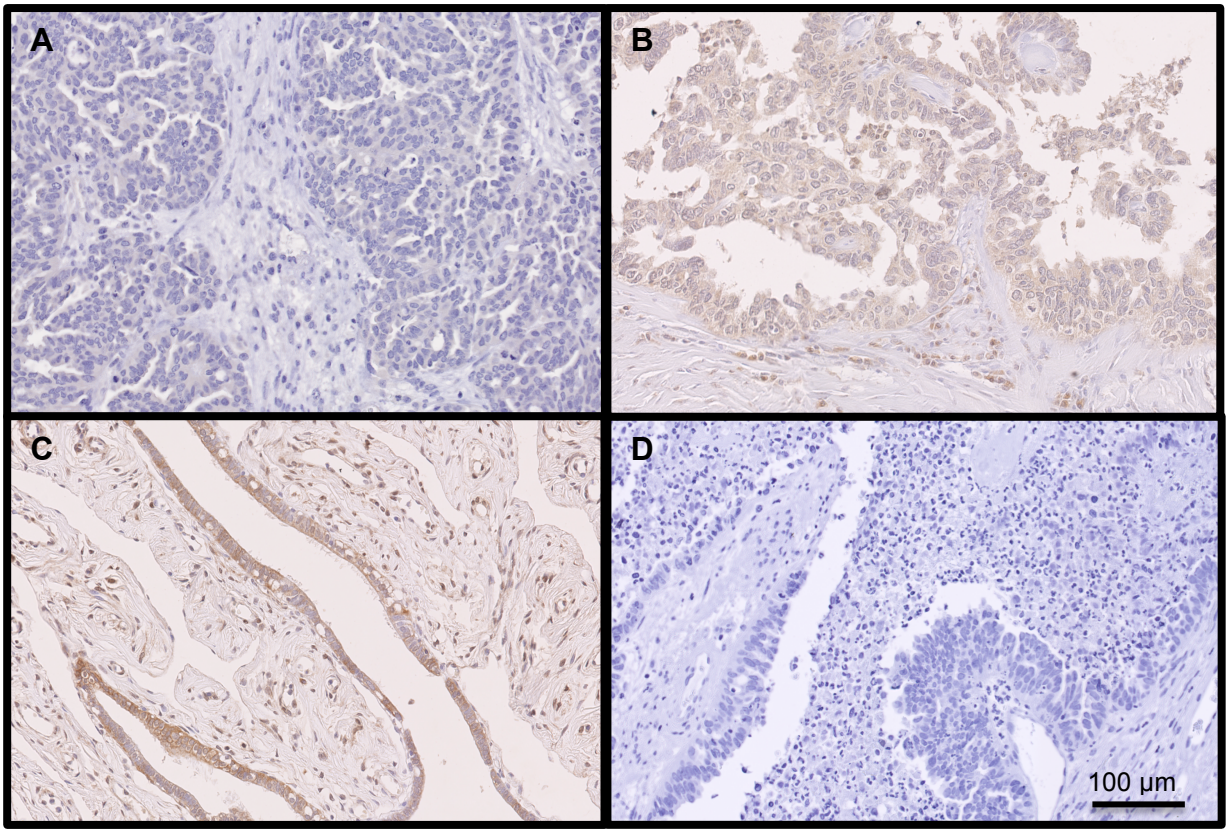

Figure 14. Immunohistochemical visualization of uPA protein expression in ovarian tumor tissue specimens.

Full-face sections were prepared from serous ovarian cancer tissue FFPE specimens and the urokinase-type plasminogen activator (uPA) protein expression in tumor cells visualized by reaction of tissue sections with anti-uPA (12.5 ng/ml) (brown) employing the DAKO Envision System. Sections were counterstained with hematoxylin (blue). **(A)** Immunoreactive score (IRS): 0 (no expression, n=13); **(B)** IRS: 1 (moderate expression; n=21); **(C)** IRS: 2 (high expression, n=16); **(D)** Negative control (Zytomed antibody diluent was applied without primary antibody). Micrographs were captured with the Hamamatsu Nanozoomer XT virtual microscope and processed with the NDP scan software (version 2.2.60).

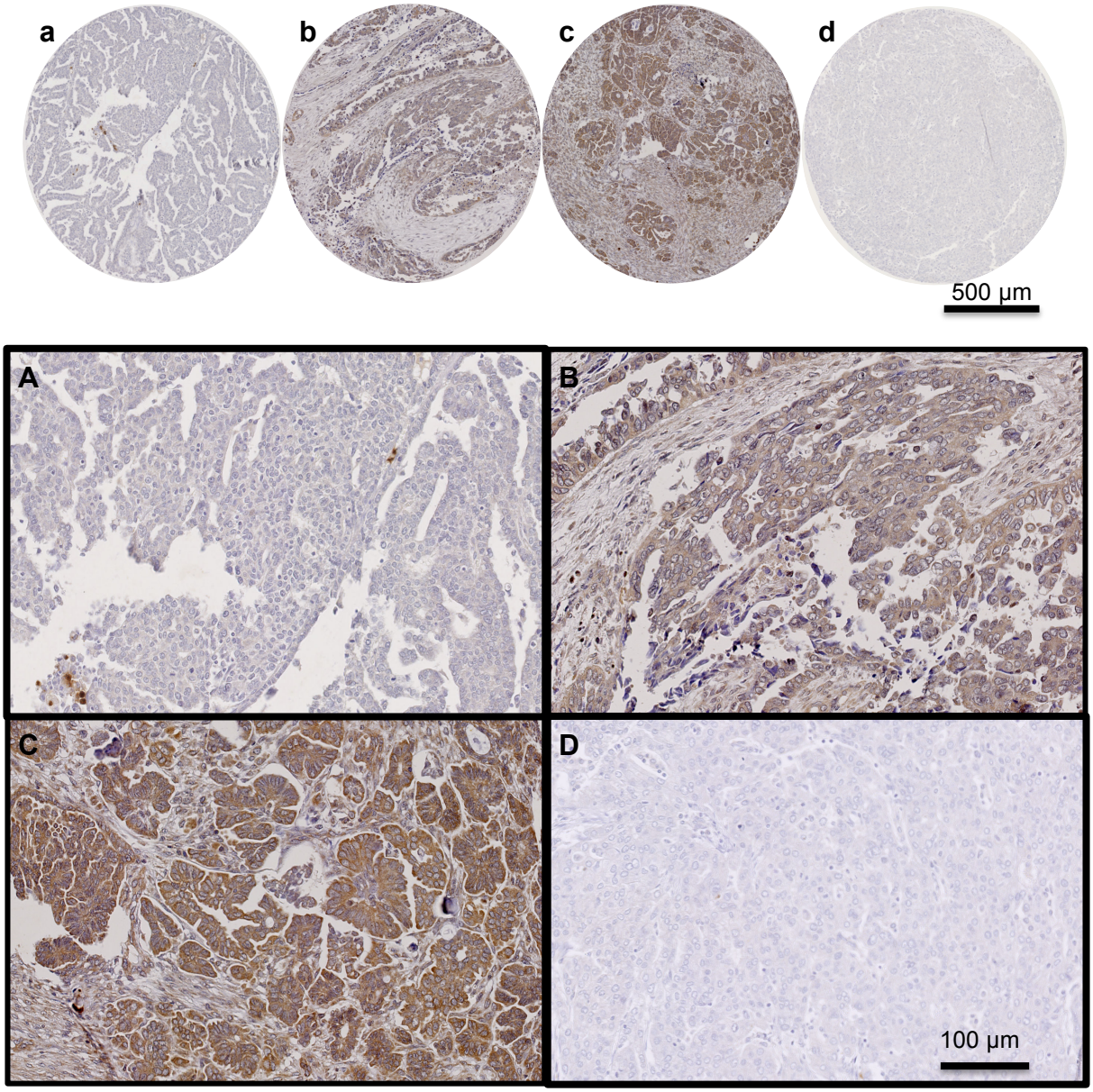

Figure 15. Immunohistochemical visualization of PAI-1 protein expression in ovarian tumor tissue specimens.

Tissue microarrays were prepared from serous ovarian cancer tissue FFPE specimens and the plasminogen-activator inhibitor type-1 (PAI-1) protein expression in tumor cells visualized by reaction of tissue sections with anti-PAI-1 (16.8 µg/ml) (brown) employing the Ventana Medical System. Sections were counterstained with hematoxylin (blue). Representative stained tumor tissue core drills with adjacent selected areas at higher magnification. **(A, a)** Immunoreactive score (IRS): 0 (no expression, n=41); **(B, b)** IRS: 1 (moderate expression; n=42); **(C, c)** IRS: 2 (high expression, n=20); **(D, d)** Negative control (Zytomed antibody diluent was applied without primary antibody). Micrographs were captured with the Hamamatsu Nanozoomer XT virtual microscope and processed with the NDP scan software (version 2.2.60).

4.4 Association of PLG and PAI-1 protein expression levels (Cohort 1) with clinical and histomorphological parameters

4.4.1 Association of PLG and PAI-1 immunoexpression with clinical parameters of ovarian cancer patients

Immunohistochemical expression of PLG and PAI-1 from cohort 1 was analyzed for potential associations with clinical parameters (Table 8). Immunoexpression of IRS = 1 and IRS = 2 was defined as positive expression, IRS = 0 as negative expression. There was no significant association observed for PLG and PAI-1 protein expression with any selected clinical parameters. On the other hand, PLG immunoexpression was significantly correlated with PAI-1 immunoexpression (*p = 0.036*, Table 9).

Table 8. Correlation of clinical characteristics with PLG and PAI-1 IRS in ovarian cancer tumor tissues (n=103).

Factor	No [a]	PLG IHC [b] negative/positive	PAI-1 IHC [b] negative/positive
Total	103	33/70	41/62
Age	103	*p* = 0.14	*p* = 0.91
≤60 years	42	10/32	17/25
>60 years	61	23/38	24/37
Residual tumor mass	103	*p* = 0.78	*p* = 0.36
0 mm	30	9/21	14/16
>0 mm	73	24/49	27/46
Ascitic fluid volume	89	*p* = 0.88	*p* = 0.98
≤500 ml	36	11/25	13/23
>500 ml	53	17/36	19/34
CA125 [c]	71	*p* = 0.86	*p* = 0.40
≤699 U/ml	36	12/24	10/26
>699 U/ml	35	11/24	13/22

[a] Number of patients
[b] Chi-square test
[c] Dichotomized into high and low levels by the median value (699 U/ml)

Table 9. Correlation of PLG with PAI-1 immunoexpression in ovarian cancer tissues (n=103).

Count	No [a]	PLG [b] negative/positive	P-value
PAI-1 [b]	103	33/70	
Negative	41	18/23	**0.036**
Positive	62	15/47	

[a] Number of patients
[b] Chi-square test

4.4.2 Association of PLG and PAI-1 immunoexpression and clinical parameters with ovarian cancer patients' progression-free survival (PFS) and overall survival (OS)

Association between clinical factors, PLG and PAI-1 immunoexpression, and patient survival (PFS, OS) were analyzed by univariate and multivariate Cox regression analysis (Table 10-11). For univariate Cox regression analysis (Table 10), age, residual tumor mass, and ascitic fluid volume were predictive factors for both PFS and OS. OC patients >60 years old experienced a higher risk of early death (HR, 1.64; 95% CI, 1.03-2.61; $p = 0.037$), and tumor progression (HR, 2.01; 95% CI, 0.82-2.35; $p = 0.005$). Patients with residual tumor mass (>0 mm) had an increased risk of death compared to tumor-free patients (HR, 3.27; 95% CI, 1.87-5.72; $p < 0.001$); and increased risk of tumor progression (HR, 3.31; 95% CI, 1.89-5.78; $p < 0.001$). Likewise, a greater volume of ascitic fluid (>500 ml) increased the risk of death (HR, 2.33; 95% CI, 1.38-3.92; $p = 0.001$) and that of disease progression (HR, 2.27; 95% CI, 1.27-4.05; $p < 0.001$). These results are displayed by Kaplan-Meier survival curves (Figure 16). Although no association was found between PLG immunoexpression and PFS, it was striking to find that positive PLG immunoexpression was significantly linked with longer OS (HR, 0.59; 95% CI, 0.37-0.94; $p = 0.026$). (see also Kaplan-Meier curves in Figure 17). Both pre-operative CA125 serum levels (figures not shown here) and PAI-1 immunoexpression were not significant indications for PFS and OS (Figure 18).

Using multivariate Cox regression analysis (Table 11), only one clinical factor, residual tumor mass showed the significant prediction for OS (HR, 2.17; 95% CI, 1.03-4.57; $p = 0.041$). Apart from that, ascitic fluid volume was the only clinical variable with significant impact for PFS (≤500 ml vs. >500 ml) (HR, 1.91; 95% CI, 0.92-3.94; $p = 0.08$). The relationship between PLG and PAI-1 and PFS/OS was examined according to the base model of analysis, including age, ascites fluid volume, and presence of residual tumor mass. Pre-operative CA125 serum was not included in the analysis because it was not statistically significant in univariate Cox analysis. PLG immunoexpression was statistically significant for OS (HR, 0.45; 95% CI, 0.25-0.82; $p = 0.009$) but not for PFS. PAI-1 immunoexpression showed no remarkable significance regarding PFS and OS.

Table 10. **Univariate Cox regression analysis (PFS and OS) with respect to clinical parameters and PLG or PAI-1 protein expression (IHC) in tumor tissues of advanced high-grade serous ovarian cancer patients (FIGO III/IV) with the treatment of adjuvant chemotherapy (n=103).**

Factor	No [a]	Progression-free survival		No [a]	Overall survival	
		HR (95% CI) [b]	*p*		HR (95% CI) [b]	*p*
Total	103			103		
Age	89			98		
≤60 years	37	**1**		40	**1**	
>60 years	52	**2.01 (0.82-2.35)**	**0.005**	58	**1.64 (1.03-2.61)**	**0.037**
Residual tumor mass	89			98		
0 mm	28	**1**		29	**1**	
>0 mm	61	**3.31 (1.89-5.78)**	**<0.001**	69	**3.27 (1.87-5.72)**	**<0.001**
Ascitic fluid volume	77			84		
≤500 ml	32	**1**		35	**1**	
>500 ml	45	**2.27 (1.27-4.05)**	**<0.001**	49	**2.33 (1.38-3.92)**	**0.001**
CA125 [c]	62			66		
≤699 U/ml	31	1		34	1	
>699 U/ml	31	1.29 (0.74-2.16)	0.393	32	1.32 (0.75-2.31)	0.335
PLG	89			98		
Negative	29	1		32	**1**	
Positive	60	0.99 (0.61-1.60)	0.958	66	**0.59 (0.37-0.94)**	**0.026**
PAI-1	89			98		
Negative	35	1		40	1	
Positive	54	0.84 (0.53-1.32)	0.454	58	1.06 (0.68-1.68)	0.779

[a]Number of patients

[b]HR: hazard ratio (CI: confidence interval) by univariate Cox regression analysis

[c]Dichotomized into high and low levels by the median value (699 U/ml)

Table 11. **Multivariate Cox regression analysis (PFS and OS) with respect to clinical parameters and PLG or PAI-1 protein expression (IHC) in tumor tissues of advanced high-grade serous ovarian cancer patients (FIGO III/IV) with the treatment of adjuvant chemotherapy (n=103).**

Factor	No [a]	Progression-free survival		No [a]	Overall survival	
		HR (95% CI) [b]	*p*		HR (95% CI) [b]	*p*
Total	77			84		
Age						
≤60 years	33	1		36	1	
>60 years	44	1.46 (0.82-2.60)	0.194	48	1.49 (0.81-2.73)	0.198
Residual tumor mass						
0 mm	26	1		27	**1**	
>0 mm	51	1.14 (0.55-2.40)	0.723	57	**2.17 (1.03-4.57)**	**0.041**
Ascitic fluid volume						
≤500 ml	32	**1**		35	1	
>500 ml	45	**1.91 (0.92-3.94)**	**0.080**	49	1.39 (0.69-2.80)	0.351
PLG						
Negative	24	1		27	**1**	
Positive	53	0.89 (0.49-1.60)	0.688	57	**0.45 (0.25-0.82)**	**0.009**
PAI-1						
Negative	28	1		31	1	
Positive	49	0.61 (0.34-1.11)	0.106	53	0.82 (0.45-1.49)	0.506

[a]Number of patients

[b]HR: hazard ratio (CI: confidence interval) by multivariate Cox regression analysis

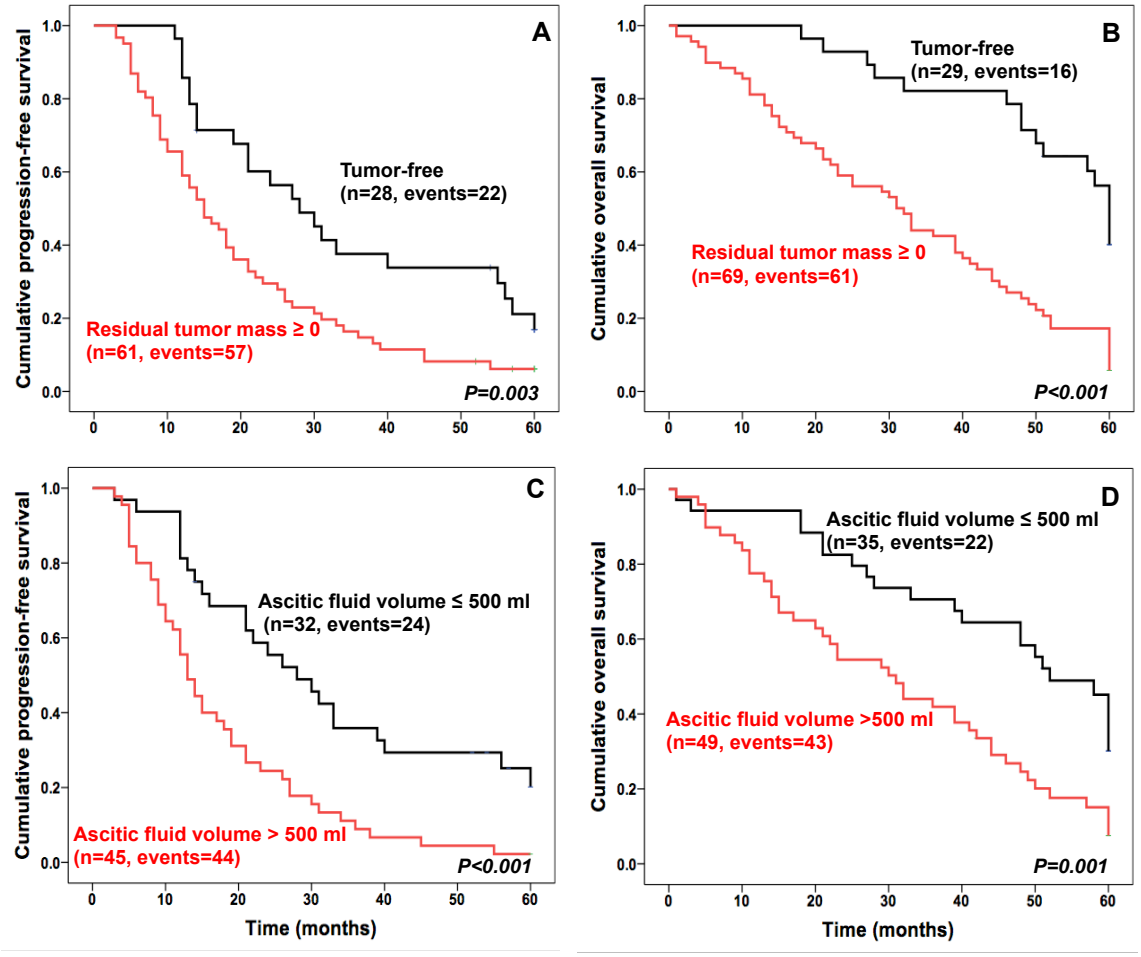

Figure 16. Probability of PFS and OS of advanced high-grade serous ovarian cancer patients (FIGO III/IV) with the treatment of adjuvant chemotherapy stratified by clinical factors tumor mass and ascitic fluid (cohort 1).

(A, B) Residual tumor mass. **(C, D)** Ascitic fluid volume. Event: PFS, disease recurrence; OS, death.

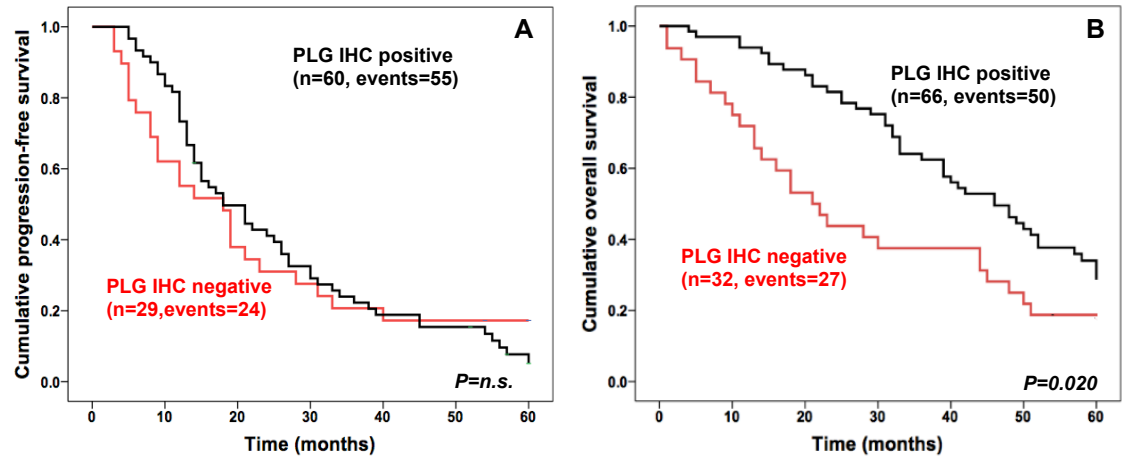

Figure 17. Probability of PFS and OS of advanced high-grade serous ovarian cancer patients (FIGO III/IV) with the treatment of adjuvant chemotherapy stratified by PLG immunoexpression (cohort 1)

Event: PFS, disease recurrence; OS, death.

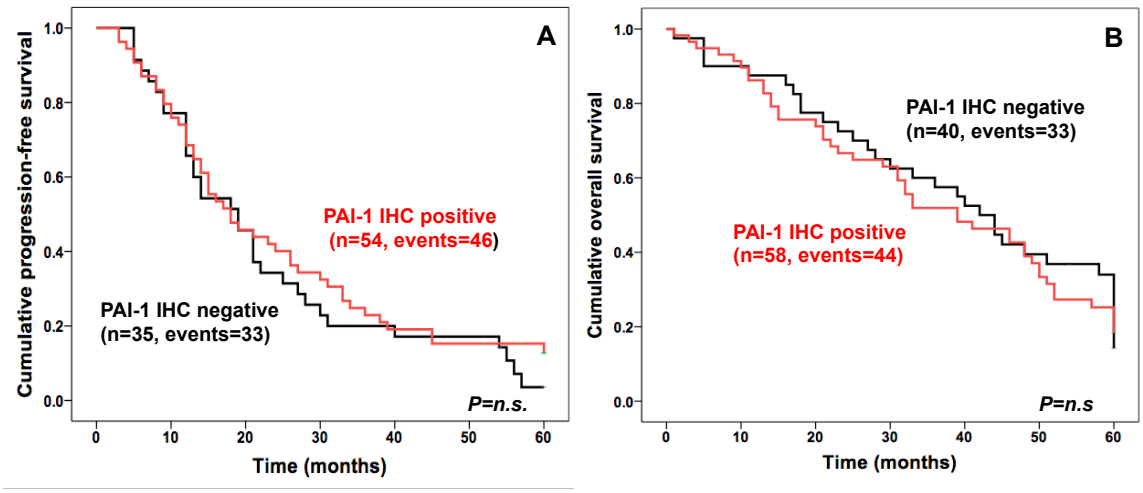

Figure 18. Probability of PFS and OS of advanced high-grade serous ovarian cancer patients (FIGO III/IV) with the treatment of adjuvant chemotherapy stratified by PAI-1 immunoexpression (cohort 1).

Event: PFS, disease recurrence; OS, death.

4.5 Analysis of immunochemical expression of uPA; mRNA expression of *PLG*, *uPA*, and *PAI-1*; and uPA/PAI-1 antigen levels in ovarian tumor tissues and association with clinical parameters (Cohort 2)

4.5.1 Association of immunoexpression of uPA, mRNA expression of *PLG*, *uPA*, and *PAI-1*, and antigen levels (ELISA) of uPA/PAI-1 with clinical parameters of ovarian cancer patients

mRNA expression of *PLG, uPA,* and *PAI-1,* immunoexpression of uPA or antigen levels of uPA and PAI-1 of all biomarkers of interest were not associated with any clinical parameters (Table 12-14).

Table 12. **Association of uPA immunoexpression (IHC) with clinical parameters in tumor tissues of advanced high-grade serous ovarian cancer patients (FIGO III/IV) with the treatment of adjuvant chemotherapy (n=50).**

Factor	No [a]	uPA IHC [b] negative/positive	*p*
Total	50	13/37	
Age	50		
≤60 years	23	5/18	
>60 years	27	8/19	0.53
Residual tumor mass	46	12/34	
0 mm	14	5/9	
>0 mm	32	7/25	0.33
Ascitic fluid volume	46	13/33	
≤500 ml	23	7/16	
>500 ml	23	6/17	0.74
CA125 [c]	46	13/33	
≤892.5 U/ml	23	7/16	
>892.5 U/ml	23	6/17	0.86

[a] Number of patients
[b] Chi-square test
[c] Dichotomized into high and low levels by the median value (892.5 U/ml)

Table 13. **Association of *PLG, uPA* and *PAI-1* mRNA expression with clinical parameters in tumor tissues of advanced high-grade serous ovarian cancer patients (FIGO III/IV) with the treatment of adjuvant chemotherapy (n=29).**

Factor	No [a]	mRNA [b]		
		PLG	***uPA***	***PAI-1***
Total	29			
Age	29			
≤60 years	17	$p = 0.88$	$p = 0.10$	$p = 0.95$
>60 years	12			
Residual tumor mass	28			
0 mm	14	$p = 0.71$	$p = 1.00$	$p = 0.71$
>0 mm	14			
Ascitic fluid volume	28			
≤500 ml	12	$p = 0.45$	$p = 0.45$	$p = 0.67$
>500 ml	16			
CA125 [c]	25			
≤892.5 U/ml	13	$p = 0.17$	$p = 0.59$	$p = 0.55$
>892.5 U/ml	12			

[a] Number of patients
[b] Mann-Whitney U test
[c] Dichotomized into high and low levels by the median value (892.5 U/ml)

Table 14. Association of uPA and PAI-1 antigen level determined by ELISA with clinical parameters in tumor tissues of advanced high-grade serous ovarian cancer patients (FIGO III/IV) with the treatment of adjuvant chemotherapy (n=45).

Factor	No [a]	Antigen level (ELISA)[b]	
		uPA	PAI-1
Total	45		
Age	45		
≤60 years	20	$p = 0.17$	$p = 0.44$
>60 years	25		
Residual tumor mass	41		
0 mm	10	$p = 0.68$	$p = 1.00$
>0 mm	31		
Ascitic fluid volume	42		
≤500 ml	22	$p = 0.45$	$p = 0.07$
>500 ml	20		
CA125 [c]	44		
≤892.5 U/ml	22	$p = 0.55$	$p = 0.57$
>892.5 U/ml	22		

[a] Number of patients
[b] Mann-Whitney U test
[c] Dichotomized into high and low levels by the median (892.5 U/ml)

4.5.2 Association of uPA immunoexpression, mRNA expression of *PLG*, *uPA*, and *PAI-1*, and antigen levels (ELISA) of uPA/PAI-1 with ovarian cancer patients' progression-free survival (PFS) and overall survival (OS)

Using univariate Cox regression analysis, residual tumor mass >0 mm was correlated with an elevated risk of disease progression in OC patients (HR, 3.45; 95% CI, 1.39-8.52; $p = 0.007$), but not significant for OS. Patients with large volume of ascitic fluid (>500 ml) had an increased risk of disease progression (HR, 2.29; 95% CI, 1.11-4.75; $p = 0.025$) and early death (HR, 2.64; 95% CI, 1.15-6.04; $p = 0.022$). Increased levels of pre-operative CA125 serum (>892.5 U/ml) are associated with increased risk of disease progression (HR, 2.49; 95% CI, 1.21-5.11; $p = 0.013$), but not significant for OS. Higher *PLG* mRNA levels are associated with a lower risk of death (HR, 0.21; 95% CI, 0.08-0.59; $p = 0.001$), presented by Kaplan-Meier survival curves (Figure 19). Although survival curves of PFS displayed that increased *PLG* mRNA expression had favorable disease outcome (log-rank test, $p = 0.044$), there was no statistically significant correlation according to Cox regression analysis (HR, 0.43; 95% CI, 0.18-1.02; $p = 0.056$). In contrast, higher *uPA* mRNA levels are associated with higher risk of death

and this result is exemplified by survival curves (HR, 3.05; 95% CI, 1.17-7.95; *p* = *0.023*) (Figure 20B), but not associated with PFS (HR, 1.83; 95% CI, 0.75-4.46; *p* = 0.183). PAI-1 mRNA expression had no correlation with PFS (HR, 0.53; 95% CI, 0.20-1.39; *p* = 0.194) and OS (HR, 0.83; 95% CI, 0.29-2.40; *p* = 0.735). Furthermore, higher antigen levels of uPA were associated with poor PFS (HR, 2.12; 95% CI, 1.04-4.32; *p* = 0.038) and OS (HR, 2.49; 95% CI, 1.11-5.6; *p* = *0.027*) (Figure 21). Higher PAI-1 antigen levels (ELISA) are only correlated with poor OS (HR, 2.29; 95% CI, 1.03-5.07; *p* = *0.040*), but not with PFS (HR, 2.03; 95% CI, 0.98-4.19; *p* = 0.057) (Figure 21). No significant result was found in association of uPA immunoexpression with PFS/OS.

In multivariate Cox regression analysis, significant predictive factors for PFS were residual tumor mass (0 mm vs. >0 mm) (HR, 3.29; 95% CI, 1.30-8.35; *p* = *0.012*), and ascitic fluid volume (≤500 ml vs. >500 ml) (HR, 2.16; 95% CI, 1.01-4.62; *p* = *0.048*), but not significant for OS. Patients with high serum levels of pre-operative CA125 (>892.5 U/ml) exhibited poor PFS (HR, 3.66; 95% CI, 1.38-9.71; *p* = *0.009*), but not significant for OS. The relationship between other markers and PFS/OS was investigated via base model, and included the following parameters: age, ascitic fluid volume, and the presence of residual tumor mass. In this model, increased mRNA levels of PLG showed a favorable disease outcome regarding OS, but not for PFS (HR, 0.26; 95% CI, 0.77-0.84; *p* = *0.025*). uPA expression concerning mRNA and protein levels (IHC/ELISA) and PAI-1 expression concerning mRNA and antigen levels had no association with either PFS or OS in patients with OC.

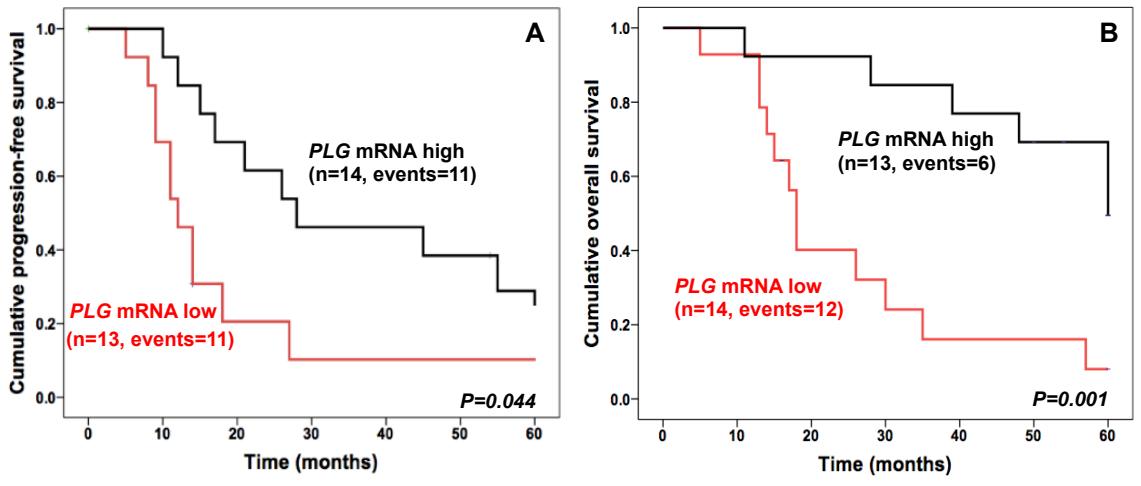

Figure 19. Probability of PFS and OS of advanced high-grade serous ovarian cancer patients (FIGO III/IV) with the treatment of adjuvant chemotherapy stratified by *PLG* mRNA expression (cohort 2).

Event: PFS, disease recurrence; OS, death.

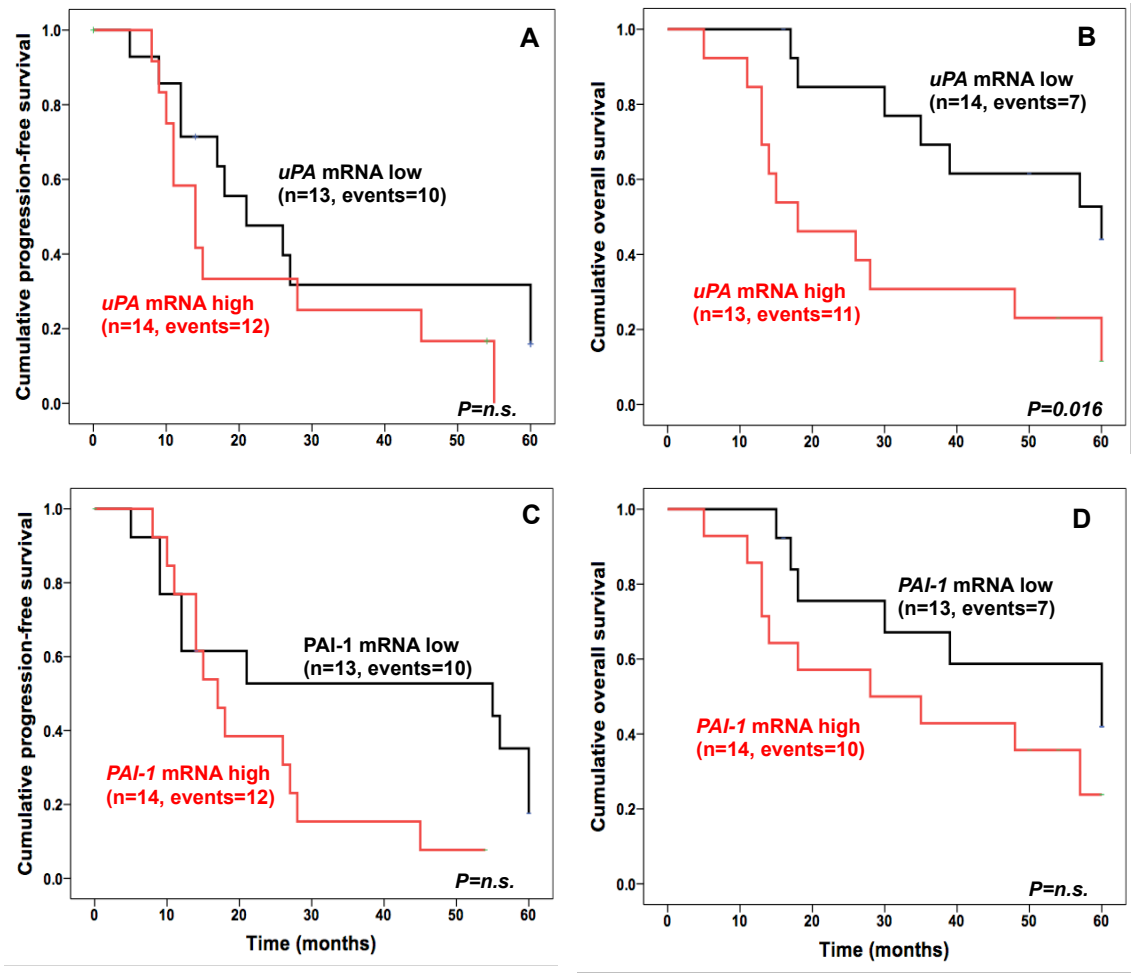

Figure 20. Probability of PFS and OS of advanced high-grade serous ovarian cancer patients (FIGO III/IV) with the treatment of adjuvant chemotherapy stratified by *uPA* and *PAI-1* mRNA expression (cohort 2).

(A) PFS and **(B)** OS curves for ovarian cancer patients in relation to *uPA* mRNA expression; (**C**) PFS and **(D)** OS curves for ovarian cancer patients in relation to *PAI-1* mRNA expression. Event: PFS, disease recurrence; OS, death.

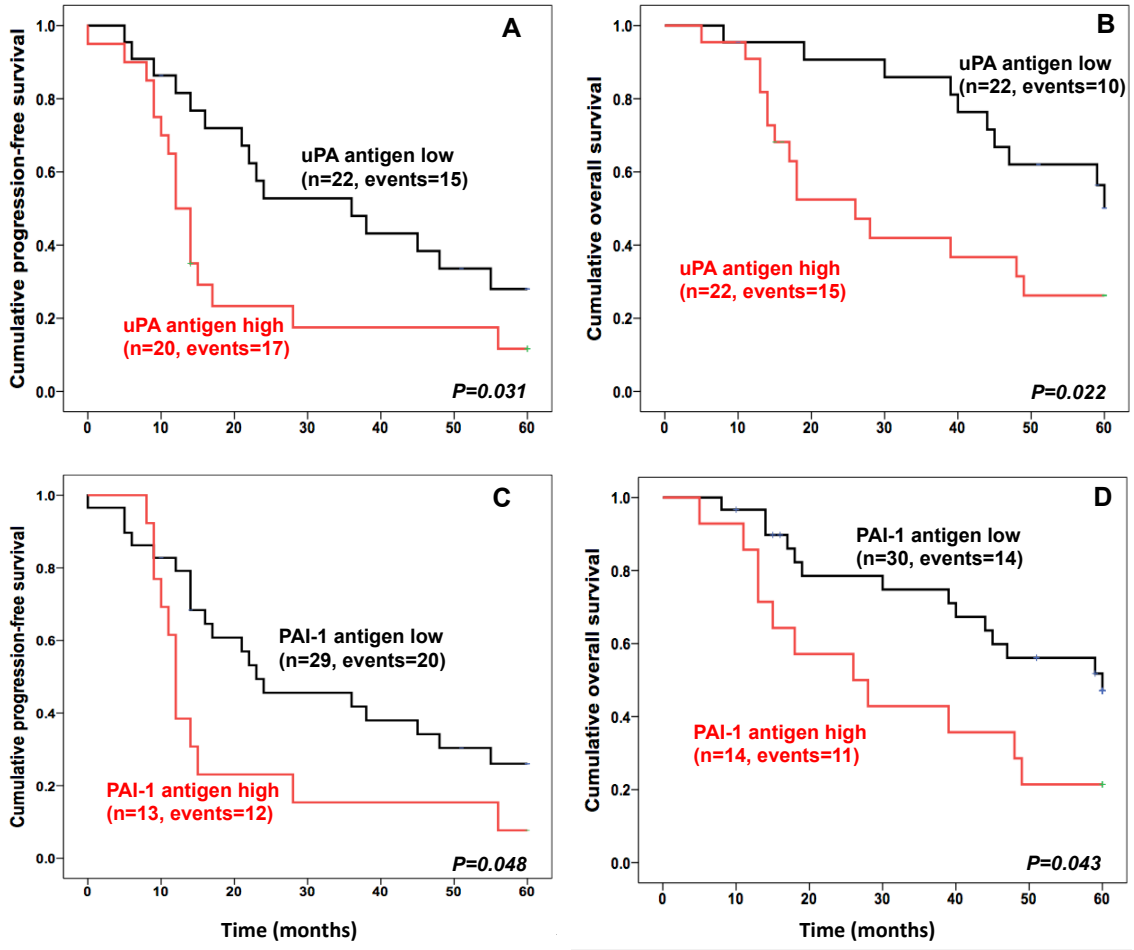

Figure 21. Probability of PFS and OS of advanced high-grade serous ovarian cancer patients (FIGO III/IV) with the treatment of adjuvant chemotherapy stratified by uPA and PAI-1 antigen levels (ELISA) (cohort 2).

(A) PFS and **(B)** OS curves for ovarian cancer patients in relation to *uPA* antigen levels; (**C)** PFS and **(D)** OS curves for ovarian cancer patients in relation to *PAI-1* antigen levels. Event: PFS, disease recurrence; OS, death.

4.6 Analysis for correlation of expression between PLG, uPA, and PAI-1 determined by IHC, qPCR, and ELISA (Cohort 2)

Application of the Mann-Whitney U test showed no correlation between PLG, uPA and PAI-1 IHC expression with mRNA levels of these markers or with ELISA in OC tissue. Spearman rank correlation analysis also demonstrated no correlation between *PLG* mRNA expression and uPA/PAI-1 at the mRNA or antigen level (ELISA). However, a statistically significant correlation between mRNA and antigen levels of uPA and PAI-1 was observed (r_s = 0.752, p *<0.001*) (Table 15). When analyzing antigen levels and mRNA levels of PAI-1, a significant correlation was also found (r_s = 0.512, p = *0.013*).

High levels of antigen were associated with high levels of mRNA for uPA and PAI-1, presented via boxplots (Figure 22).

Table 15. Correlation (R) between mRNA levels of *PLG, uPA*, and *PAI-1* and antigen levels (ELISA) of uPA/PAI-1 with the level of significance (p) determined in tumor tissue extracts of ovarian cancer.

***uPA* mRNA**	R	-0.089			
	p	0.645			
	n	29			
***PAI-1* mRNA**	R	0.003	0.549		
	p	0.987	***0.003***		
	n	27	27		
***uPA* antigen**	R	-0.211	0.752	0.555	
	p	0.321	***<0.001***	***0.006***	
	n	24	24	23	
PAI-1 antigen	R	-0.21	0.672	0.512	0.84
	p	0.324	***<0.001***	***0.013***	***<0.001***
	n	24	24	23	45
		***PLG* mRNA**	***uPA* mRNA**	***PAI-1* mRNA**	**uPA antigen**

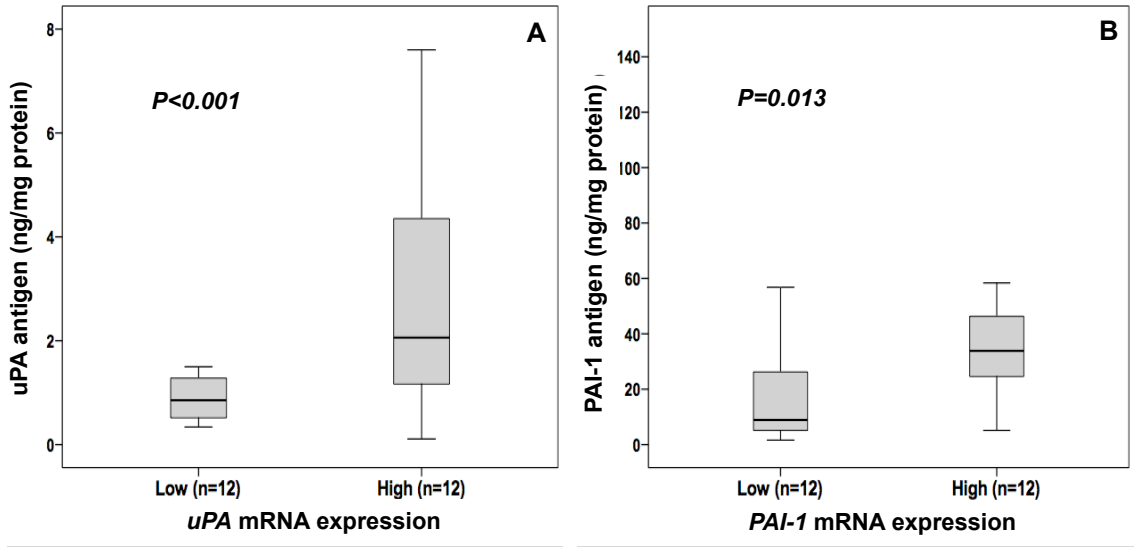

Figure 22. Boxplots of antigen concentration in ovarian cancer tumor tissues corresponding to mRNA expression for *uPA* and *PAI-1.*

(A) *uPA* and **(B)** *PAI-1* mRNA expression related to uPA/PAI-1 antigen expression (ELISA) (n=24); dichotomized into high and low levels by their median value.

Regarding the correlation of *uPA* and *PAI-1* mRNA expression, a moderated statistical significance was observed (r_s = 0.549, *p = 0.003*). The antigen level (ELISA), uPA and PAI-1 were strongly correlated (r_s = 0.84, *p <0.001*). Boxplots were drawn; representing that high expression of uPA was associated with high expression of PAI-1 at the mRNA and antigen levels (Figure 23).

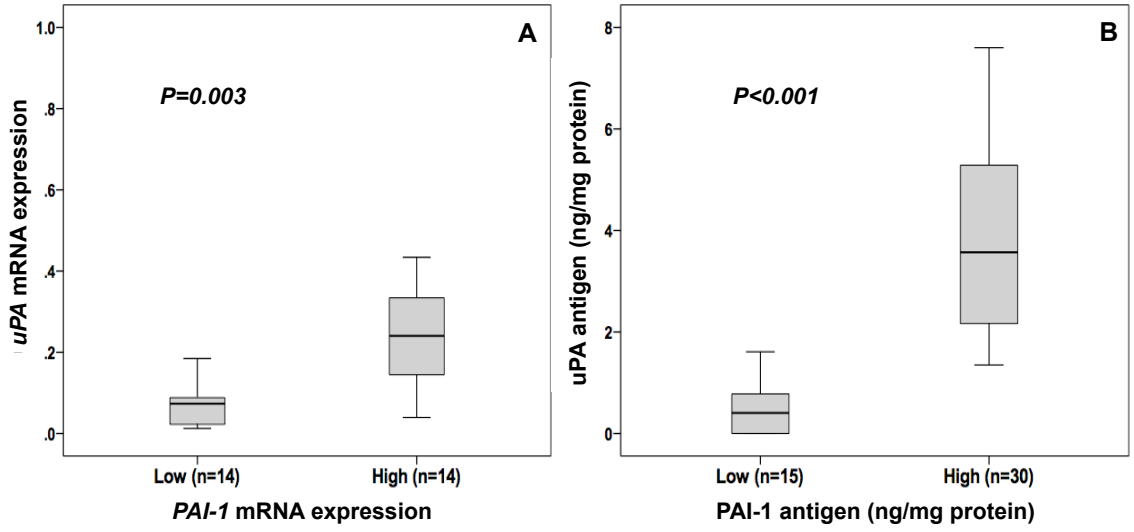

Figure 23. Correlation of uPA and PAI-1 expression (mRNA/antigen level (ELISA)) in ovarian cancer tumor tissues.

Correlation of uPA and PAI-1 expression on **(A)** mRNA level (n=28), dichotomized into high and low levels by the median value; and **(B)** antigen levels (ELISA) (n=45), dichotomized into high and low levels by cut-off value (PAI-1: 13.5 ng/mg).

5. Discussion

The majority of ovarian cancer (OC) patients are diagnosed in the advanced stage of the disease. Current therapy is based on traditional clinical factors such as tumor stage (based on FIGO) and radical reductive surgery. Despite reductive surgery with subsequent adjuvant platinum-based chemotherapy, more than half of the patients will experience early relapse and death. Therefore, it is vital to increase the precision of cancer therapeutics and clinical management, identification of molecular biomarkers of OC; particularly in advanced stages of the disease, which constitutes the majority of patients.

It has already been acknowledged that the urokinase-type plasminogen activator (uPA) system supports tumor cell invasion and metastasis. In this system, plasminogen is converted to plasmin by plasminogen activators, such as uPA, or urokinase-type plasminogen activator (tPA), which then, particularly in OC, will degrade the extracellular matrix (ECM) protein fibrin, in a process known as fibrinolysis. In cancer, the proteolytic activities of uPA and plasmin are regulated by natural inhibitors such as PAI-1, PAI-2, α2-antiplasmin, and α2-macroglobulin. Degradation of the ECM facilitates migration and dissemination of tumor cells, playing an essential role in tumor cell invasion and metastasis.

Plasminogen activation is reported to play an important role in a wide range of physiological, nonmalignant processes, such as degradation and remodelling of the ECM, cell migration, trophoblast invasion, ovulation and embryonic development, neuronal cell migration, inflammation, thrombosis, angiogenesis, as well as wound healing (Moonen et al., 1982; Dvorak et al., 1986; Sappino et al., 1989; Friedman et al., 1994; Hofmann et al., 1994; Hägglund et al., 1996; Pepper et al., 2001; Colman, 2006; Mehta et al., 2008). For instance, plasmin plays a crucial role in the degradation of the follicular wall at the time of ovulation. Many studies have reported that proteolytic activity is localized to the surface of the ovary and is activated immediately prior to ovulation (Reich et al., 1985; Xiao-Rong et al., 1993; Hägglund et al., 1996). uPA also breaks down the basement membrane components, allowing for trophoblast attachment, penetration, and degradation of the uterine mucosa (Lala et al., 1990). Both uPA and uPAR expression are associated with trophoblast invasion (Hofmann et al., 1994; Salamonsen et al., 1999). In addition, plasmin is required for removal of necrotic tissues and attributed a major role in scar remodeling during the wound repair process. In patients with plasminogen deficiency, wound-healing capacity is remarkably

decreased and fibrin degradation is limited (Mehta et al., 2008). Plasminogen-knockout mice display abolished wound healing following myocardial infarction (Creemers et al., 2000).

There is increasing evidence implying an association of the uPA system with OC. Fibrin accumulation and degradation in ovarian tumor stroma has been shown to influence tumor growth (Dvorak et al., 1986), with the protease plasmin, an important protease, partaking in this process (Wilhelm et al., 1990). When cross-linked fibrin is degraded by plasmin-induced fibrinolytic activity, fibrin fragments, including D-dimer, are produced. Elevated plasma D-dimer and fibrinogen are present in patients who died from OC correlates with risk factors such as advanced tumor stage and residual tumor mass (Koh et al., 2006; Man et al., 2015). Intriguingly, elevated D-dimer is also associated with poor prognosis in epithelial ovarian cancer (EOC) patients (FIGO II to IV) (Sakurai et al., 2014).

Elevated expression of both uPA and PAI-1 in OC is a potential prognostic indicator of poor patient outcome (Dorn et al., 2011; Zhang et al., 2013b; Mashiko et al., 2015). Most studies performed with OC tumor tissue samples analyzed mRNA expression via qPCR or antigen levels via ELISA. Only a few studies implemented IHC to study PAI-1 or uPA expression and cellular localization in ovarian tumor tissue specimens (Chambers et al., 1998; Cai et al., 2007). Even more evident, there is limited knowledge on Plasmin(ogen) (PLG) expression in ovarian tumor tissues analyzed by Western blot or ELISA (Murthi et al., 2004; Drenberg et al., 2010; van Tilborg et al., 2014). In this study, PLG expression in ovarian tumor tissues has been studied for the first time applying both IHC and qPCR technologies, and the data are correlated with uPA/PAI-1 mRNA/protein (IHC/ELISA) expression and clinical factors.

5.1 Assessment of the technical performance of PLG-, uPA-, and PAI-1-directed antibodies

PLG protein tissue expression was reported for only a few cancer types, such as colorectal cancer, breast cancer, prostate cancer, lung cancer, and liver cancer according to Human Protein Atlas (Uhlén et al., 2015). Previous studies reported that the rabbit polyclonal antibody to PLG (527557; Calbiochem, SanDiego, CA) exhibits positive staining in colorectal cancer (Yang et al., 2000; Seetoo et al., 2003); however, PLG expression analyzed by this antibody did not correlate with any clinicopathological features. In our present study, immunohistochemical staining for PLG (ab10178; Abcam, Cambridge, UK; 20 µg/ml) indicated that two-thirds of analyzed cases expressed low to moderate amounts of the PLG, which is in line with findings presented in the Human Protein Atlas (Uhlén et al., 2015).

Several studies regarding uPA and PAI-1 used antibody-based detection systems. In particular for breast cancer, immunoassays were proven to be well suited for the quantitation of uPA and PAI-1 (Jänicke et al.,1993; Benraad et al, 1996; Sweep et al., 1998; Pedersen et al., 2003; Harbeck et al., 2013; Duffy et al., 2014). In OC, uPA and PAI-1 expression, in addition to ELISA, was analyzed by IHC. This method showed moderate to strong cytoplasmic staining of tumor cells and tumor stroma cells in general (Schmalfeldt et al., 1995; Chambers et al., 1998; Koensgen et al., 2006; Cai et al., 2007).

For our study, the technical performance of the antibodies to PLG, uPA, and PAI-1 required optimization prior to assessment of protein expression via IHC. We suspected that some antibodies formed precipitates due to long-term storage of non-affinity purified primary antisera at 4°C or in a frozen state in combination with repeated freeze/thaw cycles. To overcome this, we filtered and centrifuged antibodies, and successfully removed precipitates (for details see Chapter 3.4.2 in Material and Methods and Chapter 4.1.1 in Results). Finally, protocols were established for manual staining of filtered anti-uPA, automated staining of anti-PLG and centrifuged anti-PAI-1.

5.2 Performance of qPCR assays

Given the dynamic nature of mRNA transcription and heterogeneity of tumor tissue samples, different extraction procedures or conversion efficiencies, potential variations in sample handling and in the downstream processing steps (Taylor et al., 2010), it was mandatory to establish a standardized protocol for the qPCR workflow to achieve reliable and reproducible results. To ensure validity in our test results, specificity, robustness, sensitivity, and efficiency of the qPCR reaction were assessed. Regarding test specificity, a positive control and negative controls were employed (for details see Chapter 3.6.4 in Material and Methods). Standard curves were introduced to determine reaction efficiency and sensitivity. In addition to normalization of the results with a calibrator, it was crucial to apply a housekeeping gene that was constantly expressed in both controls (calibrator) and tumor tissue samples. For the study, we used *HPRT* as the housekeeping gene, applied as previously (de Kok et al., 2005).

Standard curves for the target genes *PLG*, *uPA*, and *PAI-1* expressed in OC tumor tissues demonstrated linearity over a wide concentration range, which implied that the efficiency of amplification was consistent at varying concentrations of the target mRNAs. Multiple standard curves were used to demonstrate reproducibility and efficiency of the measurements. Standard curves for *PLG* and *uPA* confirmed reproducibility of amplification.

5.3 Demonstration of uPA/PAI-1 expression by IHC, qPCR, and ELISA

In our study, no correlation was observed between IHC staining intensity and ELISA antigen levels for both uPA and PAI-1 in OC tissue. Previous studies reported a weak correlation between values measured by IHC and ELISA when different types of tumor tissue samples were analyzed (Pappot et al. 1997; Ferrier et al., 1999). In primary human breast cancer, one study demonstrated that an optimized IHC test could be considered as a reliable alternative to the established ELISA test for determination of uPA/PAI-1 (Lang et al., 2013). However, the two techniques are not interchangeable for several reasons. At first, tissue heterogeneity introduced by sample preparation could alter results, such as FFPE sections for IHC, and frozen sections for ELISA. Second, the efficiency of detecting uPA/PAI-1 epitopes may differ for both techniques. In IHC even after an epitope retrieval step, epitopes are often masked in fixed tissue whereas epitopes may be exposed after tissue extraction for ELISA. Since the components of the plasminogen activation system may be released into the extracellular space within the tumor nest, the antigens can be recognized by ELISA, but would escape from IHC analysis. Antibodies may also react differently in extracts of fresh-frozen tissues compared to fixed tissues. More comparative studies that implement a variety of tissue processing techniques are needed to clarify whether it is, in fact, possible to exchange ELISA analysis with IHC.

Otherwise, for uPA and PAI-1 assessment, we found a strong correlation between uPA/PAI-1 mRNA expression and protein antigen level (ELISA). Previous studies also described a strong relationship between mRNA expression and antigen levels of uPA/PAI-1 in breast cancer tissue specimens (Look et al., 2002; Lamy et al., 2007; Biermann et al., 2008; Witzel et al., 2010). Harbeck et al. (2002) reported a strong correlation between uPA/PAI-1 protein expression, measured by ELISA, and clinical outcome in breast cancer patients. This finding has been validated many times by other groups (Jänicke et al.,1993; Benraad et al., 1996; Sweep et al., 1998; Foekens et al., 2000; Schmitt et al., 2011). Still, the established uPA/PAI-1 antigen determination by ELISA requires a large amount of fresh frozen tissue (Jänicke et al., 2001; Castello et al., 2006). On the other hand, qPCR, as an alternative technique, could reduce the requirement of fresh tissue material. Owing to the sensitivity and robustness of qPCR assays, the uPA/PAI-1 measurement could be accomplished routinely by qPCR with reduced consumption of clinical tissue samples.

5.4 Assessment of PLG, uPA, and PAI-1 as potential prognostic and/or predictive markers in ovarian cancer patients

In this study, we found that PLG, uPA, and PAI-1 mRNA and protein (IHC) expression have not been correlated with any clinical factors. Using univariate Cox regression analysis, clinical parameters such as advanced age, residual tumor mass, and high ascitic fluid volume emerged as markers of unfavorable outcome in advanced high-grade serous OC patients (FIGO III/IV) with the treatment of adjuvant chemotherapy. Multivariate analysis revealed that residual tumor mass is a determinant of shorter overall survival (OS) and an increase in ascitic fluid volume is associated with shorter progression-free survival (PFS). These findings were in line with previous studies demonstrating that residual tumor mass after primary surgical cytoreduction is one of the most important clinical factors to predict patient survival (Hoskins et al., 1994; Kuhn et al., 1994; Kuhn et al., 1999). Consequently, cytoreductive surgery in OC is one of the major tasks with regard to patient survival (Chi et al., 2006). Ascitic fluid volume is another clinically relevant factor related to survival in advanced OC (Lopez et al., 1996; Ayantunde et al., 2007; Kipps et al., 2013).

In our study, in advanced high-grade serous OC patients (FIGO III/IV) with the treatment of adjuvant chemotherapy and presenting with the ascitic fluid volume >500 ml suffered from a median PFS of 13 months with a 5-year OS rate of only 26%. In contrast, advanced OC patients with no ascites or ascitic fluid volume <500ml experienced a median PFS of 27 months with a 5-year OS rate of 45.7%. This result is in agreement with a report published by the SEER (surveillance, epidemiology, and end results) Cancer Statistics Review committee that advanced OC patients (FIGO III/IV) with increased ascitic fluid volume were faced with short PFS and untimely death (Howlader et al., 2015).

Although a large number of scientists are interested in investigating the PLG activation system at the molecular level in the non-malignant situation, and mainly in blood, few studies have centered on the detailed investigation of PLG expression in tumor tissues of cancer patients, and even fewer were reported for OC. Murthi et al. (2004) studied PLG-mediated uPA-activation in the context of interaction with the uPA receptor interactome. Authors reported decreased Glu-/Lys-plasminogen levels in EOC tissue compared with normal ovarian tissue. How this fits together with a report published by Drenberg et al. (2010) that elevated levels of PLG plus angiostatin were identified in the urine of EOC patients but not in that of healthy individuals, which remains unclear at present.

By uni- and multivariate analysis, we observed that elevated PLG immunoexpression is associated with prolonged OS in advanced OC patients (stage FIGO III/IV) treated with adjuvant chemotherapy. In this cohort, we observed that not only PLG protein expression but also PLG mRNA expression was related to longer OS. These results are supported by data mining of available Affymetrix microarray databases, using the online KM-plotter database (http://kmplot.com/analysis/) (Győrffy et al., 2012). For this, we employed the available 2015 combined data set and selected advanced stage FIGO III+IV OC patients data (n=414), for which mRNA expression was determined (Affymetrix probe 230931_at).

Similar to our results, in this advanced high-grade serous OC patients treated with adjuvant chemotherapy group (FIGO III/IV), Kaplan-Meier analysis revealed that elevated PLG mRNA levels were significantly associated with a better prognosis for patients (*p = 0.031*) (Figure 24). Likewise, data collected for disease-free survival of early-stage, treated breast cancer patients supported the finding that elevated PLG mRNA levels are associated with a favorable clinical outcome (Figure 25).

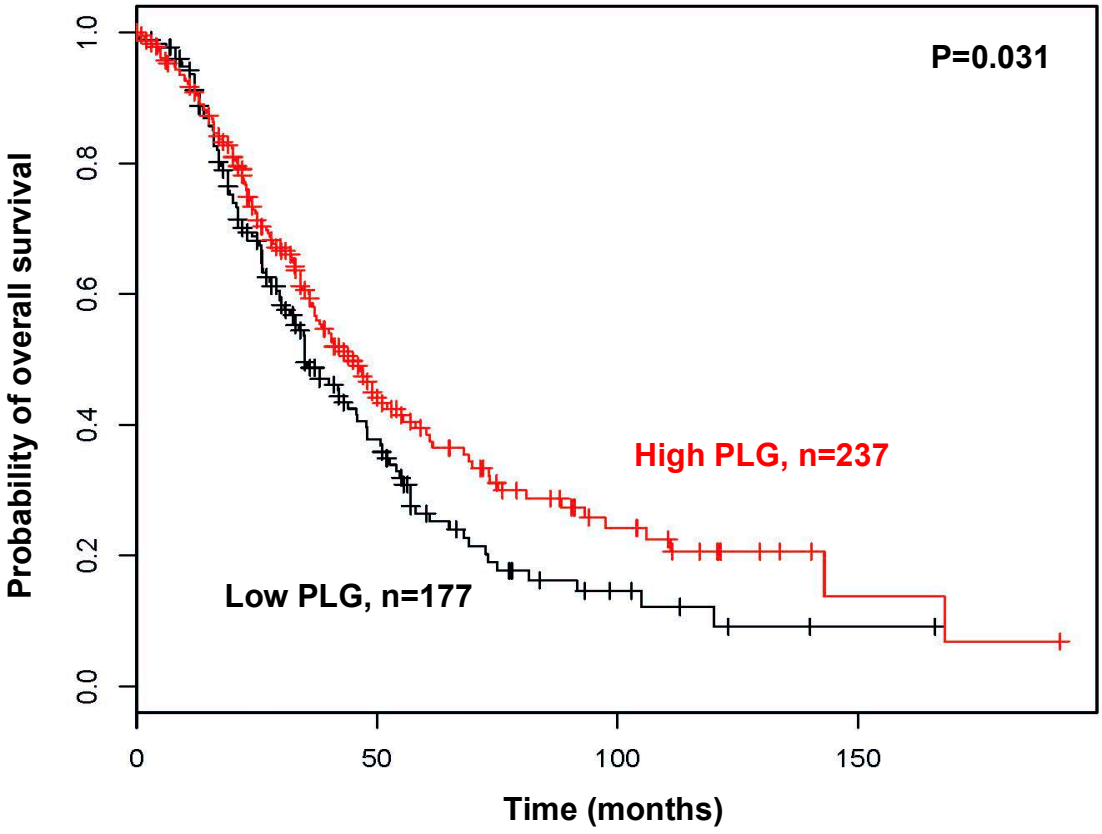

Figure 24. Probability of overall survival (OS) of advanced high-grade serous ovarian cancer patients (FIGO III/IV) with the treatment of adjuvant chemotherapy stratified by PLG mRNA expression as assessed by the Affymetrix Microarray system.

mRNA was prepared from primary tumor tissues of advanced high-grade serous ovarian cancer patients (FIGO III/IV) with > 5 years follow-up. The patients received platinum/taxane adjuvant treatment. The *PLG* mRNA expression data set investigated is part of the KM-Plotter 2015 Affymetrix data set assembled by Győrffy et al. (2012). The analysis made use of the data set obtained with the oligonucleotide 230931_at. Plotted according to Kaplan-Meier (Kaplan and Meier, 1958).

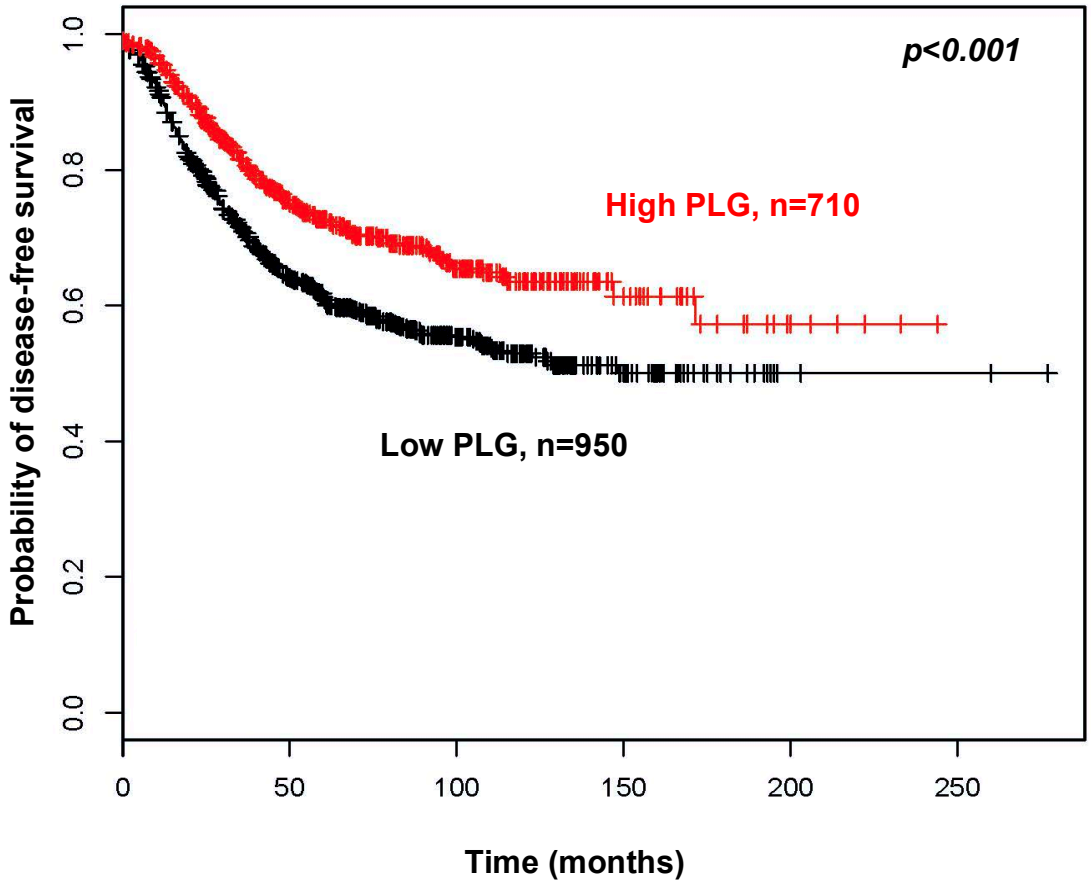

Figure 25. Probability of disease-free survival (DFS) of early breast cancer patients stratified by PLG mRNA expression as assessed by the Affymetrix Microarray system.

mRNA was prepared from primary tumor tissues of early breast cancer patients with >5 years follow-up. The *PLG* mRNA expression data set investigated is part of the KM-Plotter 2015 Affymetrix data set assembled by Győrffy et al. (2012). The analysis made use of the data set obtained with the oligonucleotide 230931_at. Plotted according to Kaplan-Meier (Kaplan and Meier, 1958).

PLG is a key member of the plasminogen activation system; in this system, plasminogen is activated to its proteolytically active form plasmin by two types of plasminogen activators, the tissue-type plasminogen activator (tPA), or by the urokinase-type plasminogen activator (HMW/LMW-uPA: high-molecular-weight/low-

molecular-weight-uPA). tPA is mainly involved in fluid-phase activation of PLG, preferentially in the blood clotting system, and its activity is enhanced by fibrin (Rijken and Lijnen, 2009; Gebbink, 2011). uPA is an important factor in the regulation of tissue-associated proteolysis (e.g. angiogenesis and wound healing, embryogenesis and pregnancy, and tissue remodeling). By binding to its receptor, uPAR (CD87), uPA is a major player in tumor invasion and metastasis. In this pathway, the latent form of uPA, pro-uPA, among other proteases, is activated by plasmin to generate the enzymatically active uPA-forms HMW-uPA and LMW-uPA. Since plasmin is a broad-acting serine protease, it may also target and inactivate uPAR, which eventually will lead to a decelerated pace of tumor invasion and metastasis. Proteases such as plasmin, uPA, and trypsin are known to cleave uPAR in the linker region between domains DI and DII, as well as within the carboxyterminal region of uPAR (Andreasen, et al., 1997; Beaufort et al., 2004; Montuori, et al., 2005). The cleavage leads to the release of soluble uPAR fragments (free DI and the truncated part encompassing DII and DIII). uPAR cleavage, mediated by uPA or plasmin, thus represents a negative-feedback mechanism to regulate cell-associated uPAR activities (Ragno et al., 2006; Rasch et al., 2008). Moreover, looking at a different feature of PLG as a modulatory molecule, it may play a role in the execution and degradation phase of the apoptotic pathway, also in cancer (Davidson, 2005).

A different feature of PLG contribution in cancer is that PLG is the parent molecular form of the angiogenesis-inhibiting molecule angiostatin (38 kDa), which encompasses several contiguous kringle modules of the parent PLG molecule. Kringles1-3 (K1-3) were mostly found to be present and are referred to as ‘angiostatin’, while other fragments, such as K1-4 displaying inhibition activity, are ‘angiostatin-like’ (Figure 26) (Javaherian et al., 2011). Angiostatin can be produced by autoproteolytic cleavage of PLG or by cleavage of PLG by different serine proteases or metalloproteinases (MMPs) (Gately et al., 1996 and 1997; Dong et al., 1998; O'Reilly et al., 1999; Kwaan et al., 2009). Angiostatin, as an endogenous inhibitor of angiogenesis, could reverse the angiogenic switch, thereby preventing vascularization in tumor growth. In preclinical studies, metastatic growth of secondary tumors was inhibited by angiostatin therapy (Javaherian et al., 2011; Folkman et al., 2012). Elevated production of angiostatin may give rise to a less malignant tumor in OC (Murthi et al., 2004). Regarding OC, van Tilborg et al. (2014) did show that both PLG and angiostatin are found in cyst fluid derived from patients afflicted with malignant ovarian tumors, whereas only small amounts of PLG and angiostatin were present in functional, non-pathological cysts. Besides angiostatin itself, the PLG kringle 5 (K5) possesses potent antiangiogenic properties with potent antitumor capacity (Perri, et al., 2007).

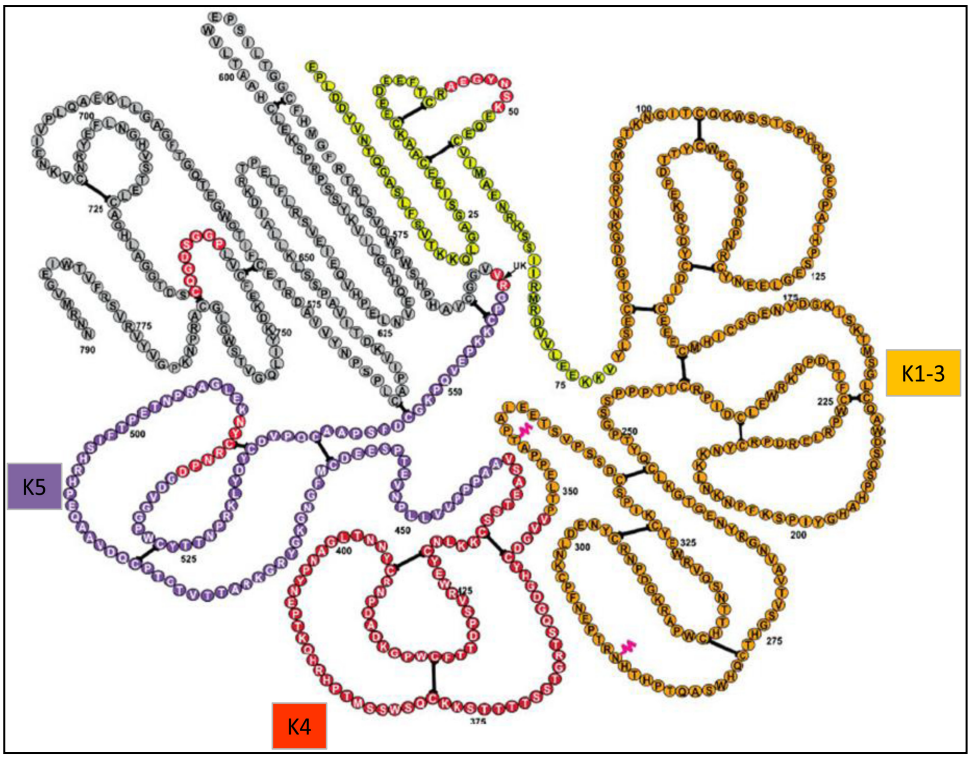

Figure 26. The full sequence of human plasminogen.

Plasminogen consists of seven structural domains: an N-terminal pre-activation peptide, 5 kringle (K) domains, and the C-terminal trypsin-like serine protease domain. Angiostatin encompasses K1-3. The recombinant angiostatin (angiostatin-like) encompasses K1-4 (Adapted from Javaherian et al., 2011).

Elevated uPA and PAI-1 expression is associated with unfavorable outcome of patients afflicted with various types of malignant tumors (Liu et al., 1995; Nordengren et al., 2002; Seetoo et al., 2003; Schmitt et al., 2010; Witzel et al., 2010; Ding et al., 2013; Al-Janabi et al., 2014; Annertz et al., 2014; Mekkawy et al., 2014; Akudugu et al., 2015; Su et al., 2015). Despite the fact that uPA and PAI-1 are upregulated in OC, their impact on ovarian tumor cells and the clinical relevance of dysregulation are still unclear (Chambers et al., 1995; van der Burg et al., 1996; Borgfeldt et al., 2001; Konecny et al., 2001; Borgfeldt et al., 2003; Cai et al., 2007; Dorn et al., 2011; Zhang et al., 2013b; Mashiko et al., 2015).

Several studies regarding OC have focused on uPA/PAI-1 antigen levels, only fewer analyzed uPA/PAI-1 mRNA expression and immunoexpression (Schmalfeldt et al., 1995; Chambers et al., 1998; Koensgen et al., 2006; Koensgen et al., 2007; Zhang et al., 2013b; Mashiko et al., 2015). Some researchers observed that mRNA expression of both *uPA/PAI-1* was higher in solid ovarian tumor than cystic ovarian tumors (Borgfeldt et al., 2001), but no study has been yet reported correlations between uPA/PAI-1 and PLG on the protein and mRNA levels. In our study, PLG expression was not associated with uPA or PAI-1 expression. The elevated uPA level is associated with clinical outcome of shorter OS in advanced high-grade serous OC patients (FIGO III/IV) treated with adjuvant chemotherapy, but not with PFS. PAI-1 did not show an association with

PFS/OS, which is probably due to the rather low number of analyzed patients in our study. Our results are in line with reports from previous clinical studies that the trend of increased amounts of uPA/PAI-1 was associated with poor clinical outcome, from benign tumors to low-malignant-potential tumors and finally to invasive and aggressive OC (Kuhn et al., 1999; Konecny et al., 2001; Schmalfeldt et al., 2001). In contrast, other studies reported that uPA/PAI-1 expression is not associated with patients' survival or even high expression was found to be related with good prognosis (Komiyama et al., 2011; Battista et al., 2014).

In addition, evaluation of the PAI-1 expression in OC is quite controversial. On the one hand, researchers observed that high levels of PAI-1 are correlated with a better prognosis than low PAI-1 expression (Komiyama et al., 2011); on the other hand, other reports showed that increased PAI-1 levels are related to malignant tumor phenotype and poor prognosis (Pappot et al., 1995; Chambers et al., 1998; Koensgen et al., 2006; Mashiko et al., 2015). In our study, Immunostaining of PAI-1 has shown that PAI-1 immunoexpression is not only presented in cancer cells but also in stromal cells of the tumor tissues, implying a coordinated action between stroma and tumor cells in the control of the proteolytic process in cancer. It is a paradox for high expression of PAI-1 is associated with malignant progression of OC. Theoretically, since PAI-1 antagonizes proteolytic plasminogen activation, thereby inhibiting ECM degradation that in turn should prevent invasion of the tumor cell. However, explanation of elevated PAI-1 related to malignant tumor is that PAI-1 triggers the turnover of uPA by complex formation and subsequent internalization of the uPAR/HMW-uPA/PAI-1 complex, which enables uPAR, but not uPA or PAI-1, to recycle to the cell surface (Mengele et al., 2010). Besides, the stromal release of both uPA and PAI-1 might result in high extracellular uPA-PAI-1 complex concentration. Owing to stimulation of uPA-PAI-1 complex combining uPAR, the efficiency of cell migration is improved compared with non-complexed uPA. The complex likely functions as a paracrine signal in tumor and endothelial cells (Borgfeldt et al., 2001).

The proposed tumor-supporting role of PAI-1 may explain the observed coordinated expression pattern of uPA and PAI-1 in tumor tissues. Several publications indicate a rather strong correlation between uPA and PAI-1 in breast cancer (Spyratos et al., 2002; Lamy et al., 2007; Hildenbrand et al., 2009; Lang et al., 2013) and OC (Konecny et al., 2001; Dorn et al., 2011; Zhang et al., 2013b). We observed a correlation between uPA and PAI-1 both at the mRNA and antigen level, which is concordant with previous results. uPA and PAI-1 supposedly regulate the activation of one another and possibly co-act in the development of OC because up-regulated expression of uPA and PAI-1 at the protein and the mRNA level is consistently found in malignant ovarian tumors. One

study reported that PAI-1 controls uPA activity but also has an impact on tumor cell adhesion and angiogenesis in breast cancer as well (Lang et al., 2013).

A strong association was found between uPA and PAI-1 at the mRNA and antigen level (ELISA), whereas no correlation was found according to immunoexpression. A possible explanation is that only selected region of tumor tissue is stained with IHC, while large amounts of protein and mRNA are extracted from tumor tissue for ELISA or qPCR (Dorn et al., 2016). However, it is of note that in IHC analysis, low PLG levels were associated with low PAI-1 levels and vice versa, indicating coordinated expression of both members of uPA system in OC (Didiasova et al., 2014).

5.5 Conclusions and outlook

The plasminogen activation system plays a significant role in tumor invasion and metastasis by means of its proteolytic activity. Plasmin(ogen) (PLG), urokinase-type plasminogen activator (uPA), uPA receptor (uPAR), and plasminogen activator inhibitor-1 (PAI-1), which are important proteolytic factors of this system, are pivotal predictive and/or prognostic cancer biomarkers, but further research regarding interaction and biological role of these markers in the malignant process is required. Apart from that, the present study explored the clinical impact of the cancer biomarkers PLG, uPA, and PAI-1 in advanced ovarian cancer (OC). At first, immunohistochemical (IHC) and quantitative polymerase chain reaction (qPCR) assays were established to assess protein and gene expression of these markers in OC tissues. All three biomarkers are expressed at the protein and gene level, providing evidence that all of these markers are involved in tumor invasion and metastasis in OC, and are associated with the clinical course of the disease.

Since it was known before that elevation of uPA and PAI-1 in OC tissues is associated with a poor prognosis of advanced OC patients, even for those treated with taxane-based chemotherapy, elevation of PLG in this type of malignancy, determined and quantified for the first time at the protein and gene level, indicates a favorable clinical outcome. This may be owing to the fact that excess production of proteolytically active plasmin from its precursor molecule plasminogen will affect a multitude of proteins, involving the destruction of uPAR, which thereby prevents binding of the uPA-PAI-1 complex to uPAR and its subsequent cellular internalization. Second to that, plasmin is also attacking and degrading the extracellular stroma protein fibrin, which is necessary for attachment and persistent survival of OC cells located in the peritoneum of advanced OC patients. Destruction of fibrin by plasmin, which ultimately will lead to detachment of OC cells from that matrix protein known as anoikis, eventually will cause

impairment of the cancer cells by losing contact with this matrix which is a site of vascularization and rich source of nutrients for the cancer cells.

Still, the relationship of PLG expression with uPA/PAI-1 expression and other factors such as cellular integrins and growth factors in the early phase of the OC disease, and its precursor borderline situation needs to be elucidated at the molecular level, related to the course of the disease and the effect of early-phase (neo)adjuvant cancer treatment.

Owing to the heterogeneity of the OC tumor tissue composition, its various histological subtypes, and resistance to certain cancer therapeutics, one must be careful in selecting the right patient groups for statistical analysis. Furthermore, the molecular tools to assess the clinical impact of cancer biomarkers at the protein and gene level should be carefully characterized prior to assessment. Finally, other preanalytical conditions must be accounted for, such as quality and storage conditions of the tumor tissues to be analyzed. Meaningful statistical analyses will require large and independent patient groups, reflecting different age groups and ethnic backgrounds, and also consider additional predictive and/or prognostic cancer biomarkers, to fully support PLG, uPA, and PAI-1 as important and clinically relevant cancer biomarkers. Thus, the present data encourages validation of the findings via future transnational cooperation.

6. Abstract

The urokinase-type plasminogen activator (uPA) system acts on both, physiologic and pathologic processes, e.g. in inflammation, thrombosis, and cancer growth. Plasmin(ogen) (PLG), uPA, and plasminogen activator inhibitor (PAI-1) are members of the plasminogen activation system, which have been implicated in tumor cell invasion and metastasis. Overexpression of uPA and PAI-1 has been associated with poor prognosis of advanced ovarian cancer patients. However, studies on the prognostic relevance of these factors are inconclusive. Up to now, research on the role of PLG in ovarian cancer has not been yet studied in details.

In this study, our aim was to establish standard operation procedures (SOPs) for immunohistochemistry staining (IHC) and quantitative polymerase chain reaction (qPCR) assays of PLG, uPA, and PAI-1, and investigate the associations and clinical relevance of these markers by protein (IHC/Enzyme-linked immunosorbent assay (ELISA)) and mRNA-based (qPCR) methods. There were two cohorts of ovarian cancer patients to be tested: in the first patients' collective, PLG and PAI-1 IHC was evaluated in 103 cases; in the second patients collective, uPA immunostaining was performed in 50

cases. Additionally, in 29 of these 50 cases, quantitative mRNA expression was determined for *PLG*, *uPA*, and *PAI-1*, and 45 of these 50 cases uPA and PAI-1 protein data were collected by ELISA.

Statistical associations between PLG, uPA, and PAI-1 were analyzed. A statistically significant correlation between uPA and PAI-1 at both the mRNA (r_s = 0.549, *p = 0.003*) and the antigen level was evident (r_s = 0.84, *p <0.001*). Furthermore, correlation of PLG and PAI-1 IHC expression was significant (*p = 0.037*). No correlation was found between uPA and PLG expression. PLG, uPA, and PAI-1 protein (IHC) and mRNA expressions showed no association with any clinical parameters, such as age, residual tumor mass, ascites, and CA125. Regarding patients survival (cohort 1), univariate Cox regression analysis showed age, residual tumor mass, and ascites to be predictive factors for both progression-free survival (PFS) and overall survival (OS) in ovarian patients. Patients aged >60 years displayed shorter PFS (HR = 2.01; *p = 0.005*) and OS (HR = 1.64; *p = 0.037*) compared with patients aged ≤60 years. Patients with residual tumor mass showed decreased PFS (HR = 3.31; *p <0.001*) and OS (HR = 3.27; *p <0.001*) compared with residual tumor-free patients. Large volume of ascitic fluid (>500 ml) was indicating shorter PFS (HR = 2.27; *p <0.001*) and OS (HR = 2.33; *p <0.001*). Following multivariate Cox regression analysis, only residual tumor mass (0 mm vs. >0 mm) was a significant predictor of OS (HR = 2.17; *p = 0.041*); and large volume of ascitic fluid (≤500 ml vs. >500 ml) was associated with shorter PFS (HR = 1.91; *p = 0.08*). Higher PLG immunoexpression indicated longer OS in both univariate (HR = 0.59; *p = 0.026*) and multivariate analysis (HR = 0.45; *p = 0.009*). In cohort 2, higher *PLG* mRNA expression was correlated with statistically longer OS (HR = 0.21; *p = 0.001*) and a trend for longer PFS (HR = 0.43, *p* = 0.056). In contrast, higher *uPA* mRNA expression represented shorter OS (HR = 3.05; *p = 0.023*). These results demonstrated that high uPA levels are related to poor prognosis; conversely, high PLG levels were related to a favorable prognostic outcome.

Overall, the work presented the first established SOPs for IHC and qPCR assays that targets the genes *PLG, uPA*, and *PAI-1*, in order to investigate whether concurrent analyses of protein-(IHC/ELISA) and RNA for all three biomarkers could serve as predictive, therapeutic, and prognostic tools for advanced high-grade serous ovarian cancer.

7. Reference

Al-Hassan, N. N., Behzadian, A., Caldwell, R., Ivanova, V. S., Syed, V., Motamed, K., & Said, N. A. (2012). Differential roles of uPAR in peritoneal ovarian carcinomatosis. *Neoplasia, 14*, 259-IN2.

Al-Janabi, O., Taubert, H., Lohse-Fischer, A., Fröhner, M., Wach, S., Stöhr, R., Keck, B., Burger, M., Wieland, W., Erdmann, K., Wirth, M. P., Wullich, B., Baretton, G., Magdolen, V., Kotzsch, M., & Füssel, S. (2014). Association of tissue mRNA and serum antigen levels of members of the urokinase-type plasminogen activator system with clinical and prognostic parameters in prostate cancer. *BioMed Research International, 2014,* 1-9.

Akudugu, J., Serafin, A., Böhm, L. (2015). Further evaluation of uPA and PAI-1 as biomarkers for prostatic diseases. *Journal of Cancer Research and Clinical Oncology, 141*, 627-631.

Anastasi, E., Marchei, G. G., Viggiani, V., Gennarini, G., Frati, L., & Reale, M. G. (2010). HE4: a new potential early biomarker for the recurrence of ovarian cancer. *Tumour Biology, 31*, 113-119.

Andreasen, P. A., Kjoller, L., Christensen, L., & Duffy, M. J. (1997). The urokinase-type plasminogen activator system in cancer metastasis: a review. *International Journal of Cancer, 72*, 1-22.

Annertz, K., Enoksson, J., Williams, R., Jacobsson, H., Coman, W. B., & Wennerberg, J. (2014). Alpha B-crystallin - a validated prognostic factor for poor prognosis in squamous cell carcinoma of the oral cavity. *Acta Otorrinolaringologica, 134*, 543-550.

Ayantunde, A., & Parsons, S. (2007). Pattern and prognostic factors in patients with malignant ascites: a retrospective study. *Annals of Oncology, 18*, 945-949.

Bast, R. C., Feeney, M., Lazarus, H., Nadler, L. M., Colvin, R. B., & Knapp, R. C. (1981). Reactivity of a monoclonal antibody with human ovarian carcinoma. *Journal of Clinical Investigation, 68*, 1331-1337.

Battifora, H. (1986). The multitumor (sausage) tissue block: Novel method for immunohistochemical antibody testing. *Laboratory Investigation, 55,* 244-248.

Battista, M. J., Mantai, N., Sicking, I., Cotarelo, C., Weyer, V., Lebrecht, A., Solbach, C., & Schmidt, M. (2014). Ki-67 as an independent prognostic factor in an unselected cohort of patients with ovarian cancer: results of an explorative, retrospective study. *Oncology Reports, 31*, 2213-2219.

Beaufort, N., Leduc, D., Rousselle, J. C., Namane, A., Chignard, M., & Pidard, D. (2004). Plasmin cleaves the juxtamembrane domain and releases truncated species of the urokinase receptor (CD87) from human bronchial epithelial cells. *FEBS Letters, 574*, 89-94.

Będkowska, G. E., Ławicki, S., Gacuta, E., Pawłowski, P., & Szmitkowski, M. (2015). M-CSF in a new biomarker panel with HE4 and CA 125 in the diagnostics of epithelial ovarian cancer patients. *Journal of Ovarian Research, 8*, 1.

Benraad, T. J., Geurts-Moespot, J., Grøndahl-Hansen, J., Schmitt, M., Heuvel, J. J. T. M., De Witte, J. H., Foekens, J. A., Leake, R. E., Brünner, N., & Sweep, C. G. J. (1996). Immunoassays (ELISA) of urokinase-type plasminogen activator (uPA): report of an EORTC/BIOMED-1 workshop. *European Journal of Cancer*, *32*, 1371-1381.

Berman, M. L. (2003). Future directions in the surgical management of ovarian cancer. *Gynecologic Oncology, 90*, S33-S39.

Biermann, J. C., Holzscheiter, L., Kotzsch, M., Luther, T., Kiechle-Bahat, M., Sweep, F. C., Span, P. N., Schmitt, M., & Magdolen, V. (2008). Quantitative RT-PCR assays for the determination of urokinase-type plasminogen activator and plasminogen activator inhibitor type 1 mRNA in primary tumor tissue of breast cancer patients: comparison to antigen quantification by ELISA. *International Journal of Molecular Medicine, 21*, 251-259.

Borgfeldt, C., Hansson, S. R., Gustavsson, B., Måsbäck, A., & Casslén, B. (2001). Dedifferentiation of serous ovarian cancer from cystic to solid tumors is associated with increased expression of mRNA for urokinase plasminogen activator (uPA), its receptor (uPAR) and its inhibitor (PAI-1). *International Journal of Cancer, 92*, 497-502.

Borgfeldt, C., Bendahl, P. O., Gustavsson, B., Långström, E., Fernö, M., Willén, R., Grenman, S., & Casslén, B. (2003). High tumor tissue concentration of urokinase plasminogen activator receptor is associated with good prognosis in patients with ovarian cancer. *International Journal of Cancer, 107*, 658-665.

Bu, X., Khankaldyyan, V., Gonzales-Gomez, I., Groshen, S., Ye, W., Zhuo, S., Pons, J., Stratton, J. R., Rosenberg, S., & Laug, W. E. (2004). Species-specific urokinase receptor ligands reduce glioma growth and increase survival primarily by an antiangiogenesis mechanism. *Laboratory Investigation, 84*, 667-678.

Bustin, S. A., Benes, V., Garson, J. A., Hellemans, J., Huggett, J., Kubista, M., Mueller, R., Nolan, T., Pfaffl, M. W., Shipley, G. L., Vandesompele, J., & Wittwer, C. T. (2009). The MIQE Guidelines: Minimum information for publication of quantitative real-time PCR experiments. *Clinical Chemistry, 55*, 611-622.

Cai, Z., Li, Y. F., Liu, F. Y., Feng, Y. L., Hou, J. H., & Zhao, M. Q. (2007). Expression and clinical significance of uPA and PAI-1 in epithelial ovarian cancer. *Ai Zheng, 26*, 312-317.

Cantero, D., Friess, H., Deflorin, J., Zimmermann, A., Bründler, M. A., Riesle, E., Korc, M., & Büchler, M. W. (1997). Enhanced expression of urokinase plasminogen activator and its receptor in pancreatic carcinoma. *British Journal of Cancer, 75*, 388.

Castello, R., Espana, F., Vazquez, C., Fuster, C., Almenar, S. M., Aznar, J., & Estelles, A. (2006). Plasminogen activator inhibitor-1 4G/5G polymorphism in breast cancer patients and its association with tissue PAI-1 levels and tumor severity. *Thrombosis Research, 117*, 487-492.

Chambers, S. K., Gertz, R. E. Jr., Ivins, C. M., & Kacinski, B. M. (1995). The significance of urokinase- type plasminogen activator, its inhibitors, and its receptor in ascites of patients with epithelial ovarian cancer. *Cancer, 75*, 1627-1633.

Chambers, S. K., Ivins, C. M., & Carcangiu, M. L. (1998). Plasminogen activator inhibitor-1 is an independent poor prognostic factor for survival in advanced stage epithelial ovarian cancer patients. *International Journal of Cancer, 79*, 449-454.

Chi, D. S., Eisenhauer, E. L., Lang, J., Huh, J., Haddad, L., Abu-Rustum, N. R., Sonoda, Y., Levine, D. A., Hensley, M., & Barakat, R. R. (2006). What is the optimal goal of primary cytoreductive surgery for bulky stage IIIC epithelial ovarian carcinoma (EOC)? *Gynecologic Oncology, 103*, 559-564.

Colman, R. W. (Ed.). (2006). *Hemostasis and thrombosis: basic principles and clinical practice*. Lippincott Williams & Wilkins.

Creemers, E., Cleutjens, J., Smits, J., Heymans, S., Moons, L., Collen, D., Daemen, M., & Carmeliet, P. (2000). Disruption of the plasminogen gene in mice abolishes wound healing after myocardial infarction. *The American Journal of Pathology*, *156*, 1865-1873.

Crippa, M. P. (2007). Urokinase-type plasminogen activator. *The International Journal of Biochemistry & Cell Biology, 39*, 690-694.

Danø, K., Rømer, J., Nielsen, B. S., Bjørn, S., Pyke, C., Rygaard, J., & Lund, L. R. (1999). Cancer invasion and tissue remodeling ‐ cooperation of protease systems and cell types. *Apmis, 107*, 120-127.

Davidson, D. (2005). Kringle 5 of human plasminogen induces apoptosis of endothelial and tumor cells through surface-expressed glucose-regulated protein 78. *Cancer Research, 65*, 4663-4672.

Davidson, B., Trope, C. G., & Reich, R. (2014). The role of the tumor stroma in ovarian cancer. *Frontiers in Oncology, 4*, 104.

De Kok, J. B., Roelofs, R. W., Giesendorf, B. A., Pennings, J. L., Waas, E. T., Feuth, T., Swinkels, D. W., & Span, P. N. (2005). Normalization of gene expression measurements in tumor tissues: comparison of 13 endogenous control genes. *Laboratory Investigation, 85*, 154-159.

De Petro, G., Tavian, D., Copeta, A., Portolani, N., Giulini, S. M., & Barlati, S. (1998). Expression of urokinase-type plasminogen activator (u-PA), u-PA receptor, and tissue-type PA messenger RNAs in human hepatocellular carcinoma. *Cancer Research, 58*, 2234-2239.

Deryugina, E. I., & Quigley, J. P. (2012). Cell surface remodeling by plasmin: a new function for an old enzyme. *Journal of Biomedicine and Biotechnology, 2012*, 564259.

Didiasova, M., Wujak, L., Wygrecka, M., & Zakrzewicz, D. (2014). From plasminogen to plasmin: role of plasminogen receptors in human cancer. *International Journal of Molecular Sciences, 15*, 21229-21252.

Ding, Y., Zhang, H., Zhong, M., Zhou, Z., Zhuang, Z., Yin, H., Wang, X., & Zhu, Z. (2013). Clinical significance of the uPA system in gastric cancer with peritoneal metastasis. *European Journal of Medical Research, 18*, 28.

Dong, Z., Yoneda, J., Kumar, R., & Fidler, I. J. (1998). Angiostatin-mediated suppression of cancer metastases by primary neoplasms engineered to produce granulocyte/macrophage colony-stimulating factor. *Journal of Experimental Medicine, 188*, 755–763.

Dorn, J., Harbeck, N., Kates, R., Gkazepis, A., Scorilas, A., Soosaipillai, A., Diamandis E., Kiechle, M., Schmalfeldt, B., & Schmitt, M. (2011). Impact of expression differences of kallikrein-related peptidases and of uPA and PAI-1 between primary tumor and omentum metastasis in advanced ovarian cancer. *Annals of Oncology, 22*, 877-883.

Dorn, J., Yassouridis, A., Walch, A., Diamandis, E. P., Schmitt, M., Kiechle, M., Wang, P., Drecoll, E., Schmalfeldt, B., Loessner, D., Kotzsch, M., & Magdolen, V. (2016). Assessment of kallikrein-related peptidase 5 (KLK5) protein expression in tumor tissue of advanced ovarian cancer patients by immunohistochemistry and ELISA: correlation with clinical outcome. *American Journal of Cancer Research, 6*, 61-70.

Drenberg, C. D., Saunders, B. O., Wilbanks, G. D., Chen, R., Nicosia, R. F., Kruk, P. A., & Nicosia, S. V. (2010). Urinary angiostatin levels are elevated in patients with epithelial ovarian cancer. *Gynecologic Oncology, 117*, 117-124.

Duffy, M. J., O'siorain, L., O'grady, P., Devaney, D., Fennelly, J. J., & Lijnen, H. J. (1988). Urokinase‐plasminogen activator, a marker for aggressive breast carcinomas. Preliminary report. *Cancer, 62*, 531-533.

Duffy, M. J. (2004). The urokinase plasminogen activator system: role in malignancy. *Current Pharmaceutical Design, 10*, 39-49.

Duffy, M. J., McGowan, P. M., Harbeck, N., Thomssen, C., & Schmitt, M. (2014). uPA and PAI-1 as biomarkers in breast cancer: validated for clinical use in level-of-evidence-1 studies. *Breast Cancer Research*, *16*, 1.

Dvorak, H. F. (1986). Tumors: Wounds that do not heal. Similarities between tumor stroma generation and wound healing. *New England Journal of Medicine, 315,* 1650-1659.

Escudero, J. M., Auge, J. M., Filella, X., Torne, A., Pahisa, J., & Molina, R. (2011) The utility of serum human epididymis protein 4 (HE4) in patients with malignant and non malignant diseases: comparison with CA125. *Clinical Chemistry, 57*, 1534-1544.

Ferlay, J., Soerjomataram, I., Ervik, M., Dikshit, R., Eser, S., Mathers, C., Rebelo, M., Parkin, D. M., Forman, D., & Bray, F. (2014). GLOBOCAN 2012 v1.1, Cancer incidence and mortality worldwide: IARC CancerBase No. 11 [Internet]. Lyon, France: International Agency for Research on Cancer. [Web page] Retrieved from http://globocan.iarc.fr, accessed on 16/01/2015.

Ferrier, C. M., de Witte, H. H., Straatman, H., van Tienoven, D. H., van Geloof, W. L., Rietveld, F. J., Sweep, C. G., Ruiter, D. J., & van Muijen, G. N. (1999). Comparison of immunohistochemistry with immunoassay (ELISA) for the detection of components of the plasminogen activation system in human tumour tissue. *British Journal of Cancer, 79*, 1534-1541.

Fisher, J. L., Mackie, P. S., Howard, M. L., Zhou, H., & Choong P. F. (2001). The expression of the urokinase plasminogen activator system in metastatic murine osteosarcoma: an *in vivo* mouse model. *Clinical Cancer Research, 7*, 1654-1660.

Foekens, J. A., Peters, H. A., Look, M. P., Portengen, H., Schmitt, M., Kramer, M. D., Brünner, N., Jänicke, F., Meijer-van Gelder, M. E., Henzen-Logmans, S. C., van Putten, W. L., & Klijn, J. G. (2000). The urokinase system of plasminogen activation and prognosis in 2780 breast cancer patients. *Cancer Research, 60*, 636-643.

Folkman, J. (2002, December). Role of angiogenesis in tumor growth and metastasis. *In Seminars in Oncology, 6*, 15-18.

Friedman, G. C., & Seeds, N. W. (1994). Tissue plasminogen activator expression in the embryonic nervous system. *Developmental Brain Research*, *81*, 41-49.

Fuessel, S., Erdmann, K., Taubert, H., Lohse-Fischer, A., Zastrow, S., Meinhardt, M., Bluemke, K., Hofbauer, L., Fornara, P., Wullich, B., & Baretton, G. (2014). Prognostic impact of urokinase-type plasminogen activator system components in clear cell renal cell carcinoma patients without distant metastasis. *BMC Cancer, 14,* 1.

Gately, S., Twardowski, P., Stack, M. S., Patrick, M., Boggio, L., Cundiff, D. L., Schnaper, H. W., Madison, L., Volpert, O., Bouck, N., Enghild, J., Kwaan, H. C., & Soff, G. A. (1996). Human prostate carcinoma cells express enzymatic activity that converts human plasminogen to the angiogenesis inhibitor, angiostatin. *Cancer Research, 56*, 4887-4890.

Gately, S., Twardowski, P., Stack, M. S., Cundiff, D. L., Grella, D., Castellino, F. J., Enghild, J., Kwaan, H. C., Lee, F., Kramer, R. A., Volpert, O., Bouck, N., & Soff, G. A. (1997). The mechanism of cancer-mediated conversion of plasminogen to the angiogenesis inhibitor angiostatin. *Proceedings of the National Academy of Sciences, 94*, 10868-10872.

Gebbink, M. F. B. G. (2011). Tissue‐type plasminogen activator‐mediated plasminogen activation and contact activation, implications in and beyond haemostasis. *Journal of Thrombosis and Haemostasis, 9,* 174-181.

Gils, A., & Declerck, P. J. (2004). The structural basis for the pathophysiological relevance of PAI-1 in cardiovascular diseases and the development of potential PAI-1 inhibitors. *Thrombosis and Haemostasis, 91*, 425-437.

Gutova, M., Najbauer, J., Gevorgyan, A., Metz, M. Z., Weng, Y., Shih, C. C., & Aboody, K. S. (2007). Identification of uPAR-positive chemoresistant cells in small cell lung cancer. *PLoS ONE, 2*, e243.

Győrffy, B., Lánczky, A., & Szállási, Z. (2012). Implementing an online tool for genome-wide validation of survival-associated biomarkers in ovarian-cancer using microarray data from 1287 patients. *Endocrine-related Cancer, 19*, 197-208.

Harbeck, N., Kates, R. E., Look, M. P., Meijer-Van Gelder, M. E., Klijn, J. G., Kruger, A., Kiechle, M., Jaenicke, F., Schmitt, M., & Foekens, J. A. (2002). Enhanced benefit from adjuvant chemotherapy in breast cancer patients classified high-risk according to urokinase-type plasminogen activator (uPA) and plasminogen activator inhibitor type 1 (n = 3424). *Cancer Research, 62*, 4617-4622.

Harbeck, N., Schmitt, M., Meisner, C., Friedel, C., Untch, M., Schmidt, M., Sweep, C. G. J., Lisboa, B. W., Lux, M. P., Beck, T., & Hasmüller, S. (2013). Ten-year analysis of the prospective multicentre Chemo-N0 trial validates American Society of Clinical Oncology (ASCO)-recommended biomarkers uPA and PAI-1 for therapy decision making in node-negative breast cancer patients. *European Journal of Cancer*, *49*, 1825-1835.

Harries, M., & Gore, M. (2002). Part I: chemotherapy for epithelial ovarian cancer-treatment at first diagnosis. *Lancet Oncology, 3*, 529-536.

Hataji, O., Taguchi, O., Gabazza, E. C., Yuda, H., D'Alessandro‐Gabazza, C. N., Fujimoto, H., Nishii, Y., Hayashi, T., Suzuki, K., & Adachi, Y. (2004). Increased circulating levels of thrombin‐activatable fibrinolysis inhibitor in lung cancer patients. *American Journal of Hematology, 76*, 214-219.

Häckel, C. G., Krueger, S., Grote, H. J., Oshiro, Y., Hodges, S., Johnston, D. A., Johnson, M. E., Roessner, A., Ayala, A. G., & Czerniak, B. (2000). Overexpression of cathepsin B and urokinase plasminogen activator is associated with increased risk of recurrence and metastasis in patients with chondrosarcoma. *Cancer, 89*, 995-1003.

Hägglund, A. C., Ny, A., Liu, K., & Ny, T. (1996). Coordinated and cell-specific induction of both physiological plasminogen activators creates functionally redundant mechanisms for plasmin formation during ovulation. *Endocrinology*, *137*, 5671-5677.

Heinemann, V., Ebert, M. P., Laubender, R. P., Bevan, P., Mala, C., & Boeck, S. (2013). Phase II randomised proof-of-concept study of the urokinase inhibitor upamostat (WX-671) in combination with gemcitabine compared with gemcitabine alone

in patients with non-resectable, locally advanced pancreatic cancer. *British Journal of Cancer, 108,* 766-770.

Henry, N. L., & Hayes, D. F. (2012). Cancer Biomarkers. *Molecular Oncology, 6*, 140-146.

Herceg, G. H., Herceg, D., Kralik, M., Kulic, A., Bence-Zigman, Z., Tomic-Brzac, H., Bracic, I., Kusacic-Kuna, S., & Prgomet, D. (2013). Urokinase plasminogen activator and its inhibitor type-1 as prognostic factors in differentiated thyroid carcinoma patients. *Otolaryngology-Head and Neck Surgery, 149*, 533-540.

Higuchi, R., Fockler, C., Dollinger, G., & Watson, R. (1993). Kinetic PCR analysis: Real-time monitoring of DNA amplification reactions. *Biotechnology, 11*, 1026-1030.

Hildenbrand, R., Schaaf, A., Dorn-Beineke, A., Allgayer, H., Sütterlin, M., Marx, A., & Stroebel, P. (2009). Tumor stroma is the predominant uPA-, uPAR-, PAI-1-expressing tissue in human breast cancer: prognostic impact. *Histology and Histopathology, 24*, 869-877.

Hofmann, G. E., Glatstein, I., Schatz, F., Heller, D., & Deligdisch, L. (1994). Immunohistochemical localization of urokinase-type plasminogen activator and the plasminogen activator inhibitors 1 and 2 in early human implantation sites. *American Journal of Obstetrics and Gynecology, 170*, 671-676.

Hofmann, R., Lehmer, A., Buresch, M., Hartung, R., & Ulm, K. (1996). Clinical relevance of urokinase plasminogen activator, its receptor, and its inhibitor in patients with renal cell carcinoma. *Cancer, 78,* 487-492.

Hoskins, W. J., McGuire, W. P., Brady, M. F., Homesley, H. D., Creasman, W. T., Berman, M., Ball, H., & Berek, J. S. (1994). The effect of diameter of largest residual disease on survival after primary cytoreductive surgery in patients with suboptimal residual epithelial ovarian carcinoma. *American Journal of Obstetrics and Gynecology, 170*, 974-979.

Howlader, N., Noone, A. M., Krapcho, M., Neyman, N., Aminou, R., Waldron, W., Altekruse, S. F., Kosary, C. L., Ruhl, J., Tatalovich, Z., Cho, H., Mariotto, A., Eisner, M. P., Lewis, D. R., Chen, H. S., Feuer, E. J., & Cronin, K. A. (Eds). (2015). SEER Cancer

Statistics Review, 1975-2011, National Cancer Institute; Bethesda [Web page] Retrieved from http://seer.cancer.gov/csr/1975_2009_pops09/.

Hsu, D. W., Efird, J. T., & Hedley-Whyte, E. T. (1995). Prognostic role of urokinase-type plasminogen activator in human gliomas. *The American Journal of Pathology, 147*, 114.

Javaherian, K., Lee, T. Y., Sjin, R. M. T. T., Parris, G. E., & Hlatky, L. (2011). Two endogenous antiangiogenic inhibitors, endostatin and angiostatin, demonstrate biphasic curves in their antitumor profiles. *Dose-Response, 9*, 369-376.

Jänicke, F., Schmitt, M., Ulm, K., Grösser, W., & Graeff, H. (1989). Urokinase-type plasminogen activator antigen is a predictor of early relapse in breast cancer. *Lancet, 28*, 1049.

Jänicke, F., Schmitt, M., Pache, L., Ulm, K., Harbeck, N., Höfler, H., & Graeff, H. (1993). Urokinase (uPA) and its inhibitor PAI-1 are strong and independent prognostic factors in node-negative breast cancer. *Breast Cancer Research and Treatment*, *24*, 195-208.

Jänicke, F., Prechtl, A., Thomssen, C., Harbeck, N., Meisner, C., Untch, M., Sweep, C. F., Selbmann, H. K., Graeff, H., Schmitt, M., & German Chemo N0 Study Group. (2001). Randomized adjuvant chemotherapy trial in high-risk, lymph node-negative breast cancer patients identified by urokinase-type plasminogen activator and plasminogen activator inhibitor type 1. *Journal of the National Cancer Institute*, *93*, 913-920.

Ji, F., Chen, Y. L., Jin, E. Y., Wang, W. L., Yang, Z. L., & Li, Y. M. (2005). Relationship between matrix metalloproteinase-2 mRNA expression and clinicopathological and urokinase-type plasminogen activator system parameters and prognosis in human gastric cancer. *World Journal of Gastroenterology, 11*, 3222-3226.

Kanno, Y., Kuroki, A., Minamida, M., Kaneiwa, A., Okada, K., Tomogane, K., Takeuchi, K., Ueshima, S., Matsuo, O., & Matsuno, H. (2008). The absence of uPAR attenuates insulin-induced vascular smooth muscle cell migration and proliferation. *Thrombosis Research, 123*, 336-341.

Kaplan, E. L., & Meier, P. (1958). Nonparametric estimation from incomplete observations. *Journal of the American Statistical Association, 53*, 457-481.

Kauff, N. D., Domchek, S. M., Friebel, T. M., Lee, J. B., Roth, R., Robson, M. E., Barakat, R. R., Norton, L., Offit, K., Rebbeck, T. R., & the PROSE Study Group. (2006). Multi-center prospective analysis of risk-reducing salpingo-oophorectomy to prevent BRCA-associated breast and ovarian cancer. *Journal of Clinical Oncology*, *2006 ASCO Annual Meeting Proceedings Part I, 24*, 1003.

Kenny, H. A., Leonhardt, P., Ladanyi, A., Yamada, S. D., Montag, A., Im, H. K., Jagadeeswaran, S., Shaw, D. E., Mazar, A. P., & Lengyel, E. (2011). Targeting the urokinase plasminogen activator receptor inhibits ovarian cancer metastasis. *Clinical Cancer Research, 17*, 459-471.

Kipps, E., Tan, D. S., & Kaye, S. B. (2013). Meeting the challenge of ascites in ovarian cancer: new avenues for therapy and research. *Nature Reviews Cancer, 13*, 273-282.

Kobayashi, H., Fujishiro, S., & Terao, T. (1994). Impact of urokinase-type plasminogen activator and its inhibitor type 1 on prognosis in cervical cancer of the uterus. *Cancer Research, 54*, 6539-6548.

Kodama, J., Miyagi, Y., Seki, N., Tokumo, K., Yoshinouchi, M., Kobashi, Y., Okuda, H., & Kudo, T. (1999). Serum c-reactive protein as a prognostic factor in patients with epithelial ovarian cancer. *European Journal of Obstetrics & Gynecology and Reproductive Biology, 82*, 107-110.

Koensgen, D., Mustea, A., Denkert, C., Sun, P. M., Lichtenegger, W., & Sehouli, J. (2006). Overexpression of the plasminogen activator inhibitor type-1 in epithelial ovarian cancer. *Anticancer Research, 26,* 1683-1689.

Koensgen, D., Mustea, A, Klaman, I., Sun, P., Zafrakas, M., Lichtenegger, W., Denkert, C., Dahl, E., & Sehouli, J. (2007). Expression analysis and RNA localization of PAI-RBP1 (SERBP1) in epithelial ovarian cancer: association with tumor progression. *Gynecologic Oncology, 107*, 266-273.

Koh, S. C., Khalil, R., Lim, F. K., Ilancheran, A., & Choolani, M. (2006). The association between fibrinogen, von Willebrand Factor, antithrombin III, and D-dimer levels and survival outcome by 36 months from ovarian cancer. *Clinical and Applied Thrombosis/Hemostasis, 12*, 3-8.

Kohler, M. F., Kerns, B. J., Humphrey, P. A., Marks, J. R., Bast Jr, R. C., & Berchuck, A. (1993). Mutation and overexpression of p53 in early-stage epithelial ovarian cancer. *Obstetrics and Gynecology, 81*, 643-650.

Komiyama, S., Aoki, D., Saitoh, E., Komiyama, M., & Udagawa, Y. (2011). Biological significance of plasminogen activator inhibitor-1 expression in ovarian clear cell adenocarcinoma. *European Journal of Gynaecological Oncology, 32*, 611-614.

Konecny, G., Untch, M., Pihan, A., Kimmig, R., Gropp, M., Stieber, P., Hepp, H., Slamon, D., & Pegram, M. (2001). Association of urokinase-type plasminogen activator and its inhibitor with disease progression and prognosis in ovarian cancer. *Clinical Cancer Research, 7*, 1743-1749.

Kuhn, W., Pache, L., Schmalfeldt, B., Dettmar, P., Schmitt, M., Jänicke, F., & Graeff, H. (1994). Urokinase (uPA) and PAI-1 predict survival in advanced ovarian cancer patients (FIGO III) after radical surgery and platinum-based chemotherapy. *Gynecologic Oncology, 55*, 401-409.

Kuhn, W., Schmalfeldt, B., Reuning, U., Pache, L., Berger, U., Ulm, K., Harbeck, N., Späthe, K., Dettmar, P., Höfler, H., Jänicke, F., Schmitt, M., & Graeff, H. (1999). Prognostic significance of urokinase (uPA) and its inhibitor PAI-1 for survival in advanced ovarian carcinoma stage FIGO IIIc. *British Journal of Cancer, 79*, 1746-1751.

Kuhn, W., Rutke, S., Späthe, K., Schmalfeldt, B., Florack, G., von Hundelshausen, B., Pachyn, D., Ulm, K., & Graeff, H. (2001). Neoadjuvant chemotherapy followed by tumor debulking prolongs survival for patients with poor prognosis in International Federation of Gynecology and Obstetrics Stage IIIC ovarian carcinoma. *Cancer, 92*, 2585-2591.

Kwaan, H. C., & McMahon, B. (2009). The role of plasminogen-plasmin system in cancer. *Coagulation in Cancer*, 148, 43.

Kwaan, H. C., Mazar, A. P., & McMahon, B. J. (2013). The apparent uPA/PAI-1 paradox in cancer: more than meets the eye. In Seminars in thrombosis and hemostasis. *Thieme Medical Publishers, 39*, 382-391.

Lala, P. K., & Graham, C. H. (1990). Mechanisms of trophoblast invasiveness and their control: the role of proteases and protease inhibitors. *Cancer and Metastasis Reviews*, *9*, 369-379.

Lamy, P. J., Verjat, T., Servanton, A. C., Paye, M., Leissner, P., & Mougin, B. (2007). Urokinase-type plasminogen activator and plasminogen activator inhibitor type-1 mRNA assessment in breast cancer by means of NASBA: correlation with protein expression. *Journal of Clinical Pathology, 128*, 404-413.

Lang, D. S., Heilenkötter, U., Schumm, W., Behrens, O., Simon, R., Vollmer, E., & Goldmann, T. (2013). Optimized immunohistochemistry in combination with image analysis: a reliable alternative to quantitative ELISA determination of uPA and PAI-1 for routine risk group discrimination in breast cancer. *Breast, 22*, 736-743.

Law, R. H., Abu-Ssaydeh, D., & Whisstock, J. C. (2013). New insights into the structure and function of the plasminogen/plasmin system. *Current Opinion in Structural Biology, 23*, 836-841.

Law, R. H., Caradoc-Davies, T., Cowieson, N., Horvath, A. J., Quek, A. J., Encarnacao, J. A., Steer, D., Cowan, A., Zhang, Q., Lu, B. G., & Pike, R. N. (2012). The X-ray crystal structure of full-length human plasminogen. *Cell Reports, 1,* 185-190.

Ledermann, J. A., Raja, F. A., Fotopoulou, C., Gonzalez-Martin, A., Colombo, N., Sessa, C., & ESMO, Guidelines Working Group. (2013). Newly diagnosed and relapsed epithelial ovarian carcinoma: ESMO Clinical Practice Guidelines for diagnosis, treatment and follow-up. *Annals of Oncology, 24*, vi24–vi32.

Leurer, C., & Shafaat Ahmed, R. (2015). Plasminogen activator system—diagnostic, prognostic and therapeutic implications in breast cancer. A concise review of molecular pathology of breast cancer. Book edited by Mehmet Gunduz, Published: March 25, 2015.

Li, H., Ye, X., Mahanivong, C., Bian, D., Chun, J., & Huang, S. (2005). Signaling mechanisms responsible for lysophosphatidic acid-induced urokinase plasminogen activator expression in ovarian cancer cells. *Journal of Biological Chemistry, 280*, 10564-10571.

Liu, G., Shuman, M. A., & Cohen, R. L. (1995). Co-expression of urokinase, urokinase receptor and PAI-1 is necessary for optimum invasiveness of cultured lung cancer cells. *International Journal of Cancer, 60*, 501-506.

Look, M. P., van Putten, W. L., Duffy, M. J., Harbeck, N., Christensen, I. J., Thomssen, C., Kates, R., Spyratos, F., Fernö, M., Eppenberger-Castori, S., Sweep, C. G., Ulm, K., Peyrat, J. P., Martin, P. M., Magdelenat, H., Brünner, N., Duggan, C., Lisboa, B. W., Bendahl, P. O., Quillien, V., Daver, A., Ricolleau, G., Meijer-van Gelder, M. E., Manders, P., Fiets, W. E., Blankenstein, M. A., Broët, P., Romain, S., Daxenbichler, G., Windbichler, G., Cufer, T., Borstnar, S., Kueng, W., Beex, L. V., Klijn, J. G., O'Higgins, N., Eppenberger, U., Jänicke, F., Schmitt, M., & Foekens, J. A. (2002). Pooled analysis of prognostic impact of urokinase-type plasminogen activator and its inhibitor PAI-1 in 8377 breast cancer patients. *Journal of the National Cancer Institute, 94*, 116-128.

Lopez, R. I., Paul, J., Atkinson, R., Soukop, M., Kitchener, H., Fullerton, W., Duncan, I., Kennedy, J., Davis, J., Maclean, A., Cassidy, J., Pyper, E., & Kaye, S. B. (1996). Prognostic factor analysis, for patients with no evidence of disease after initial chemotherapy for advanced epithelial ovarian carcinoma. *International Journal of Gynecological Cancer, 6*, 8-14.

Loskutoff, D. J., Linders, M., & Keijer, J. (1987). Structure of the human plasminogen activator inhibitor 1 gene: nonrandom distribution of introns. *Biochemistry, 26*, 3763-3768.

Luo, L. Y., Katsaros, D., Scorilas, A., Fracchioli, S., Bellino, R., van Gramberen, M., de Bruijn, H., Henrik, A., Stenman, U. H., Massobrio, M., van der Zee, A. G., Vergote, I., & Diamandis, E. P. (2003). The serum concentration of human kallikrein 10 represents a novel biomarker for ovarian cancer diagnosis and prognosis. *Cancer Research, 63*, 807-811.

Malgaretti, N., Bruno, L., Pontoglio, M., Candiani, G., Meroni, G., Ottolenghi, S., & Taramelli, R. (1990). Definition of the transcription initiation site of human plasminogen gene in liver and non hepatic cell lines. *Biochemical and Biophysical Research Communications, 173*, 1013-1018.

Man, Y. N., Wang, Y. N., Hao, J., Liu, X., Liu, C., Zhu, C., & Wu, X. Z. (2015). Pretreatment plasma D-dimer, fibrinogen, and platelet levels significantly impact

prognosis in patients with epithelial ovarian cancer independently of venous thromboembolism. *International Journal of Gynecological Cancer*, 25, 24-32.

Mashiko, S., Kitatani, K., Toyoshima, M., Ichimura, A., Dan, T., Usui, T., Ishibashi, M., Shigeta, S., Nagase, S., Miyata, T., & Yaegashi, N. (2015). Inhibition of plasminogen activator inhibitor-1 is a potential therapeutic strategy in ovarian cancer. *Cancer Biology & Therapy, 16*, 253-260.

Mazar, A. P., Ahn, R. W., & O'Halloran, T. V. (2011). Development of novel therapeutics targeting the urokinase plasminogen activator receptor (uPAR) and their translation toward the clinic. *Current Pharmaceutical Design, 17*, 1970-1978.

McMahon, B. J., & Kwaan, H. C. (2015). Components of the plasminogen-plasmin system as biologic markers for cancer. *In Advances in Cancer Biomarkers, Springer Netherlands*, 145-156.

Mehta, R., & Shapiro, A. D. (2008). Plasminogen deficiency. *Haemophilia, 14*, 1261-1268.

Mekkawy, A. H., Pourgholami, M. H., & Morris, D. L. (2014). Involvement of urokinase-type plasminogen activator system in cancer: an overview. *Medicinal Research Reviews, 34*, 918-956.

Memarzadeh, S., Kozak, K. R., Chang, L., Natarajan, S., Shintaku, P., Reddy, S. T., & Farias-Eisner, R. (2002). Urokinase plasminogen activator receptor: Prognostic biomarker for endometrial cancer. *Proceedings of the National Academy of Sciences of the United States of America, 99*, 10647-10652.

Mengele, K., Napieralski, R., Magdolen, V., Reuning, U., Gkazepis, A., Sweep, F., Brünner, N., Foekens, J., Harbeck, N., & Schmitt, M. (2010). Characteristics of the level-of-evidence-1 disease forecast cancer biomarkers uPA and its inhibitor PAI-1. *Expert Review of Molecular Diagnostics, 10*, 947-962.

Meyer, J. E., Brocks, C., Graefe, H., Mala, C., Thäns, N., Bürgle, M., Rempel, A., Rotter, N., Wollenberg, B., & Lang, S. (2008). The oral serine protease inhibitor WX-671–first experience in patients with advanced head and neck carcinoma. *Breast Care, 3,* 20-24.

Molina, R., Escudero, J. M., Augé, J. M., Filella, X., Foj, L., Torné, A., Lejarcegui, J., & Pahisa, J. (2011). HE4 a novel tumour marker for ovarian cancer: comparison with CA 125 and ROMA algorithm in patients with gynaecological diseases. *Tumour Biology, 32*, 1087-1095.

Montuori, N., Visconte, V., Rossi, G., & Ragno, P. (2005). Soluble and cleaved forms of the urokinase-receptor: degradation products or active molecules. *Thrombosis and Haemostasis, 93*, 192-198.

Moonen, G., Grau-Wagemans, M. P., & Selak, I. (1982). Plasminogen activator–plasmin system and neuronal migration. *Nature, 298,* 753-755.

Moore, R. G., Brown, A. K., Miller, M. C., Skates, S., Allard, W. J., Verch, T., Steinhoff, M., Messerlian, G., DiSilvestro, P., Granai, C. O., & Bast, R. C. Jr. (2007). The use of multiple novel tumor biomarkers for the detection of ovarian carcinoma in patients with a pelvic mass. *Gynecologic Oncology, 108*, 402-408.

Moore, R. G., Jabre-Raughley, M., Brown, A. K., Robison, K. M., Miller, M. C., Allard, W. J., Kurman, R. J., Bast, R. C., & Skates, S. J. (2010). Comparison of a novel multiple marker assay vs the risk of malignancy index for the prediction of epithelial ovarian cancer in patients with a pelvic mass. *American Journal of Obstetrics and Gynecology, 203*, 228-226.

Möbus, V., Gerharz, C. D., Press, U., Moll, R., Beck, T., Mellin, W., Pollow, K., Knapstein, P. G., & Kreienberg, R. (1992). Morphological, immunohistochemical and biochemical characterization of 6 newly established human ovarian carcinoma cell lines. *International Journal of Cancer, 52*, 76-84.

Murthi, P., Barker, G., Nowell, C. J., Rice, G. E., Baker, M. S., Kalionis, B., & Quinn, M. A. (2004). Plasminogen fragmentation and increased production of extracellular matrix-degrading proteinases are associated with serous epithelial ovarian cancer progression. *Gynecologic Oncology, 92*, 80-88.

Nekarda, H., Schmitt, M., Ulm, K., Wenninger, A., Vogelsang, H., Becker, K., Roder, J. D., Fink, U., & Siewert, J. R. (1994). Prognostic impact of urokinase-type plasminogen

activator and its inhibitor PAI-1 in completely resected gastric cancer. *Cancer Research, 54*, 2900-2907.

Nekarda, H., Schlegel, P., Schmitt, M., Stark, M., Mueller, J. D., Fink, U., & Siewert, J. R. (1998). Strong prognostic impact of tumor-associated urokinase-type plasminogen activator in completely resected adenocarcinoma of the esophagus. *Clinical Cancer Research, 4*, 1755-1763.

Nordengren, J., Fredstorp, Lidebring, M., Bendahl, P. O., Brünner, N., Fernö, M., Högberg, T., Stephens, R. W., Willén, R., & Casslén, B. (2002). High tumor tissue concentration of plasminogen activator inhibitor 2 (PAI-2) is an independent marker for shorter progression-free survival in patients with early stage endometrial cancer. *International Journal of Cancer, 97*, 379-385.

Nordgard, O., Kvaloy, J. T., Farmen, R. K., & Heikkila, R. (2006). Error propagation in relative real-time reverse transcription polymerase chain reaction quantification models: the balance between accuracy and precision. *Analytical Biochemistry, 356*, 182-193.

Novokhatny, V., Medved, L., Mazar, A., Marcotte, P., Henkin, J., & Ingham, K. (1992). Domain structure and interactions of recombinant urokinase-type plasminogen activator. *Journal of Biological Chemistry, 267,* 3878-3885.

Nykjaer, A., Conese, M., Christensen, E. I., Olson, D., Cremona, O., Gliemann, J., & Blasi, F. (1997). Recycling of the urokinase receptor upon internalization of the uPA: serpin complexes. *The EMBO Journal*, 2610-2620.

O'Brien, T. J., Beard, J. B., Underwood, L. J., & Shigemasa, K. (2002). The CA125 gene: a newly discovered extension of the glycosylated N-terminal domain doubles the size of this extracellular superstructure. *Tumour Biology, 23,* 154-169.

Ohtani, H., Pyke, C., Dan, Ø., & Nagura, H. (1995). Expression of urokinase receptor in various stromal - cell populations in human colon cancer: Immunoelectron microscopical analysis. *International Journal of Cancer, 62,* 691-696.

O'Reilly, M. S., Wiederschain, D., Stetler-Stevenson, W. G., Folkman, J., & Moses, M. A. (1999). Moses Regulation of angiostatin production by matrix metalloproteinase-2 in a model of concomitant resistance. *Journal of Biological Chemistry, 274*, 29568-29571.

Ovarian cancer. (n.d.). American Cancer Society. [Web page] Retrieved August 02, 2016, from http://www.cancer.org/cancer/ovariancancer/index.

Ovarian cancer statistics. (2015). Cancer Research UK. [Web page] Retrieved August 02, 2016, from http://www.cancerresearchuk.org/health-professional/cancer-statistics/statistics-by-cancer-type/ovarian-cancer#heading-Zero.

Pappot, H., Gårdsvoll, H., Rømer, J., Pedersen, A. N., Grøndahl-Hansen, J., Pyke, C., & Brünner, N. (1995). Plasminogen activator inhibitor type 1 in cancer: therapeutic and prognostic implications. *Biological Chemistry Hoppe-Seyler, 376*, 259-267.

Pappot, H., Skov, B. G., Pyke, C., & Grøndahl-Hansen, J. (1997). Levels of plasminogen activator inhibitor type 1 and urokinase plasminogen activator receptor in non-small cell lung cancer as measured by quantitative ELISA and semiquantitative immunohistochemistry. *Lung Cancer, 17,* 197-209.

Pedersen, A. N., Mouridsen, H. T., Tenney, D. Y., & Brünner, N. (2003). Immunoassays of urokinase (uPA) and its type-1 inhibitor (PAI-1) in detergent extracts of breast cancer tissue. *European Journal of Cancer Prevention, 39*, 899-908.

Pedersen, N., Schmitt, M., Rønne, E., Nicoletti, M. I., Høyer-Hansen, G., Conese, M., Giavazzi, R., Dano, K., Kuhn, W., & Jänicke, F. (1993). A ligand-free, soluble urokinase receptor is present in the ascitic fluid from patients with ovarian cancer. *Journal of Clinical Investigation, 92*, 2160-2167.

Pepper, M. S. (2001). Role of the matrix metalloproteinase and plasminogen activator–plasmin systems in angiogenesis. *Arteriosclerosis, Thrombosis, and Vascular Biology*, *21*, 1104-1117.

Permuth-Wey & Sellers. (2009). Epidemiology of ovarian cancer. *Cancer Epidemiology: Modifiable Factors, 413-437.*

Perri, S. R., Martineau, D., François, M., Lejeune, L., Bisson, L., Durocher, Y., & Galipeau, J. (2007). Plasminogen Kringle 5 blocks tumor progression by antiangiogenic and proinflammatory pathways. *Molecular Cancer Therapeutics, 6*, 441-449.

Petersen, T. E., Martzen, M. R., Ichinose, A., & Davie, E. W. (1990). Characterization of the gene for human plasminogen, a key proenzyme in the fibrinolytic system. *Journal of Biological Chemistry, 265*, 6104-6111.

Piironen, T., Haese, A., Huland, H., Steuber, T., Christensen, I. J., Brünner, N., Danø, K., Høyer-Hansen, G., & Lilja, H. (2006). Enhanced discrimination of benign from malignant prostatic disease by selective measurements of cleaved forms of urokinase receptor in serum. *Clinical Chemistry, 52*, 838-844.

Ploug, M. (2003). Structure-function relationships in the interaction between the urokinase-type plasminogen activator and its receptor. *Current Pharmaceutical Design, 9*, 1499-1528.

Polterauer, S., Vergote, I., Concin, N., Braicu, I., Chekerov, R., Mahner, S., Woelber, L., Cadron, I., Van Gorp, T., Zeillinger, R., Castillo-Tong, D. C., & Sehouli, J. (2012). Prognostic value of residual tumor size in patients with epithelial ovarian cancer FIGO stages IIA-IV: analysis of the OVCAD data. *International Journal of Gynecological Cancer, 22*, 380-385.

Prat, J. (2012). New insights into ovarian cancer pathology. *Annals of Oncology, 23*, x111-x117.

Ragno, P. (2006). The urokinase receptor: a ligand or a receptor? Story of a sociable molecule. *Cellular and Molecular Life Sciences CMLS, 63*, 1028-1037.

Rasch, M. G., Lund, I. K., Almasi, C. E., & Hoyer-Hansen, G. (2008). Intact and cleaved uPAR forms: diagnostic and prognostic value in cancer. *Frontiers in Bioscience, 13*, 6752-6762.

Rasmussen, R. (2001). Quantification on the LightCycler. In Rapid cycle real-time PCR. *Springer Berlin Heidelberg*, 21-34.

Reich, R., Miskin, R., & Tsafriri, A. (1985). Follicular plasminogen activator: involvement in ovulation. *Endocrinology*, *116*, 516-521.

Ren, F., Shi, H., Zhang, G., & Zhang, R. (2013). Expression of deleted in liver cancer and plasminogen activator inhibitor 1 protein in ovarian carcinoma and their clinical significance. *Journal of Experimental & Clinical Cancer Research, 32*, 60.

Riisbro, R., Christensen, I. J., Nielsen, H. J., Brunner, N., Nilbert, M., & Fernebro, E. (2005). Preoperative plasma soluble urokinase plasminogen activator receptor as a prognostic marker in rectal cancer patients. An EORTC-Receptor and Biomarker Group collaboration. *The International Journal of Biological Markers, 20*, 93-102.

Rijken, D. C., & Lijnen, H. R. (2009). New insights into the molecular mechanisms of the fibrinolytic system. *Journal of Thrombosis and Haemostasis, 7*, 4-13.

Roett, M. A., & Evans, P. (2009). Ovarian cancer: an overview. *American Academy of Family Physicians, 80*, 609-616.

Roy, D. M., & Walsh, L. A. (2014). Candidate prognostic markers in breast cancer: focus on extracellular proteases and their inhibitors. *Breast Cancer, 6*, 81-91.

Ruijter, J., Pfaffl, M., Zhao, S., Spiess, A., Boggy, G., Blom, J., Rutledge, R. G., Sisti, D., Lievens, A., De Preter, K., Derveaux, S., Hellemans, J., & Vandesompele, J. (2013). Evaluation of qPCR curve analysis methods for reliable biomarker discovery: bias, resolution, precision, and implications. *Methods, 59*, 32-46.

Sakurai, M., Satoh, T., Matsumoto, K., Shikama, A., Michikami, H., Tasaka, N., Nakamura, Y., Nakao, S., Ochi, H., Onuki, M., & Minaguchi, T. (2014). High pretreatment plasma D-dimer Levels are associated with poor prognosis in patients with ovarian cancer independently of venous thromboembolism and tumor extension. *International Journal of Gynecological Cancer: Official Journal of the International Gynecological Cancer Society, 25*, 593-598.

Salamonsen, L. A. (1999). Role of proteases in implantation. *Reviews of Reproduction*, *4*, 11-22.

Sappino, A. P., Huarte, J., Belin, D., & Vassalli, J. D. (1989). Plasminogen activators in tissue remodeling and invasion: mRNA localization in mouse ovaries and implanting embryos. *The Journal of Cell Biology*, *109*, 2471-2479.

Schmalfeldt, B., Kuhn, W., Reuning, U., Pache, L., Dettmar, P., Schmitt, M., Jänicke, F., Höfler, H., & Graeff, H. (1995). Primary tumor and metastasis in ovarian cancer differ in their content of urokinase-type plasminogen activator, its receptor, and inhibitors types 1 and 2. *Cancer Research, 55*, 3958-3963.

Schmalfeldt, B., Prechtel, D., Harting, K., Spathe, K., Rutke, S., Konik, E., Fridman, R., Berger, U., Schmitt, M., Kuhn, W., & Lengyel, E. (2001). Increased expression of matrix metalloproteinases (MMP)-2, MMP-9, and the urokinase-type plasminogen activator is associated with progression from benign to advanced ovarian cancer. *Clinical Cancer Research, 7,* 2396-2404.

Schmitt, M., Mengele, K., Schueren, E., Sweep, F. C., Foekens, J. A., Brünner, N., Laabs, J., Malik, A., & Harbeck, N. (2007). European Organisation for Research and Treatment of Cancer (EORTC) Pathobiology Group standard operating procedure for the preparation of human tumour tissue extracts suited for the quantitative analysis of tissue-associated biomarkers. *European Journal of Cancer, 43,* 835-844.

Schmitt, M., Mengele, K., Napieralski, R., Magdolen, V., Reuning, U., Gkazepis, A., Gkazepis, A., Sweep, F., Brünner, N., Foekens, J., & Harbeck, N. (2010). Clinical utility of level-of-evidence-1 disease forecast cancer biomarkers uPA and its inhibitor PAI-1. *Expert Review of Molecular Diagnostics, 10*, 1051-1067.

Schmitt, M., Harbeck, N., Brünner, N., Jänicke, F., Meisner, C., Mühlenweg, B., Jansen, H., Dorn, J., Nitz, U., Kantelhardt, E. J., & Thomssen, C. (2011). Cancer therapy trials employing level-of-evidence-1 disease forecast cancer biomarkers uPA and its inhibitor PAI-1. *Expert Review of Molecular Diagnostics, 11*, 617–634.

Schmitt, M., Magdolen, V., Yang, F., Kiechle, M., Bayani, J., Yousef, G. M., Scorilas, A., Diamandis, E. P., & Dorn, J. (2013). Emerging clinical importance of the cancer biomarkers kallikrein-related peptidases (KLK) in female and male reproductive organ malignancies. *Radiology and Oncology, 47*, 319-329.

Scholler, N., Fu, N., Yang, Y., Ye, Z., Goodman, G. E., Hellström, K. E., & Hellström, I. (1999). Soluble member(s) of the mesothelin/megakaryocyte potentiating factor family are detectable in sera from patients with ovarian carcinoma. *Proceedings of the National Academy of Sciences, 96*, 11531-11536.

Scholler, N., & Urban, N. (2007). CA125 in ovarian cancer. *Biomarkers in Medicine, 1,* 513-523.

Seetoo, D. Q., Crowe, P. J., Russell, P. J., & Yang, J. L. (2003). Quantitative expression of protein markers of plasminogen activation system in prognosis of colorectal cancer. *Journal of Surgical Oncology, 82*, 184-193.

Shetty, S., Kumar, A., Johnson, A., Pueblitz, S., & Idell, S. (1995). Urokinase receptor in human malignant mesothelioma cells: role in tumor cell mitogenesis and proteolysis. *The Journal of Physiology, 268,* L972-L982.

Simmons, A. R., Baggerly, K., & Bast, R. C. Jr. (2013). The emerging role of HE4 in the evaluation of epithelial ovarian and endometrial carcinomas. *Oncology (Williston Park), 27*, 548-556.

Spyratos, F., Bouchet, C., Tozlu, S., Labroquere, M., Vignaud, S., Becette, V., Lidereau, R., & Bieche, I. (2002). Prognostic value of uPA, PAI-1 and PAI-2 mRNA expression in primary breast cancer. *Anticancer Research, 22*, 2997-3003.

Stephens, R. W., Nielsen, H. J., Christensen, I. J., Thorlacius-Ussing, O., Sørensen, S., Danø, K., & Brünner, N. (1999). Plasma urokinase receptor levels in patients with colorectal cancer: relationship to prognosis. *Journal of the National Cancer Institute, 91*, 869-874.

Stoppelli, M. P., Corti, A., Soffientini, A., Cassani, G., Blasi, F., & Assoian, R. K. (1985). Differentiation-enhanced binding of the amino-terminal fragment of human urokinase plasminogen activator to a specific receptor on U937 monocytes. *Proceedings of the National Academy of Sciences of the United States of America, 82*, 4939-4943.

Su, C. Y., Liu, Y. P., Yang, C. J., Lin, Y. F., Chiou, J., Chi, L. H., Lee, J. J., Wu, A. T., Lu, P. J., Huang, M. S., & Hsiao, M. (2015). Plasminogen activator inhibitor-2 plays a leading prognostic role among protease families in mon-small cell lung cancer. *PLoS One, 10*, e0133411.

Su, S. C., Lin, C. W., Yang, W. E., Fan, W. L., & Yang, S. F. (2016). The urokinase-type plasminogen activator (uPA) system as a biomarker and therapeutic target in human malignancies. *Expert Opinion on Therapeutic Targets, 20*, 551-566.

Sweep, C. G., Geurts-Moespot, J., Grebenschikov, N., De Witte, J. H., Heuvel, J. J., Schmitt, M., Duffy, M. J., Jänicke, F., Kramer, M. D., Foekens, J. A., & Brünner, N. (1998). External quality assessment of trans-European multicentre antigen determinations (enzyme-linked immunosorbent assay) of urokinase-type plasminogen activator (uPA) and its type 1 inhibitor (PAI-1) in human breast cancer tissue extracts. *British Journal of Cancer*, *78*, 1434.

Sweep, F. C., Thomas, C. M., & Schmitt, M. (2006). Analytical aspects of biomarker immunoassays in cancer research. *In Biomarkers in Breast Cancer* (pp. 17-30). Humana Press.

Swiercz, R., Wolfe, J. D., Zaher, A., & Jankun, J. (1998). Expression of the plasminogen activation system in kidney cancer correlates with its aggressive phenotype. *Clinical Cancer Research, 4*, 869-877.

Tan, Y., Hilmy, M. H., Hung, H., & Tan, P. H. (2013). Initial experience with tissue microarray in a surgical pathology laboratory: technical considerations. *Journal of Histotechnology, 2,* 113-117.

Taylor, S., Wakem, M., Dijkman, G., Alsarraj, M., & Nguyen, M. (2010). A practical approach to RT-qPCR-Publishing data that conform to the MIQE guidelines. *Methods, 50*, S1-5.

Terry, K. L., Sluss, P. M., Skates, S. J., Mok, S. C., Ye, B., Vitonis, A. F., & Cramer, D. W. (2004). Blood and urine markers for ovarian cancer: a comprehensive review. *Disease Markers, 20*, 53.

Uhlén, M., Fagerberg, L., Hallström, B. M., Lindskog, C., Oksvold, P., Mardinoglu, A., Sivertsson, Å., Kampf, C., Sjöstedt, E., Asplund, A., Olsson, I., Edlund, K., Lundberg, E., Navani, S., Szigyarto, C. A., Odeberg, J., Djureinovic, D., Takanen, J. O., Hober, S., Alm, T., Edqvist, P. H., Berling, H., Tegel, H., Mulder, J., Rockberg, J., Nilsson, P., Schwenk, J. M., Hamsten, M., von Feilitzen, K., Forsberg, M., Persson, L., Johansson,

F., Zwahlen, M., von Heijne, G., Nielsen, J., & Pontén, F. (2015). Tissue-based map of the human proteome. *Science, 347*, 1260419.

Ulisse, S., Baldini, E., Sorrenti, S., & D'Armiento, M. (2009). The urokinase plasminogen activator system: a target for anti-cancer therapy. *Current Cancer Drug Targets, 9*, 32-71.

van de Craen, B., Scroyen, I., Vranckx, C., Compernolle, G., Lijnen, H. R., Declerck, P. J., & Gils, A. (2012). Maximal PAI-1 inhibition *in vivo* requires neutralizing antibodies that recognize and inhibit glycosylated PAI-1. *Thrombosis Research, 129*, e126–e133.

van der Burg, M. E., Henzen-Logmans, S. C., Berns, E. M., van Putten, W. L., Klijn, J. G., & Foekens, J. A. (1996). Expression of urokinase-type plasminogen activator (uPA) and its inhibitor PAI-1 in benign, borderline, malignant primary and metastatic ovarian tumors. *International Journal of Cancer, 69*, 475-479.

van Nagell, J. R., DePriest, P. D., Reedy, M. B., Gallion, H. H., Ueland, F. R., Pavlik, E. J., & Kryscio, R. J. (2000). The efficacy of transvaginal sonographic screening in asymptomatic women at risk for ovarian cancer. *Gynecologic Oncology, 77*, 350-356.

van Tilborg, A. A., Sweep, F. C., Geurts-Moespot, A. J., Wetzels, A. M., de Waal, R. M., Westphal, J. R., & Massuger, L. F. (2014). Plasminogen activators are involved in angiostatin generation *in vivo* in benign and malignant ovarian tumor cyst fluids. *International Journal of Oncology, 44*, 1394-1400.

Vassalli, J. D., Baccino, D., & Belin, D. (1985). A cellular binding site for the Mr 55,000 form of the human plasminogen activator, urokinase. *The Journal of Cell Biology, 100*, 86-92.

Vincenza Carriero, M., Franco, P., Vocca, I., Alfano, D., Longanesi-Cattani, I., Bifulco, K., Mancini, A., Caputi, M., & Stoppelli, M. P. Structure, function and antagonists of urokinase-type plasminogen activator. (2009). *Frontiers in Bioscience (Landmark Edition), 1,* 3782-3794.

Visintin, I., Feng, Z., Longton, G., Ward, D. C., Alvero, A. B., Lai, Y., Tenthorey, J., Leiser, A., Flores-Saaib, R., Yu, H., Azori, M., Rutherford, T., Schwartz, P. E., & Mor, G.

(2008). Diagnostic markers for early detection of ovarian cancer. *Clinical Cancer Research, 14*, 1065-1072.

Wang, Y., Dang, J., Johnson, L. K., Selhamer, J. J., & Doe, W. F. (1995). Structure of the human urokinase receptor gene and its similarity to CD59 and the Ly-6 family. *European Journal of Biochemistry, 227*, 116-122.

Wilhelm, O., Hafter, R., Henschen, A., Schmitt, M., & Graeff, H. (1990). Role of plasmin in the degradation of the stroma-derived fibrin in human ovarian carcinoma. *Blood*, *75*, 1673-1678.

Winter, W. E., 3rd, Maxwell, G. L., Tian, C., Carlson, J. W., Ozols, R. F., Rose, P. G., Markman, M., Armstrong, D. K., Muggia, F., McGuire, W. P., & Gynecologic Oncology Group Study. (2007). Prognostic factors for stage III epithelial ovarian cancer: a Gynecologic Oncology Group Study. *Journal of Clinical Oncology, 25,* 3621-3627.

Witzel, I. D., Milde-Langosch, K., Wirtz, R. M., Roth, C., Ihnen, M., Mahner, S., Zu Eulenburg, C., Jänicke, F., & Müller, V. (2010). Comparison of microarray-based RNA expression with ELISA-based protein determination of HER2, uPA and PAI-1 in tumour tissue of patients with breast cancer and relation to outcome. *Journal of Cancer Research and Clinical Oncology, 136*, 1709-1718.

World Cancer Report, 2014. World Health Organization (2014. pp. Chapter 5.12. ISBN 5629283204298).

Xiao-Rong, P., Hsueh, A. J., & Tor, N. Y. (1993). Transient and cell-specific expression of tissue-type plasminogen activator and plasminogen-activator-inhibitor type 1 results in controlled and directed proteolysis during gonadotropin-induced ovulation. *European Journal of Biochemistry*, *214*, 147-156.

Xue, Y., Bodin, C., & Olsson, K. (2012). Crystal structure of the native plasminogenreveals an activation-resistant compact conformation. *Journal of Thrombosis and Haemostasis, 10*, 1385-1396.

Yang, J. L., Seetoo, D., Wang, Y., Ranson, M., Berney, C. R., Ham, J. M., Russell, P. J., & Crowe, P. J. (2000). Urokinase-type plasminogen activator and its receptor in

colorectal cancer: independent prognostic factors of metastasis and cancer-specific survival and potential therapeutic targets. *International Journal of Cancer, 89,* 431-439.

Zhang, L., Zhao, Z. S., Ru, G. Q., & Ma, J. (2006). Correlative studies on uPA mRNA and uPAR mRNA expression with vascular endothelial growth factor, microvessel density, progression and survival time of patients with gastric cancer. *World Journal of Gastroenterology, 12,* 3970-3976.

Zhang, Y., Kenny, H. A., Swindell, E. P., Mitra, A. K., Hankins, P. L., Ahn, R. W., Gwin, K., Mazar, A. P., O'Halloran, T. V., & Lengyel, E. (2013a). Urokinase plasminogen activator system–targeted delivery of nanobins as a novel ovarian cancer therapy. *Molecular Cancer Therapeutics, 12*, 2628-2639.

Zhang, W., Ling, D., Tan, J., Zhang, J., & Li, L. (2013b). Expression of urokinase plasminogen activator and plasminogen activator inhibitor type-1 in ovarian cancer and its clinical significance. *Oncology Reports, 29*, 637-645.

8. Appendix

8.1 Standard operation procedure for immunohistochemical assessment of uPA protein expression

Protocol is a manual procedure by applying the Envision/polymer method without pressure-cooking.

1	**Deparaffinization and rehydration of tissue section in xylene and descending row of graded alcohols:** 2 x 10 min xylene, 2 x 100% ethanol, 1 x 96% ethanol, 1 x 70% ethanol, each one for 5 min at room temperature (RT).
2	**Washing step:** 5 min washing with TBST (Tris-buffer with 0.05% Tween-20), with intervening buffer changes at RT.
3	**Blocking of endogenous peroxidase activity:** Incubation of tissue sections with 3% H_2O_2 (hydrogen peroxide) (45 ml distilled H_2O + 5 ml 30% H_2O_2), 20 min at RT.
4	**Washing step:** 5 min washing with tap water at RT.
5	**Washing step:** 5 min washing with TBST, intervening buffer changes at RT.
6	**Apply primary antibody against uPA:** Dilute antibody before use with ready-to-use antibody diluent (Dako) at a dilution rate of 1:400 (working solution concentration: 12.5 ng/ml), applying 100 µl. Apply 100 µl antibody diluent instead of primary antibody as the negative control. Incubation overnight at 4°C.
7	**Washing step:** 5 min washing with TBST, intervening buffer changes.
8	**Apply the polymer-one-step mixture from Zytomed:** Apply 120 µl/slide and incubate for 30 min at RT.
9	**Washing step:** 5 min washing with TBST, with intervening buffer changes, RT.
10	**Apply the DAB high-contrast substrate:** Apply 120 µl/slide of DAB high-contrast substrate from Zytomed (a mixture of 1 ml buffer and 50 µl DAB chromogen for 10 slides) and incubate for 8 min at RT.
11	**Washing step:** 5 min washing with TBST, with intervening buffer changes, RT.
12	**Counterstain:** With hematoxylin, 1 min, RT.
13	**Blue dyeing:** Rinse under flowing tap water, 3 min, then transfer to distilled H_2O, 1 min.
14	**Dehydrate in ascending row of** 70% ethanol, 1 x 96% ethanol, 2 x 100% ethanol, 2 x xylene, each for 3 min at RT.
15	**Cover glass sealing:** Use Pertex mounting medium.

8.2 Standard operation procedure for immunohistochemical assessment of PLG and PAI-1 protein expression

The automated immunohistochemical staining procedure protocol is programm No.998 in Ventana Medical Systems.

1. Deparaffinization.	31. Apply primary antibody, incubation for 1 h.
2. 75°C, incubation for 8 min (Cycle 1).	32. 37°C, incubation for 4 min.
3. Incubation for 8 min (Cycle 2).	33. Wash with reaction buffer.
4. 37°C, incubation for 4 min.	34. Apply 2nd antibody (anti-mouse IgG), incubation for 30 min.
5. Washing step.	35. Wash with reaction buffer
6. Pretreatment.	36. Apply one drop of Blocker D, incubation for 4 min.
7. CC1 (Cell Conditioning 1) antigen retrieval solution.	37. Apply one drop of SA-HRP (steptavidin-horseradish peroxidase) D, incubation for 16 min.
8. 93°C, incubation for 8 min (CC1).	38. Wash with reaction buffer.
9. 100°C, incubation for 4 min (CC1).	39-41. Repeat position 38.
10. CC1 incubation for 4 min (RT).	42. Apply one drop of DAB H_2O_2, liquid coverslip solution (LCS) and incubation for 8 min.
11-19 Repeat step 10.	43. Wash with reaction buffer.
20. Incubate for 8 min.	44. Apply one drop of Copper D and incubation for 4 min.
21. Wash with reaction buffer.	45. Wash with reaction buffer.
23. EZ Prep solution.	46. Counterstain.
24. SSC (Sodium Chloride Sodium. Citrate buffer solution).	47. Apply one drop of hematoxylin, LCS (Counterstain), incubation for 4 min.
25. 37°C, incubation for 4 min.	48. Wash with reaction buffer.
26. Wash with reaction buffer.	50. Post counterstain.
27. Inhibitor D.	51. Apply one drop of bluing reagent (Post Counterstain), incubation for 4 min.
28. Apply one drop of Inhibitor D, incubation for 4 min.	52. Wash with reaction buffer.
29. Wash with reaction buffer.	53. Wash with reaction buffer.
30. Antibody step.	

8.3 Antibody characteristics

Antigen	Species	Stock solution (mg/ml)	Working solution	Method
PLG	Monoclonal mouse IgG1	2	1:100	Ventana automatic staining
PAI-1	Monoclonal mouse IgG1	0.42	1:25 (after centrifugation)	Ventana automatic staining
uPA	Monoclonal mouse IgG1	1	1:400 (after filtration)	EnVision manual staining

8.4 Standard dilutions

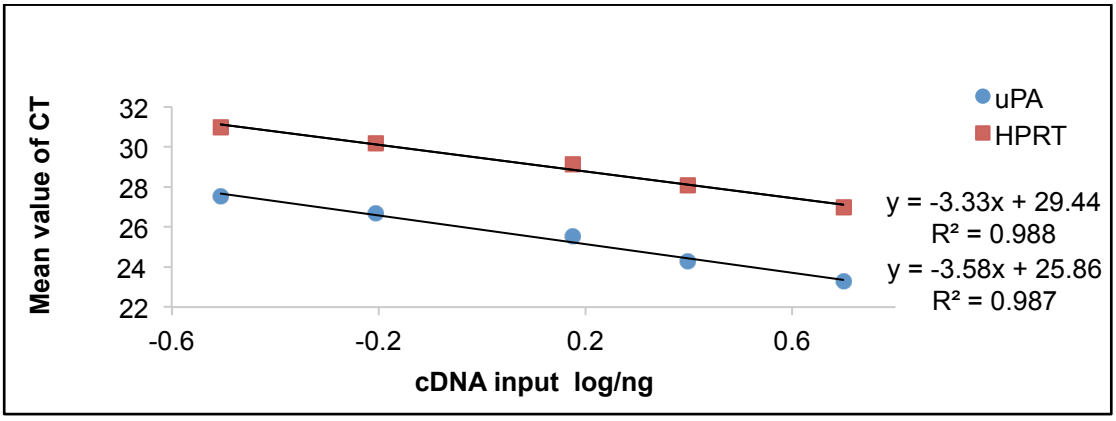

Figure A. Exemplary dilution series for *uPA* cDNA and *HPRT* cDNA by qPCR.

The reference gene is *HPRT*. Total RNA was extracted from the ovarian cancer cell line OV-MZ-6 and reverse transcribed (cDNA input range: 0.3125-5 ng). *uPA*: slope = -3.58, E = 1.90; *HPRT*: slope = -3.33, E = 1.99.

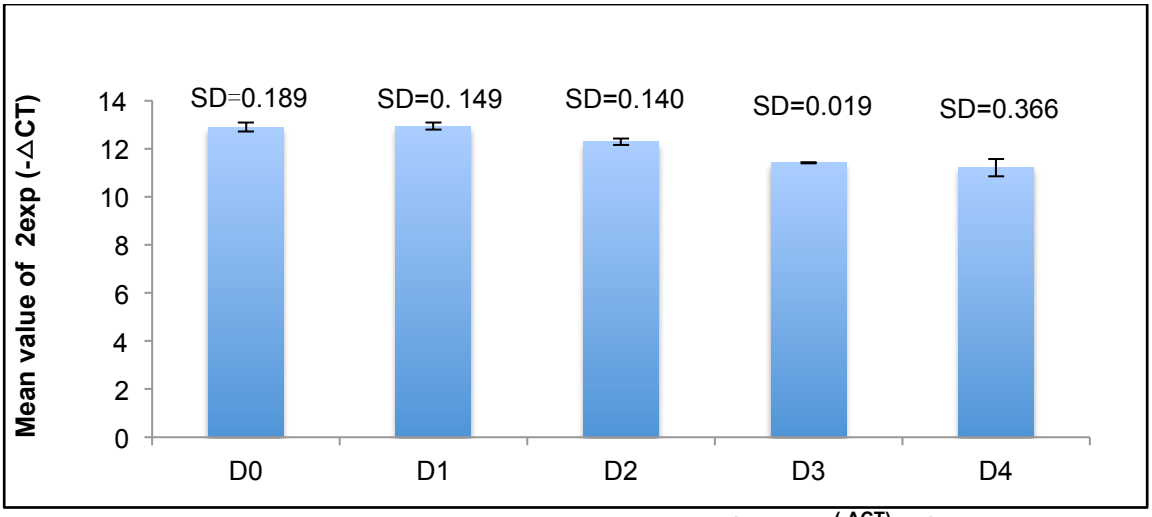

Figure B. Mean values and standard deviations of 2exp $^{(-\Delta CT)}$ of individually diluted samples representing two independent *uPA* qPCR experiments. Normalization against *HPRT* cDNA.

Overview over two separate qPCR experiments representing five dilutions for the *uPA* qPCR assay. 1:2 fold dilution steps, from the first dilution (D0) to the fifth dilution (D4) are displayed (cDNA from OV-MZ-6 cells; cDNA input range: 0.3125-5 ng).

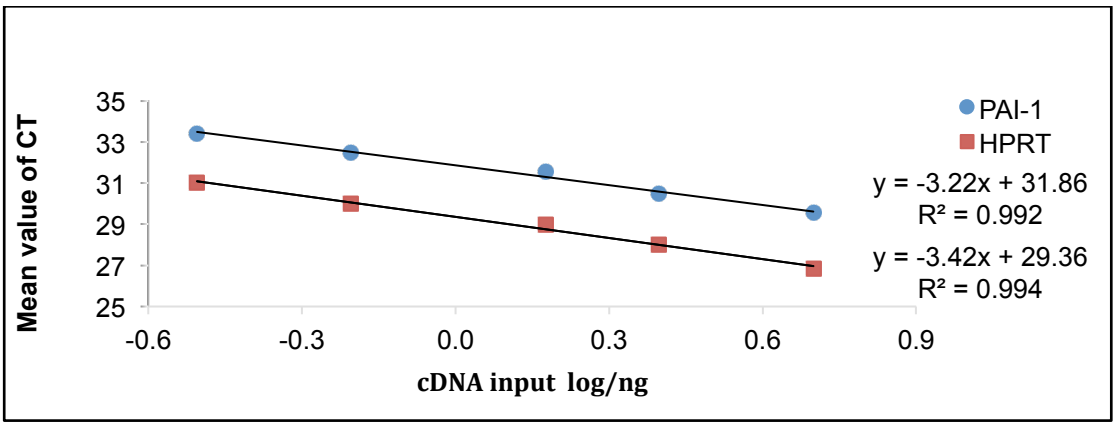

Figure C. Exemplary dilution series for *PAI-1* cDNA and *HPRT* cDNA by qPCR.

The reference gene is *HPRT*. Total RNA was extracted from the ovarian cancer cell line OV-MZ-6 and reverse transcribed (cDNA input range: 0.3125-5 ng). *PAI-1*: slope = -3.22, E = 1.96; *HPRT*: slope = -3.42, E = 2.04.

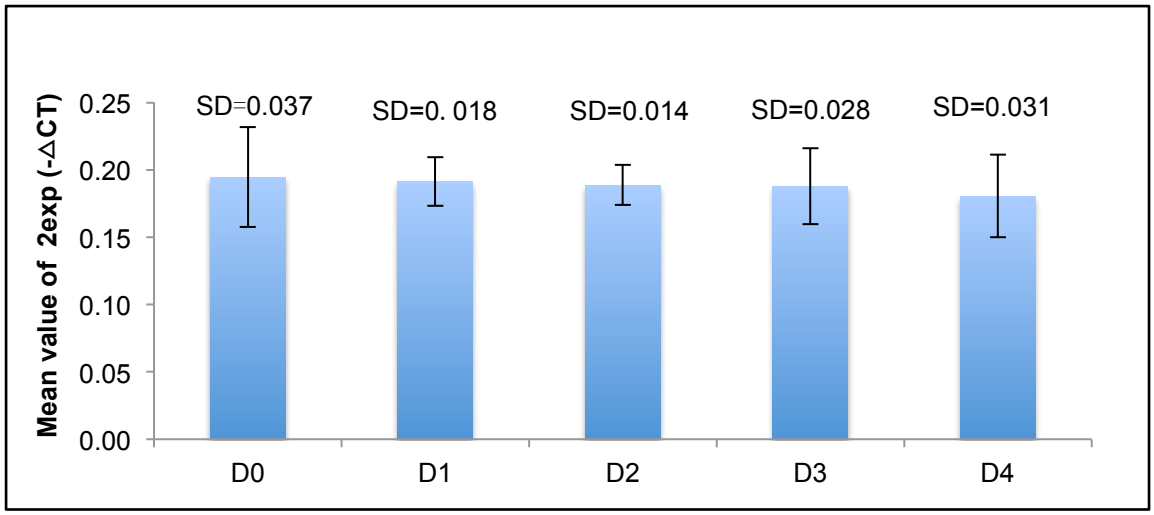

Figure D. Mean values and standard deviations of 2exp $^{(-\Delta CT)}$ of individually diluted samples representing six independent *PAI-1* qPCR experiments. Normalization against HPRT cDNA.

Overview over six separate qPCR experiments representing five dilutions for the *PAI-1* qPCR assay. 1:2 fold dilution steps, from the first dilution (D0) to the fifth dilution (D4) are displayed (cDNA from OV-MZ-6 cells; cDNA input range: 0.3125-5 ng).

8.5 Abbreviations

Ab	Antibody
cDNA	Complementary deoxyribonucleic acid
CI	Confidence interval
Conc.	Concentration
DAB	3,3'-Diaminobenzidine
DNA/cDNA	Deoxyribonucleic acid/complementary DNA
DNase	Deoxyribonuclease
DMSO	Dimethyl sulfoxide
dNTP	Deoxynucleotide nucleoside triphosphate
ECM	Extracellular matrix
EDTA	Ethylenediaminetetraacetic acid
e.g.	Exempli Gratia (for example)
ELISA	Enzyme-linked immunosorbent assay
etc.	Et cetera (and so forth)
FFPE	Formalin-fixed paraffin-embedded
FIGO	Fédération Internationale de Gynécologie et d'Obstétrique
g	Gravity
h	Hour
H&E-staining	Hematoxylin and eosin-staining
HR (95% CI)	Hazard ratio (95% confidence interval)

HRP	Horseradish peroxidase
HPRT	Hypoxanthine-guanine phosphoribosyltransferase
IgG	Immunoglobulin G
IHC	Immunohistochemistry
kb	Kilobase
kDa	Kilodalton
KLK	Kallikrein-related peptidase
mAb	Monoclonal antibody
mg/ml	Milligrams per milliliter
min	Minute
ml	Milliliter
mRNA	Messenger ribonucleic acid
NaOH	Sodium hydroxide
ng/ml	Nanograms per milliliter
No.	Number
µl	Microliter
OS	Overall survival
PAI-1	Plasminogen-activator inhibitor type 1
PBS	Phosphate-buffered saline
PCR	Polymerase chain reaction
PFS	Progression-free survival
pH	Potential of hydrogen
PLG	Plasmin(ogen)
RLT	RNeasy lysis buffer
RNase	Ribonuclease
r_s	Spearman's rank correlation coefficient
RT	Reverse transcription
SEER	Surveillance, epidemiology, and end results
SOP	Standard-operating-procedure
SSC	Sodium chloride plus sodium citrate buffer solution
TBST	Tris-buffered saline with 0.05% Tween 20
TMA	Tissue microarray
uPA	Urokinase-type plasminogen activator
uPAR	uPA receptor
vs.	Versus
°C	Degree Celsius
% (w/v)	Percent weight/volume
% (v/v)	Percent volume/volume

9. Acknowledgments

First and foremost, I would like to offer my sincerest gratitude and thanks to my supervisor Univ.-Prof. Dr. rer. nat. Dr. med. habil. Manfred Schmitt, Frauenklinik, Klinikum rechts der Isar, TUM. He has fully supported my experiments and thesis writing with his broad knowledge and unlimited patience.

I am deeply grateful to my co-supervisor, Prof. Dr. rer. nat. habil. Viktor Magdolen as well, Frauenklinik, Klinikum rechts der Isar, TUM. He has always been there to give me advice during the course of my work.

Thanks for support to the head and chair of the Frauenklinik, Klinikum rechts der Isar, TUM, Prof. Dr. med. Marion Kiechle that my research could be carried out smoothly.

Dr. rer. nat. Rudolf Napieralski's technical guidance, insightful teaching and constructive criticism throughout my research helped me a lot. His great experience helped me to focus on the center aspect of my study.

I am also indebted to Prof. Dr. med. Axel Karl Walch and Ulrike Buchholz, Helmholtz Zentrum, Munich, who gave me the chance to work in their facility and also taught me ovarian cancer pathology. I am also thankful for the exchange study experience by Prof. Andreas Scorilas, University of Athens, Greece.

Prof. Dr. rer. nat. Matthias Kotzsch, University of Dresden, introduced me to statistical methods. His teaching encouraged me to conduct the statistical analyses.

Finally, I am thankful to several colleagues of the Frauenklilnik, Klinikum rechts der Isar, TUM. PD Dr. med. Julia Dorn, Dr. rer. nat. Sandra Diersch, Dr. rer. nat. Christof Seidl, Daniela Hellmann, Elisabeth Schüren, Sabine Creutzburg, and Anke Benge. They gave me guidance and various forms of support to conduct my experiments.

During my work, I was blessed to cooperate with a friendly group of fellow students and international exchange students. They are Dr. Brittney Harrington, Dr. Konstantinos Mavridis, Dr. Kleita Michaelidou, Nancy Ahmed, Thirza Singer, Ping Wang, Feng Yang and Caixia Zhu.

I would also like to acknowledge my Chinese master supervisors Prof. Dr. Beihua Kong and Prof. Dr. Xiaohui Deng, Shandong University, P.R. China. Their knowledgeable suggestions and continuous support are highly appreciated.

Finally, I am really thankful to my parents, my husband and other relatives for supporting my doctoral studies at my home university and abroad. Their enormous understanding and belief in me motivated me and encouraged me to complete my scientific work.